universität wien

MASTERARBEIT / MASTER'S THESIS

Titel der Masterarbeit / Title of the Master's Thesis

„Development of a targeted LC-MS/MS method for the simultaneous detection of recently discovered bile acid conjugates"

verfasst von / submitted by

Daniel Wasinger, BSc

angestrebter akademischer Grad / in partial fulfilment of the requirements for the degree of

Master of Science (MSc)

Wien, 2022 / Vienna 2022

Studienkennzahl lt. Studienblatt / degree programme code as it appears on the student record sheet:	UA 066 659
Studienrichtung lt. Studienblatt / degree programme as it appears on the student record sheet:	Masterstudium Lebensmittelchemie
Betreut von / Supervisor:	Univ.-Prof. Dipl.-Ing. Dr. Benedikt Warth, Bakk.

Table of contents

Acknowledgements

I would first and foremost like to thank Prof. Dr. Benedikt Warth for allowing me the opportunity to write my thesis within his Global Exposomics & Biomonitoring working group, as well as offering advice whenever necessary, and providing the invaluable experience of what it feels like to be part of the scientific community. I would also like to thank all the members of the working group, especially Manuel Pristner, who also provided excellent supervision throughout my entire project. I was honored to be able to operate on instruments at the Mass Spectrometry Centre at the Faculty of Chemistry of the University of Vienna and would like to thank the staff for providing assistance whenever necessary. Furthermore, I want to thank my parents, Thomas and Zuzana, who have done everything in their power to enable me to get this far, as well as my girlfriend, Katharina, who's loving support never waned even at the worst of times. Finally, I want to thank my friends who had to endure me rejecting their invitations countless times during these busy times, yet never stopped thinking of me.

Thank you!

Abstract

The human gut hosts a plethora of microorganisms, known as the gut microbiome. The combined metabolome of the different phyla, genera and strains affect all tissues of the host, deeply implicated in health and disease of individuals. Bile acids synthesized by the host and secreted into the gut lumen are also subject of microbial conversion. Recently, new bile acid – amino acid conjugates created by the microbiome have been discovered as part of a previously unknown mechanism of interaction, giving rise to a new class of metabolites. These molecules have already been associated with inflammatory diseases and as such the role they possibly play could be of great interest. However, this requires means of sensitive and accurate detection, which can be difficult to establish for novel compounds. This thesis aimed to develop a targeted MS/MS method for the detection of the newly discovered conjugates. In order to circumvent the problem of unavailable standard material necessary for the acquisition of measurement parameters, conjugates were synthesized using coupling chemistry. To simplify the process, a batch synthesis procedure of reacting all amino acids with a single bile acid at a time was employed. Overall, this resulted in the synthesis of 120 compounds that were tuned on a triple quadrupole mass spectrometer. The same batches were utilized in the establishment of the HPLC method, where three different columns and four eluent systems were tested before optimizing the gradient. Though absolute and accurate quantification was not feasible, this method could still be utilized in a qualitative and semi-quantitative manner. The method was tested using plasma and fecal samples obtained from a cohort of extremely premature infants, of which a subgroup suffered from neurodevelopmental impairments. The aim was to investigate the conjugated bile acid profile and find a potential link between bile acid conjugates and pathological outcome in the cohort.

Zusammenfassung

Der menschliche Darm beherbergt eine Fülle von Mikroorganismen, die als Darmmikrobiom bekannt sind. Das kombinierte Metabolom der verschiedenen Stämme, Gattungen und Arten wirkt sich auf alle Gewebe des Wirts aus und ist maßgeblich an Gesundheit und Krankheit des Menschen beteiligt. Gallensäuren, die vom Wirt synthetisiert und in das Darmlumen abgegeben werden, sind ebenfalls Gegenstand mikrobieller Umwandlung. Kürzlich wurden neue Gallensäuren-Aminosäuren-Konjugate entdeckt, deren Entstehungsmechanismus durch die Interaktion mit dem Mikrobiom bisher unbekannt war und zu einer neuen Klasse von Metaboliten führt. Diese Moleküle konnten bereits mit Entzündungskrankheiten in Verbindung gebracht werden, weshalb die Rolle, die sie dabei möglicherweise spielen, von großem Interesse ist. Dafür sind jedoch empfindliche und genaue Nachweismethoden erforderlich, die bei neuartigen Verbindungen anfangs nur schwer zu etablieren sind, da diese Substanzen nicht kommerziell erhältlich sind. In diesem Projekt sollte demnach eine gezielte MS/MS-Methode für den Nachweis der neu entdeckten Konjugate entwickelt werden. Da die für die Erfassung der Messparameter erforderlich Referenzmaterialien noch nicht erwerblich sind, wurden die nötigen chemischen Standardsubstanzen durch Kopplungschemie selbst synthetisiert. Zur Vereinfachung des Prozesses wurde ein Batch-Syntheseverfahren angewandt, bei dem alle Aminosäuren jeweils mit einer einzelnen Gallensäure umgesetzt wurden. Insgesamt führte dies zur Synthese von 120 Verbindungen, die verwendet wurden um eine LC-MS Methode mithilfe eines Triple-Quadrupol-Massenspektrometer zu entwickeln und optimieren. Für die Optimierung der HPLC-Methode wurden drei verschiedene Säulen und vier Eluentensysteme getestet. Obwohl eine absolute und genaue Quantifizierung nicht durchführbar war, kann diese Methode dennoch auf qualitative und semi-quantitative Weise eingesetzt werden. Die Methode wurde mittels Plasma- und Fäkalproben aus einer Kohorte extrem frühgeborener Säuglinge getestet, von denen ein Teil an neurologischen Entwicklungsstörungen litt. Ziel war es, das Profil der konjugierten Gallensäuren zu untersuchen und einen möglichen Zusammenhang zwischen Gallensäurekonjugaten und pathologischen Folgen in der Kohorte zu finden.

1 Introduction

1.1 The gut microbiome and its microbial metabolome

The gut of humans and similar organisms hosts a wide variety of microorganisms, where the species present can be highly diverse and strongly dependant on environmental factors and diet. The interindividual diversity is so vast, that even the possibility of personal identification via metagenomic code has been suggested.[1] Functions attributed to the microbiome range from being described as a protective aid, to facilitating breakdown of more complex carbohydrates (dietary fiber), as well as impacting energy metabolism and amino acid homeostasis.[2–4] As such, the interaction of microbiome and host has been recognized to be vital for the upkeep of health.[5] The global effects exerted by commensal microbes can be further confirmed in studies based on differences in metabolic profiles between conventional and germ-free (GF) mice. Many molecules could be found exclusively in the serum and tissues of animals with a functional gut microbiome and around 10% of features that are common within both groups differ significantly in concentration.[6,7]

Among the most impacted metabolites are those derived from tryptophan. Through enzymes such as tryptophanase found in certain bacterial species, indole can be created through cleavage of an alanine moiety from tryptophan.[8] Dietary tryptophan is intercepted and partially metabolized by the gut microflora, resulting in lower levels of serum tryptophan in the host.[7] In addition, phase II metabolites as a response to the introduction of indole, such as indoxyl sulfate, can also be found. This is also true for many phase II metabolites of other molecules, which appear highly elevated, or exclusively in conventional mice, such as hippuric acid and cinnamoylglycine.[7] Other bacteria have been found to be able to further transform indole to indole-3-propionic acid (IPA), which features strong antioxidative properties.[9]

Another set of microbiome-related metabolites of great interest that are well studied are short-chain fatty acids (SCFAs). This group is so heavily implicated in host health that causal relationships between microbiome SCFA production and metabolic diseases such as type 2 diabetes have been proposed.[10] They are created from undigestible, fibrous material that passes the small intestine and is then available for fermentation by the microbiota. Major products include formate, acetate, propionate and butyrate and the pathways have already been elucidated and are well understood.[11,12] Butyrate has been found to have dramatic effects on the gut epithelium,[13] and SCFAs in general appear to stimulate gene expression for tight junction proteins.[14] Tight junctions are the interstitial space between two adjacent epithelial cells and therefore are of paramount importance in the paracellular exchange of substances and the overall integrity of the gut barrier. Dysfunction of the gut barrier is associated with diseases of metabolic and inflammatory nature.[15] The regulatory function of SCFAs

appears to extend to affecting glucose and lipid metabolism positively as well, explaining an inverse association with obesity.[16]

Considering all of this, it is easy to see why interest and research in the field of microbiome research has picked up significantly in the past years. Investigation of microbiome-derived metabolites like SCFAs is largely enabled by state-of-the-art analytical tools such as mass spectrometry with the ability for highly sensitive detection of numerous analytes in a single measurement.[17] While a significant amount of the work done on microbiome research is focused on bacteria, these are not the only microorganisms present in the gut. Viruses, phages, fungi and other microorganisms make up a significant part of the biome inhabiting our gut.[18] The interaction between all these different actors is still not well understood and so it requires much more research to completely unveil the connections between the gut microbiome and the health of the host.

1.2 Bile acids

Bile acids are synthesized in the liver of humans and account for the vast majority of organic compounds in the bile.[19] They are end products of the cholesterol metabolism and the carboxyl group in combination with the sterol frame gives them the amphipathic characteristic necessary to fulfil their physiological function as emulsifiers of ingested fats and oils.[19,20] For this purpose, they are further conjugated with taurine or glycine at the acid moiety forming bile salts.[21] After release into the small intestine, they are eventually reabsorbed as part of the enterohepatic cycle and stored in the gallbladder. This process is exceedingly efficient, such that more than 85% of bile salts released are recovered.[21] When in the lumen those bile salts, consisting of conjugates of the two endogenous bile acids cholic acid and chenodeoxycholic acid, are subject to the microbiome and can be altered, resulting in secondary bile acids and different bile acid conjugates.[22]

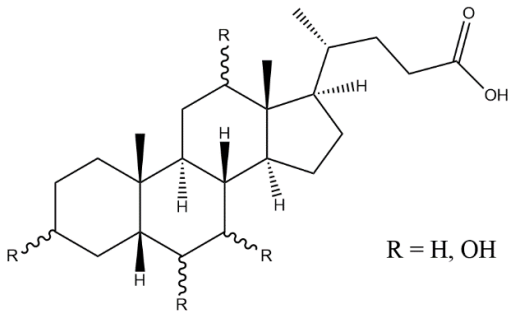

Figure 1. General structure of bile acids, featuring the sterol backbone and acid moiety.

Besides their role as detergents to facilitate lipid uptake, bile acids are also known to have regulatory functions. Their ability to activate nuclear receptors (e.g. Farnesoid X receptor "FXR") and G protein coupled receptor TGR5, as well as numerous other signalling pathways affecting a multitude of tissues,

including even the brain and its function.[23,24] Bile acids can affect glucose metabolism in similar fashion as insulin in liver cells and boost the uptake after a meal.[25] Concerning lipids, bile acids are self-regulating through activating negative feedback of their own synthesis through FXR.[26] Furthermore chenodeoxycholic acid is even used as a pharmaceutical drug for treating gallstones.[27] While this further showcases the strong regulatory functions of bile acids in the human body, they have also been shown to be a major regulator of the gut microbiome, affecting its community structure.[28] Due to their amphiphilic nature, bile acids are potent antimicrobial agents, damaging and inducing lysis in bacteria that lack mechanisms for their uptake and metabolism.[29] In the same manner, the secondary bile acids created by the microbiome exhibit altered interaction with human receptors while depleting the primary bile acid pool, affecting host metabolism with a possible role in neurological diseases.[30]

Recently, novel conjugates of different amino acids, namely phenylalanocholic acid, tyrosocholic acid and leucocholic acid, have been described and an association with Inflammatory bowel disease (IBD) was discovered.[31] Their origin has also been traced back to the activity of the microbiome, revealing an entirely new mechanism of the bile acid – microbiome interaction. Some of these conjugates were shown in follow-up cell assays to be effective agonists of the pregnane X receptor, a receptor often targeted by drugs to treat IBD.[32,33] Microorganisms that have been found to be able to synthesize such compounds (e.g. Bacteria of the genus *Clostridium*) have also been correlated with greater occurrences of developmental disorders in children.[34] As such, there is considerable interest to determine the exact nature and role these new conjugated bile acids may play in disease formation, with researchers already developing methods for their detection.[35]

1.3 High-performance liquid chromatography

As a preface, all the presented information in this chapter is in reference to the book "Liquid Chromatography, Fundamentals and Instrumentation", 2nd ed., 2017, if not otherwise specified by additional references.[36]

1.3.1 History and general concept

There is no doubt that high-performance liquid chromatography (HPLC) has established itself as one of the most important techniques in the analysis of chemical mixtures. Especially in the life sciences it enables the thorough investigation into various areas of clinical importance, such as drug pharmacokinetics, modes of action and metabolic response. The earliest precursor to modern HPLC can be found within the works by Moore, Stein and Spackman in 1958 on the analysis of amino acids using ion exchange chromatography, featuring automatic pumps, efficient columns and continuous detection via calorimetry. The development of electrospray interfaces in the late 1980s heralded the introduction of mass spectrometry (MS) as a universal detector for HPLC and is now one of the most

popular techniques. In general, the concept of HPLC, and every other chromatographic technique, lies in the separation of compounds on the basis of their interaction between a mobile phase (eluent) and a stationary phase (column material). As such, two compounds with distinctly different affinity to either phase will be retained for longer or shorter times, depending on the materials used, and leave the column in narrow bands, which can then be analyzed separately from each other using applicable detectors (UV, MS, etc.).

1.3.2 Columns and different types of stationary phases

The first part of the development of a HPLC method lies in the selection of an appropriate column. Modern HPLC columns are stainless steel cylinders because they are both inert and able to withstand high pressures. The hollow inner tube featuring the actual stationary phase has diameters usually ranging between 2 – 4 mm and a length between 50 and 250 mm. Great importance is put on manufacturing columns where the inner diameter is constant over the length, as even slight fluctuations can result in large changes in the linear velocity of eluents and thus retention times of analytes. This space is either outfitted with a rigid monolithic element or tightly packed with uniform particles of various sizes, forms and functionalities, which in the end is responsible for the greatest changes in efficiency and selectivity among different columns. The main goal is to introduce a homogenous body with a very large surface area to volume ratio, leading to enhanced mass transfer kinetics and eventually results in the separation of analytes. Replaceable guard- or pre-columns made from the same material are used in many cases to protect the far more valuable analytical HPLC column from debris. As for the material of the column packing, porous silica is by far the most used for its mechanic stability and general robust nature. The siloxane network is quite stable in the pH ranges 1 – 9 and the surface silanol groups can be modified with various other functional groups such as n-alkyl silanes, allowing for very broad application. Alternatively, core-shell particles, where the silica is fused onto a solid core instead of using the fully porous materials, are used in some applications by manufacturers to greatly narrow down the particle size distribution within a column and reduce back pressure while keeping efficiencies high.

Originally, HPLC was performed with non-functionalized or bare silica, known today as normal phase (NP) HPLC. This required the use of organic solvents as eluents and water trapped on the hydrophilic surface often interfered with the establishment of stable retention times. Functionalization of silica with n-octadecyl (C18) lead to reversed phase (RP) chromatography, enabling the possibility of injecting and separating aqueous samples using water as an eluent. Nowadays a broad variety of different functionalized columns are available, each offering different properties. Recent trends in research on the omics scale aim to analyze as many constituents as possible from very complex biological fluids, rendering simple functionalized HPLC columns inadequate for resolving this

complexity fully. Utilizing two columns in parallel with different modalities or multifunctional columns that feature multiple interactive sites on the bound ligand may be required to capture the full chemical spectrum of a sample.[37] A brief overview of selected techniques employing different mobile and stationary phases and their distinguishing characteristics can be found in Tab. 1.

Table 1. A list featuring common chromatographic techniques and a brief explanation about their characteristics and application.

Chromatographic technique	Basic concept
Normal phase chromatography (NPC)	Considered the original LC mode. Stationary phase consists of polar groups such as unbonded silica and non-polar solvents are used as eluents (hexane, dichloromethane, etc.).
Reversed-phase chromatography (RPC)	The most commonly used LC mode today. Stationary phase features non-polar functionality such as alkyl-groups of varying length while mixtures of water and an organic solvent (e.g. methanol, acetonitrile) are used as solvents.
Hydrophilic interaction chromatography (HILIC)	A twist on conventional NPLC that is able to use similar solvents as RPLC. Polar stationary phases such as bare silica or those modified with amino, diol or other polar functional groups are run with highly organic solvent mixtures and at least 2.5% water. A water-rich layer is formed on the surface of the stationary phase to enable the interaction of polar compounds and their elution is expedited by increasing the water content over time.
Hydrophobic interaction chromatographic (HIC)	A mild method for protein separation that preserves their tertiary structure. The stationary phase features hydrophobic ligands (e.g. alkyls, phenyls) linked by spacers. The interaction between ligands and non-polar moieties on large biomolecules in the presence of salts is responsible for the retention. Liberation of target compounds is achieved by reducing the salt concentration with gradient or step elution.
Size-exclusion chromatography (SEC)	A method that separates molecules based on their molecular mass and finds great use in the analysis of synthetic polymers. Smaller components of a mixture will be able to enter and be retained by the inert, porous stationary phase while larger ones will pass by more quickly. Thus, this technique can be thought of as “inverse-sieving”.
Affinity chromatography	Uses biological agents such as hormone receptors or antigens immobilized on solid supports as a stationary phase to selectively retain certain analytes and subsequently eluting them using buffers.

1.3.3 Eluents and their role in chromatography

Another large impact on method development is the choice of the eluent systems. Firstly, the two major modes of elution are isocratic (one eluent, held constant) and gradient (two or more eluents with changing composition over time). Isocratic elution is often simpler in development as the composition need not be adjusted over time and it serves to simply find a solvent mixture where compounds of interest are distinguishably separated with satisfactory peak shapes. This can often be the preferred method for molecules with similar polarities. If polarities of the compounds in the mixture span a wider range, a gradient elution might become necessary to ensure acceptable retention times and peak shapes. As such, gradient elution, using multiple pumps and solvents, is considered the standard for methods that span a wide range of chemically different compounds. Elution starts with solvents of weaker elution strength on a given stationary phase (e.g. water in RP-HPLC) and gradually introduces more of the stronger eluent (e.g. organic solvents such as methanol or acetonitrile in RP-HPLC). This eluent ratio increase can be done in a linear fashion or stepwise and can also feature temporary plateaus, where the ratio is held constant (isocratic), in order to provide the best separation and resolution of analytes. This is followed by the execution of a gradient with a very high percentage of the stronger eluent as a cleaning step to flush out strongly retained molecules. A run is finished by a short period of the same eluent composition used at the start of the run, resulting in the equilibration of the column and guaranteeing the same starting conditions for the next injection. The choice of solvents, addition of additives and the gradient design are highly dependent on the nature of the potential analytes and the stationary phase used. Considering this, it becomes apparent that the iterative process of HPLC method development may in some cases require considerable time investment for reaching optimal results.

1.4 Mass spectrometry

The information in this chapter is based on the book “Mass Spectrometry”, 2008, unless otherwise specified by additional references.[38]

Mass spectrometry (MS) refers to a field of techniques that measure the mass-to-charge ratio of molecules after ionization, enabling the discrimination of analytes with different masses. Since mass is an integral part of all matter, mass spectrometry can theoretically be applied to any compound, compared to many other analytical methods that need to exploit specific chemical or structural elements. The only prerequisite is sufficient ionization of the target, as all mass analysers rely in some way on the use of magnetic or electric fields to derive the mass in relation to the charge of a particular molecule or particle. Because of this, MS is also considered a destructive analytical technique, since analytes need to be fundamentally changed in order to be measured and can no longer be retrieved

afterwards. The main body of a mass spectrometer can be divided into three vital parts: Ion source, mass analyser and detector.

1.4.1 Ion sources

The role of the ion source of a mass spectrometer is to convert molecules and particles into an ionic, gaseous state so they can be separated based on their mass-to-charge ratio by the following mass analyser. While many ion sources invented over the years were indispensable at the time and contributed to further development of mass spectrometry and its hyphenation to other technologies, not all of them find regular use today. As such, only a selection will be discussed in detail with special focus on application in LC.

However, some historical context is necessary to understand why certain techniques established itself in LC-MS over others: All mass spectrometers rely on very low pressures within their mass analysers to ensure collisions between particles do not interfere with analysis to a significant extent. This worked well in the favour of combining gas chromatography (GC) with MS, as particles were already in the gas phase and the low carrier gas flow in capillary columns was perfectly suited for the high vacuum requirements. The most widely used ionization technique at the time became electron ionization (EI), in which a tungsten filament under strong electric current generates a high-power electron beam. Gas-phase molecules passing through the beam from the GC inlet would then be ionized on contact. This is known as a very harsh form of ionization and causes fragmentation of molecules, which can aid in their identification. However, not all molecules can be subjected to GC measurements without going through laborious and time-consuming derivatization procedures. Since LC can span a much larger variety of analytes, the search for suitable interfaces that could connect it to MS as a detector became of great interest. The biggest issue was the complete opposite of required operation parameters, as the high pressures and lower temperatures of LC made reconciliation with the preferred electron ionization at the time highly incompatible. As such, the development of ionization methods that can be operated at atmospheric pressures was a crucial step for LC-MS to gain traction.[39]

Electrospray ionization (ESI) stands out among others for this purpose and is the most prominent ion source in LC-MS today. It is based on the formation of a so-called Taylor cone on the tip of a needle under high electric potential with up to 4 kV (see Fig. 2 for illustration). A polar, volatile solvent is pushed through the needle, causing charged particles of same polarity to be ejected from the cone in solvent droplets. Auxiliary flow of heated nitrogen aids in the evaporation process of said droplets until they are small enough that the repelling charges on the inside break the surface tension and fission occurs, creating even smaller droplets. The process then repeats until charged analytes are in the gas phase, fulfilling the requirement for analysis via MS. The transfer unit on the inlet of the mass

spectrometer then guides the analyte ions to the mass analyser. The atmospheric pressure conditions at which ESI can be performed are not the only advantages that make it the preferred method for LC-MS. Especially on modern instruments, the polarity of the needle can be switched very quickly. This enables the effective and simultaneous analysis of molecules that may be more sensitive to either negative or positive ionization. However, a drawback of ESI is the lack of ionization potential for molecules of low polarity, leading to a severe drop in efficiency. The sensitivity is also dependent on the concentration of analytes in the needle, which are constantly diluted through the relatively high flow rates in conventional HPLC apertures. The by far biggest issue for ESI, is signal suppression caused by competing elements of sample matrix that coelute with analytes. This means, that the signal strength of an analyte is always going to be subject to the sample environment and makes sample preparation procedures all the more important for reproducible results, especially when the goal is quantitation.

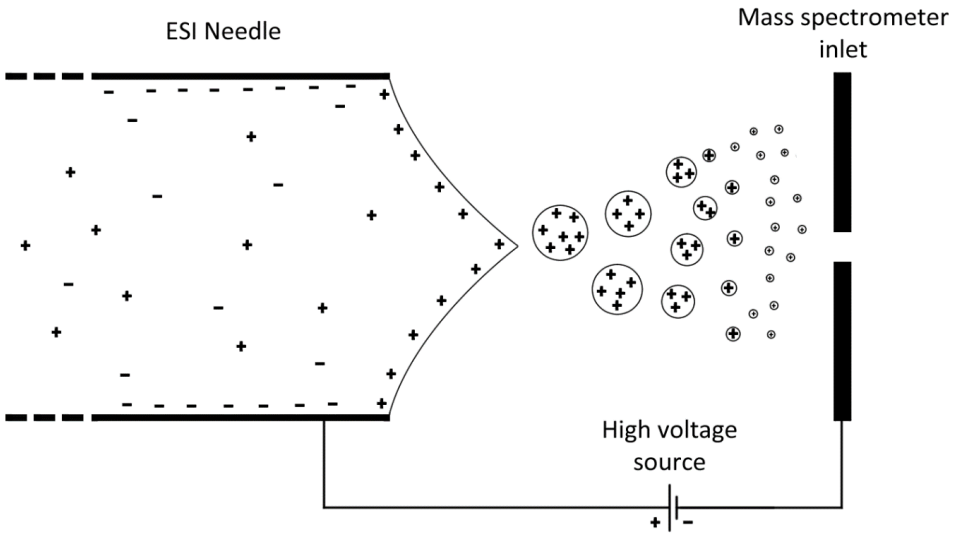

Figure 2. Cross-section of an ESI needle and a schematic overview of the processes at hand.

Another possible and relatively popular ion source for LC-MS is atmospheric pressure chemical ionization (APCI). Here, a spray is formed through a pneumatic nebulizer instead of using electric means. The spray ejects droplets past a corona discharge electrode in close proximity to the inlet of the mass spectrometer. Particles that are ionized this way will be transferred into the mass analyser and subjected to analysis. The major advantage over ESI is, that APCI can effectively ionize compounds of lower polarity and mass and can thus provide a complementary ion source for molecules that are difficult to ionize with ESI. For even more difficult to ionize, non-polar compounds an alternative exists

in atmospheric pressure photoionization (APPI), which works similar to EI but features a photon beam instead of an electron beam to excite molecules and induce ionization. However, this source is very inefficient and often requires the addition of dopants (e.g. toluene, acetone) to transfer charges onto analytes.

1.4.2 Mass analysers

The part of a mass spectrometer that is responsible for the separation of the charged species received from the ion source is called mass analyser. As mentioned, these devices work on the basis of electromagnetism and so the discriminating factor between particles is their mass-to-charge ratio (m/z). Depending on the principle and the working machinery, mass analysers can be broken down into distinct categories. For example, time-of-flight (TOF) instruments rely on exact pulses of energy to accelerate analytes and derive the m/z over the time it takes for them to reach the detector at the end of the flight path. Meanwhile, instruments like orbitraps and cyclotrons derive the information about charged molecules in relation to their oscillating frequency, either directly or through excitation, after trapping them in a potential well. What analyser to use depends first and foremost on the desired information and workload: High-resolution machines with high mass accuracy, giving m/z values of multiple decimals, will give more detailed information, greatly aiding in the exploration of unknown compounds and are employed at the forefront of omics research. However, deconvoluting the amount and complexity of information that can be gathered this way is no easy task and tends to be a time-consuming process. On the other hand, when information on compounds is well known and instead their concentration in certain media becomes of greater interest, low-resolution mass spectrometry generally features higher throughput and can reach very low limits of detection/quantification.

A mass analyser of particular versatility is the quadrupole mass filter. It is characterized by a set of four rods, that are arranged symmetrically to surround a flight path. A constant direct-current (DC) in addition to an oscillating radio frequency (RF) potential is applied to all of them. Opposite rods share the same connection, while adjacent ones differ in polarity. As such, the two pairs of rods always share the same magnitude of potential, while being opposite in sign. Ions that are introduced between the rods will then experience electrostatic deflection in dependence of the DC and RF fields. Through precise modulation of these fields, only particles within a narrow m/z range can pass on a stable trajectory and are thus transferred to the detector, while others are discharged by impact on the rods (see Fig. 3 for illustration). With higher RF frequencies and lower molecule velocity the resolution of quadrupoles increases, since analytes spend longer between the rods to be properly filtered. However, the mass accuracy of quadrupoles is generally considered to be rather poor and instead, most quadrupoles are operated to achieve a bit more than unit resolution (being able to differentiate between analytes that differ in 1 Da). Their main advantages are found in maintenance of good speed

and sensitivity, while being very cheap and small in comparison to other analysers. In fact, they are often incorporated into other devices as a filter option, since lowering or removing the DC voltage can let ions of broad m/z ranges through, which are then further discriminated by more sensitive analysers following thereafter. When used as the primary mass analyser, quadrupoles can only accurately detect one ionic species at a time. This means that sensitivity is decreased when scanning a broad m/z range, as relevant ions entering from the source outside of their scan window will not be detected. When monitoring narrow m/z windows or single ions the sensitivity is much improved with good reproducibility, leading to quadrupoles often being employed in questions regarding quantification. Especially in a triple quadrupole (QqQ) setup, where three quadrupoles are linked in succession with the second one employed as a collision cell for fragmentation, this effect is enhanced as multiple different scan modes can be employed. The duty cycle (the time it takes to complete a particular scan operation) of QqQ can be very low when filtering for limited amounts of analytes. This means, multiple data points can be collected over a chromatographic peak when coupled to online LC separation and the resulting extracted ion chromatogram can then be integrated and used to quantitate analytes with the help of reference standards.

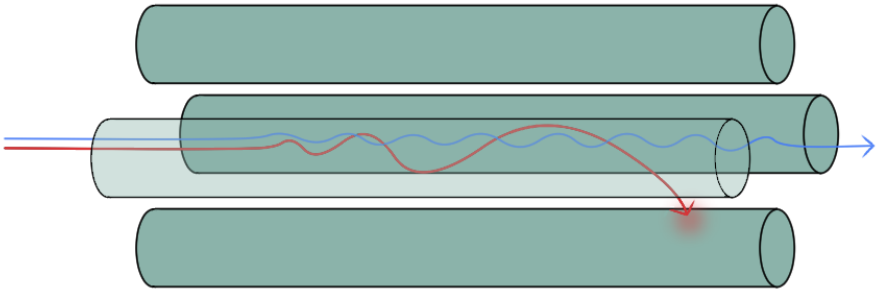

Figure 3. Schematic construction of a quadrupole. The red arrow represents an ion that does not meet the requirements set by DC and RF current for a stable trajectory and experiences more and more deflection as it passes through the quadrupole. The ion on the blue path is currently being monitored and therefore has perfect conditions to pass to the detector.

1.4.3 Fragmentation

Structurally different molecules can still exhibit the same mass (isobaric) and therefore even in high-resolution mass spectrometry, a differentiation based on mass alone is often inadequate. Ions can be subjected to controlled fragmentation processes, breaking the analyte apart in a characteristic manner and thereby providing additional information about the fragmented ion and its structure. The fragments created by this process can then again be subjected to additional mass selection. This is referred to as tandem mass spectrometry, MS/MS or MS^n with *n-1* being the number of fragmentation steps (>2 only available in ion trapping devices).

In the case of triple quadrupoles, the second quadrupole (or often a hexapole/octapole nowadays) is filled with an inert gas (e.g. nitrogen, argon). By accelerating the ions passing through the first quadrupole (Q1), a specific kinetic energy is added to them as they enter the second quadrupole (Q2). A part of this energy is converted to inner energy (vibration/rotation) upon impact with the inert gas particles, eventually leading to chemical bonds within the analyte (parent ion) breaking and causing the creation of the respective fragments (product ions). The third quadrupole (Q3) can then again filter or scan for those fragments, passing them to the detector for a signal. This enables a wide array of options and scan modes as outlined in Tab. 2. However, devices can be vastly different in collision cell and accelerator geometry, used inert gas, its respective pressure and otherwise, depending on the manufacturer. This makes transferring optimized measurement parameters between different instruments extremely difficult.

Table 2. Scan modes available to QqQ instruments and their operation principle.

Scan mode	Description
Product Ion Scan	Q1 is set to filter a constant *m/z*, while Q3 scans for all fragments of the isolated ions. This gives more information on the target compound by showing what constituents it breaks apart into.
Precursor Ion Scan	Q3 is set to filter a constant m/z, while Q1 scans a wide range of potential precursors. If a certain functional group is known to create intense fragments, this mode can help find compounds carrying said group in unknown mixtures.
Neutral Loss Scan	Q1 scans a defined m/z range while Q3 scans another m/z range corresponding to Q1 minus the mass of a fragment known to depart from the precursor as a neutral particle (e.g. H_2O or NH_3).
Selected/Multiple Reaction Monitoring (SRM/MRM)	Q1 filters for a specific precursor, while Q3 filters for a specific product of this precursor. These precursor/product pairs are called transitions and enable high selectivity. It is the standard mode used for quantitation. In SRM only one product ion is monitored while in MRM multiple products are scanned to further increase selectivity. Usually only the most intense product ion peak is used for integrative quantitation (quantifier ion) while additional fragments are used as further proof of identification (qualifier ions). Specifying scan windows on the basis of retention time further increases sensitivity, as scans for given analytes are only executed when they can be expected to elute from online methods. This is referred to as scheduled SRM/MRM (sSRM/sMRM).

1.4.4 Detectors

The oldest detectors for MS were physical, photoactive plates. The ions were dispersed along the entire length of the plate according to their m/z and could then be analysed after the experiment. Of course, with the dawn of the digital age the photoplate detector became obsolete very quickly for

almost all applications and is only very sparsely found today in spark source MS. More often found than photoplates today, are faraday cups that collect charged particles and relay the signal gathered from the discharge on their walls. They are robust and reliable in design, but are lacking in sensitivity, often requiring very strong amplification of the low signal strength.

The most common detectors used today in MS are electron multiplier dynodes, which are secondary electron emission electrodes that are impacted by incoming ions and cause a number of electrons to be released. Through the geometry of the detector and potential gradients, the same event is repeated multiple times. The anode at the end is finally reached by a cascade of electrons, resulting in a heavily amplified signal. These dynodes can be arranged in multiple different ways, such as discretely lined up elements, continuous, bent tubes or in multichannel plates featuring many hollow, cylinder-like channels. All have their advantages and disadvantages, and which one is used often depends on the compatibility with the mass analyser to create the best signal possible and introduce minimal noise.

1.5 Coupling reactions and synthesis-based reverse metabolomics

Due to the great importance of peptides in biological chemistry, a vast amount of research has been conducted on the efficient creation of amide bonds between two amino acid residues.[40] Often, amide bonds can also be found in important pharmaceutical drugs as well.[41–43] In most cases, these coupling procedures involve the activation of the carboxyl group by introducing an electron-withdrawing group, followed by the subsequent attack from the amino group to form an amide. Spontaneous elimination of water from carboxylic acids to enable this attack without activation is possible, but requires high temperatures that are damaging to many substrates.[44] The reactions are usually very similar and preferred reagents depend on multiple factors, such as employed solvents, desired stability of intermediates and inhibition of side reactions.[40] However, critical evaluation on the topic is often lacking due to the sheer amount of available reagents that are sparsely tested against each other.[45]

Carbodiimides such as dicyclohexylcarbodiimide (DCC) or N-(3-Dimethylaminopropyl)-N'-ethylcarbodiimide (EDC) are some of the most well-known coupling reagents.[46] Carboxylic acids are quick to react with carbodiimides and form O-acylisourea intermediates that then react with amines to form the desired products (Fig. 4). However, due to their high reactivity, many side reactions can occur, reducing yield and introducing impurities.[47] One potential measure to avoid those side reactions are additives like for example 1-hydroxy-7-azabenzotriazole.[48]

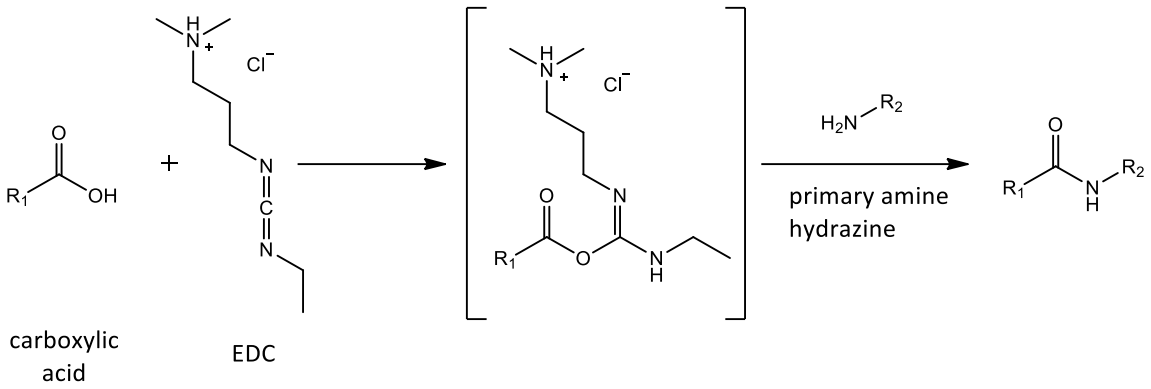

Figure 4. Reaction equation for the activation of a carboxylic acid with EDC and subsequent attack by a primary amine or hydrazine. The reaction is very fast and can lead to multiple side products that are not shown.

Another different coupling method, utilizing triphenylphosphine (TPP) and 2,2'-dipyridyldisulfide (DPDS), dates back to a discovery by Mukaiyama in 1971.[49] These reagents have been used in a variety of other studies, mostly for the derivatization of carboxylic acids with fluorescence markers or moieties that result in very intense fragments in tandem MS.[50–52] The reagents function very well in organic solvents such as acetonitrile and are therefore ideal for reactions with molecules that have poor water solubility like bile acids.[51] The mechanism behind the reaction is detailed in Fig. 5.[53] TPP and DPDS form a complex leading the central phosphorus to create a reactive intermediate with the carboxyl group. This enables the attack by primary amines or hydrazines forming the amide bond, while the phosphine is being eliminated as an oxide.

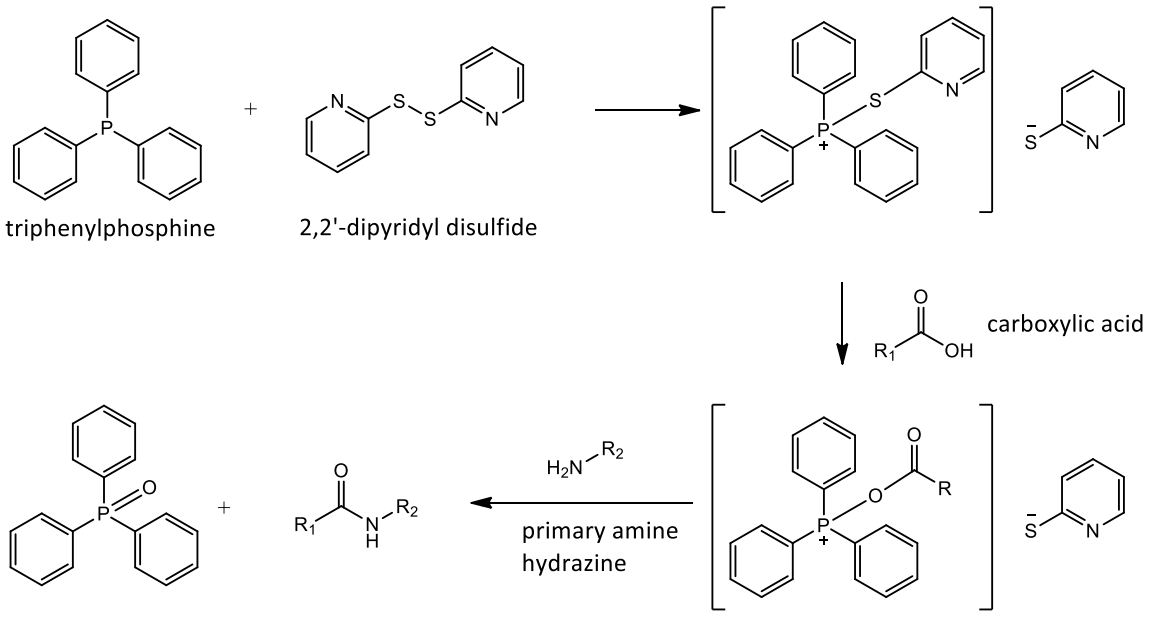

Figure 5. Reaction mechanism of the formation of an amide bond between a carboxylic acid and a primary amine after activation via TPP and DPDS.

The indiscriminate nature and easy execution of these coupling reactions, creating simple bonds between similar molecules, opens up an interesting angle for the quick investigation into suspected metabolites, as outlined by Dorrestein *et al*.[33] Their approach, coined under the name "synthesis-based reverse metabolomics" aims to leverage synthetic means to create highly likely but unconfirmed metabolites. These synthesis products can then be used to generate MS/MS fragment spectra and gain the necessary information to conduct experiments or search public databases on matches pertaining to the new structures. Given that only around 2% – 10% of MS features found in metabolomics studies can be annotated to known structures, the chance to find new compounds of interest through this innovative technique may well be worth the time investment.[54] As a demonstration of the principle, the group of Dorrestein *et al.* synthesized various bile acid – amino acid conjugates (BA-AAs) inspired by recent discoveries.[31,55] The procedure was simple and fast, yielding more than 16,000 matching results in public metabolomics databases using the mass spectrometry search tool MASST.[56]

Combining the results of public metabolomics database searches with the respective metadata of the data sets (e.g. sample origin, health status, matrix, etc.) can give insight into potential correlations with certain diseases and further increase the pool of compounds of interest.[57] Of course, even in the event that novel metabolites are found in this manner, further research into their *in vivo* creation, role and possible mode of action is needed. This idea merely constitutes a different approach to conventional methods of structure elucidation, which require compound isolation from the sample and lack the throughput necessary to keep up with modern omics workflows.[33]

2 Aims and objectives

The overall aim of this work was the development of a LC-MS/MS method for the semi-quantitation of recently described bile acid amino acid conjugates and the application of the resulting method to biological samples in proof-of-principle experiments. The scope of this work concisely summarized extends to the following points:

1. Development and optimization of an effective batch synthesis procedure for the creation of the desired bile acid amino acid conjugate reference standards that are required for the development of the LC-MS/MS method and as reference standards during measurements.

2. Establishment and optimization of an LC-MS/MS method able to separate isobaric bile acids and their respective isobaric conjugates.

3. Application of the developed and optimized method on plasma and fecal samples obtained from a cohort of extremely premature infants to explore possible connections between pathological development and the bile acid conjugate profiles in further studies.

3 Materials and methods

3.1 Chemicals

Water (LC-MS grade) was purchased from VWR Chemicals, while ACN and MeOH (LC-MS grade) were purchased from Honeywell Riedel de-Haën. Formic acid (FA) from ScienTEST/Promochem was used as an additive in the HPLC Eluents. Cholic acid (CA), deoxycholic acid (DCA), ursodeoxycholic acid (UDCA), hyodeoxycholic acid (HDCA), chenodeoxycholic acid (CDCA) and lithocholic acid (LCA) were all purchased from Sigma-Aldrich. Taurine was also purchased from Sigma-Aldrich and dissolved in Water (200 mM). Unprotected amino acids used in the synthesis of conjugates were thankfully received from the Department of Biological Chemistry, University of Vienna. As for the coupling reagents, both triphenylphosphine (TPP) and 2,2'-dipyridyldisulfide (DPDS) were purchased from Sigma-Aldrich. Isotopically labeled d4-ursodeoxycholic acid, used as an internal standard, was purchased from Cambridge Isotope Laboratories at a concentration of 100 µg/mL in MeOH.

3.2 Synthesis of bile acid amino acid conjugates

A schematic overview of the process can be seen in Fig. 6. Where possible, amino acids were dissolved in pure Water to yield stock solutions of 100 mM which were later diluted during the creation of mixes for the batch synthesis of conjugates. Solutions of the coupling reagents TPP and DPDS were freshly prepared to a concentration of 10 mM before every synthesis. From the AA and Taurine stock solutions as outlined above, two mixes with 10 AAs each were created to separate isobaric molecules (Tab. 3). Concentration of each AA and Taurine within the mixes was 2 mM. Batches for tuning were created by incubating 40 µL of one bile acid (2.5 mM) with 40 µL each of 10 mM TPP and DPDS for 1 min after vortexing, following the addition of 5 µL AA Mix and 75 µL ACN. The reaction volumes were left on a Thermo-Shaker (TS-100, Biosan) at 60 °C for 30 min. Then, 300 µL of ACN were added. In total, this yielded 12 batches of BA-AAs (six different bile acids with two mixes each). Taurine conjugates were synthesized in the same manner. From each batch 150 µL were combined and the resulting mixture evaporated and reconstituted in 150 µL ACN to act as a concentrated standard mix that could be used for LC-method development and for the creation of a spiked matrix sample for quality control (QC).

Table 3. Mixtures that were used in the batch synthesis of conjugates. Gln and Lys, Leu and Ile, and Asn and Orn have indistinguishable m/z values on low resolution MS instruments and had to be separated for the procedure to be effective.

Mix "AA1"	Mix "AA2"
Ala	Asp
Arg	Glu
Asn	Gly
Gln	Ile
His	Lys
Leu	Orn
Met	Tau
Phe	Trp
Ser	Tyr
Thr	Val

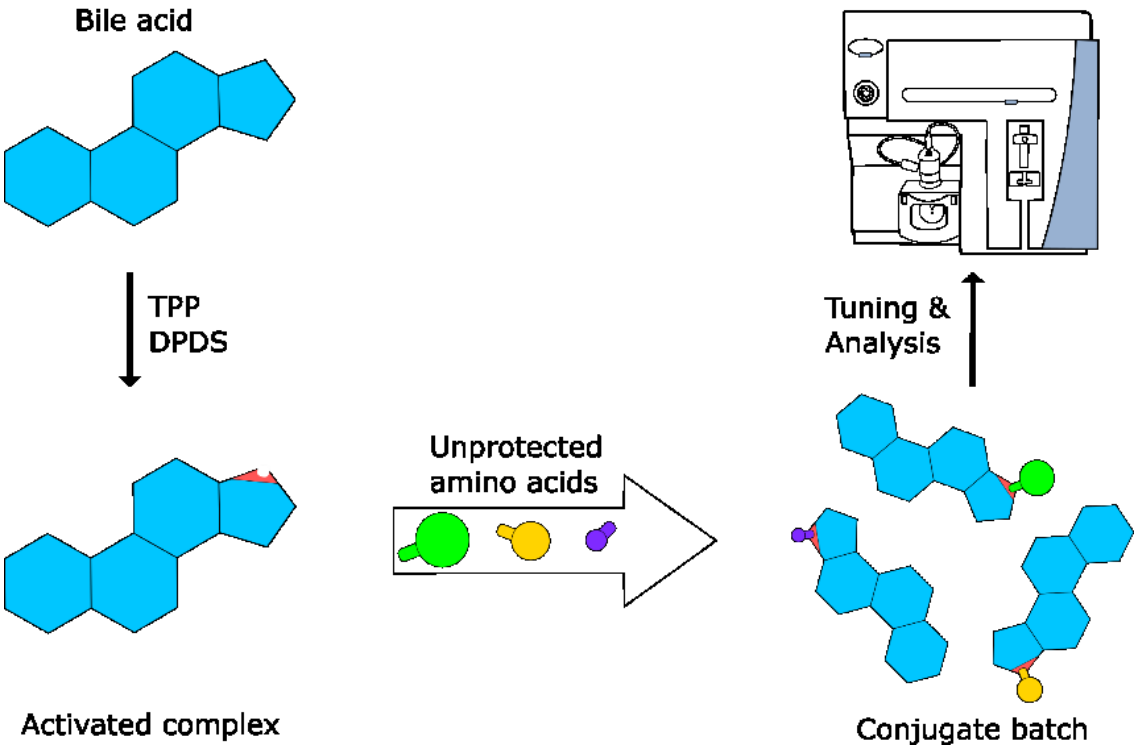

Figure 6. Schematic overview of the batch synthesis process, featuring the activation of a bile acids, followed by subjecting the activated complex to multiple amino acids to form a mixture of conjugates that could then be tuned and analyzed on the TSQ Vantage triple quadrupole mass spectrometer.

3.3 Tuning of analytes and development of MRM method

Using a T-piece, complementary LC-flow (0.2 mL/min) was added to the syringe pump operated at 10 µL/min to minimize use of standard material and simulate conditions closer to chromatographic separation runs. Capillary and vaporizer temperatures, as well as ESI gas parameters were automatically optimized on a model compound (cholic acid) and left constant over all analytes, as they cannot be adjusted quickly enough during a run to apply to the MRM windows. Mass to charge ratios corresponding to the expected $[M-H]^-$ ions of each conjugate were scanned for in MS1 in negative mode. After confirming a signal of adequate intensity and stability, an automatic adjustment of the S-Lens to maximize intensity was followed by a scan for a maximum of 8 product ions, spanning a range of 5 to 50 eV collision energy in 10 steps, for each conjugate. Common fragmentation patterns included elimination of the bile acid, elimination of the amino acid and further fragmentation of the amino acid to recognized patterns in literature.[58] The data from the resulting tuning files was then used to create a MRM method file where retention times and windows could be adjusted along with the development process. As a minimum of two transitions (quantifier and qualifier ions) is usually desirable in MRM methods, the two most intense product ions of each conjugate were chosen. In rare cases only one truly abundant product ion could be determined. The detailed transition list can be found in section 4 (Tab. 4).

3.4 Sample origin and sample preparation

The samples used for the proof-of-principle experiments were obtained from a cohort of extremely premature infants from the Medical University of Vienna and constitute the main body of research for other projects. Within the cohort there were two groups, one with pathological neurophysiological development (PAT) and one with age-adequate neurophysiological development (CTR).[59] The aim of the project was to investigate both groups in regard of relative abundance of bile acids and their amino acid conjugates. As samples were taken at days 3, 7 and 28 after birth and upon reaching term age, these samples also have the advantage of showing potential changes in accordance with time.

The matrix extracts that were spiked with concentrated conjugate mix to be used as quality control were obtained from commercially available pooled plasma and infant feces samples kindly provided by Dr. Lukas Wisgrill from the Medical University of Vienna. These samples were prepared in the same manner as the premature infant samples, detailed below.

3.4.1 Sample preparation of plasma samples

The infant plasma samples had already been extracted for a different experiment and aliquots had been prepared for measurements using the method described in this work. The extraction protocol that was used is described as follows: Prior to extraction, samples were stored at -80 °C and then kept on ice during the entire process. After vortexing, 200 µL of extraction solvent (ACN/MeOH, 1:1 v/v) were added to 50 µL sample. In some cases of limited sample material, a smaller volume of <50 µL had to be used while keeping the sample to solvent ratio the same (1:4). Following additional vortexing, the samples were sonicated in an ice bath for 15 min. Samples were stored at -20 °C overnight to facilitate protein precipitation. Supernatants of samples were transferred to a new tube after centrifugation at 18,000g and 4 °C for 10 min. At this point, aliquots for the bile acid conjugate experiments were taken and stored at -80 °C. Prior to measurement, d4-UDCA was added to every sample as internal standard to a final concentration of 2 µM. Afterwards the samples were transferred to LC vials and stored at -80 °C until measurement.

3.4.2 Sample preparation of fecal samples

The wet feces samples were first dried over a weekend on a SpeedVac concentrator (Labconco) at 4 °C. For each mg of dried feces sample, 25 µL of water was added to the sample. The samples were homogenized using a bead shaker (4 m/s, MP FastPrep-24 5G) for 10 seconds. Following centrifugation at 18,000g and 4 °C for 10 min, a volume equaling half the water added before homogenization was removed and frozen immediately for further biochemical assays. ACN/MeOH (1:1, v/v) at a volume equaling 4 times that of the remaining water was added to the tube containing the sample residue and again homogenized using a bead shaker (4 m/s, MP FastPrep-24 5G) for 10 seconds. Afterwards the samples were sonicated in an ice bath for 10 min and stored at -20 °C overnight to facilitate protein precipitation. After centrifugation at 18,000g and 4 °C for 10 min, the supernatants were transferred to new tubes and evaporated using the SpeedVac concentrator (Labconco) at 4 °C. The dried samples were reconstituted back to the original volume using a mixture of H_2O/ACN/MeOH (1:2:2 v/v) including the internal standard d4-UDCA (2 µM). All samples were once again vortexed and sonicated in an ice bath for 10 min and centrifuged at 18,000g and 4 °C for 10 min. The supernatants were transferred to LC vials and stored at -20 °C until measurement.

3.5 Analysis

3.5.1 LC-MS/MS analysis

Measurements were performed using a Dionex Ultimate 3000 UHPLC system coupled to a TSQ Vantage triple quadrupole mass spectrometer, operated with a heated electrospray ionization source (HESI; Thermo Scientific, Vienna, Austria). Sequences were created using the software "Xcalibur", which also served as a communication tool between the systems. Chromatographic separation of the compounds was achieved on an Atlantis T3 column (3 µm, 3 mm × 150 mm) equipped with a VanGuard precolumn (3 µm; Waters, Vienna, Austria). The column oven was maintained at 40 °C, while the autosampler was kept at 5 °C. All solvents used for mobile phases were of LC-MS grade quality. Eluent A was water with 0.1% formic acid. Eluent B was a mixture of acetonitrile and methanol (1:1, v/v) with 2% water and 0.1% formic acid. The total run time of the method was 21 min with a flow rate of 0.6 mL/min following a gradient as described: 0–1 min at 5% B; rise to 50% B until 1.5 min; rise to 95% B until 10 min; 10–13 min at 95% B; sharp drop to 75% B min and maintain until 19 min; re-equilibrate at 5% B until 21 min. Negative ESI mode was used to acquire the scheduled multiple reaction monitoring (sMRM) data. The ion source parameters were as follows: Capillary temperature of 300 (°C), vaporizer temperature of 300 (°C), sheath gas pressure of 40 (Arb), aux valve flow of 10 (Arb), declustering potential of 14 (V), collision gas pressure of 1.5 (mTorr) and a spray voltage of 3000 (V). Scan windows for all compounds were set according to expected drift. The cycle time was set to 0.600 (s), while Q1 and Q3 peak width was kept at 0.7 (FWHM). To reduce introduction of unwanted pollution into the MS system, a divert valve was used that switched all flow directly to waste from 0.5-2.5 min.

3.5.2 Evaluation of LC-MS/MS data

The evaluation of the resulting peaks in the MRM-Chromatograms was done using Skyline (MacCoss Lab Software, 21.1.0.568).[60] Many signals found were at very low intensity close to noise level, indicating low concentrations in vivo. Since this method was developed with self-synthesized standards of unknown purity and concentration (more details in section "Batch synthesis viability") for semi-quantitation, absolute quantitative results could not be obtained. For qualitative evaluation, arbitrary requirements were enacted for a peak to be viable, namely a minimum peak height of 1.0E2 and the presence of all transitions in similar ratio to QCs. The peak picking was manually checked for all analytes in all samples to ensure correct peak integration.

4 Results and discussion

4.1 Batch synthesis viability and limitations

The idea to synthesize conjugates in batches rather than single steps was originally pursued to simplify synthesis and increase time efficiency. Since a similar procedure had already been successfully applied in other work, confidence in a favorable outcome was high.[33] A major concern, however, was the use of unprotected amino acids. Amino acids, by nature of their composition, feature both a carboxyl group and an amino moiety on the same molecule. Simple coupling reactions aim at the activation of a carboxyl group for the subsequent attack of an amine to occur. This fact was thought to make unprotected amino acids prone to polymerize in presence of the employed coupling reagents. One preventive measure to control this behavior as much as possible, was keeping the excess of activation reagents low. This appeared to be sufficient, as no significant amounts of byproducts could be detected. As cysteine features a comparatively reactive thiol group and it has been shown in other work that conjugates of cysteine are very rare and appear irrelevant, it was excluded from the batch synthesis process and the method itself.[33] A different strategy that could be sought out in the future in hopes for higher yields could be the use of carbodiimides with N-hydroxysuccinimide to create an activated, dry-stable bile acid intermediate that can be isolated, reconstituted and then react with amino acids without fear of polymerization.[61]

The need for two separate amino acid mixtures, rather than one mixture encompassing all conjugating molecules, was unavoidable, as the method was developed for low resolution mass spectrometry. The difference in mass of the amino acids Gln and Lys, as well as Asn and Orn is very small and the separation on mass alone would require high resolution mass spectrometers. Even in the case of high resolution MS the isomeric bile acids CDCA, DCA, HDCA and UDCA and their conjugates would have to be prepared seperately, as they share exact same mass without distinct fragments.[62] Nontheless, being able to prepare 2 mixes rather than 20 single step reactions already constitutes a significant improvement in terms of time and efficiency.

4.2 LC-MS/MS method optimization

4.2.1 MS tuning of bile acids and their respective conjugates

Overall, the tuning of the synthesized conjugates from the mixtures proved to be without major problems and validates the process as done by the Dorrestein lab at UCSD, CA. For specific amino acids however, the signals of the conjugates in mixture were not sufficient to extract fragment patterns so that single synthesis had to be employed, as was the case for Asn, Asp and Glu. Whether this is due to lower synthetic yields through competition or change in ionization capability of the resulting conjugates could not been evaluated for sure. Some other conjugates that were deemed problematic, namely Trp-CA, Tyr-CA, Ala-UDCA, Ser-UDCA and Thr-UDCA, were also re-synthesized in single steps to check the integrity of the values obtained from the batch synthesis mixtures. In all cases the major fragments were the same in the resulting tuning files of both single and batch synthesis, further confirming viability of the batch synthesis approach. The full transition list can be found in Tab. 4.

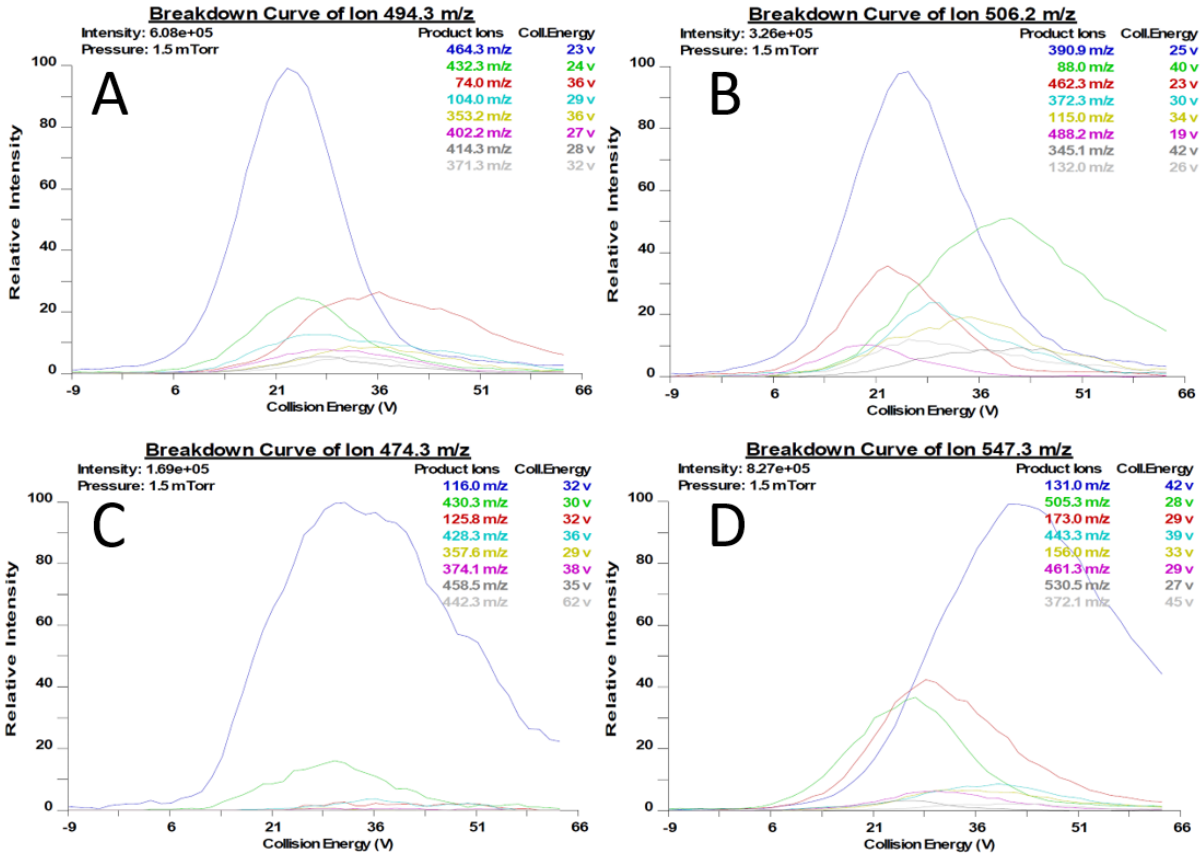

Figure 7. A selection of breakdown curves obtained from the tuning process, showing the most viable product ions and their optimal collision energies for a given compound. **A:** Ser-CA, **B:** Asp-DCA, **C:** Val-LCA, **D:** Arg-UDCA

Table 4. All analyte-specific LC-MS/MS-Parameters used in the method, including compound names, abbreviation, retention time (RT), m/z of precursor and product ions in negative ESI mode, collision energy (CE) and S-Lens values.

Compound	Abbr.	RT	Precursor	Product	CE	S-Lens
		min	m/z	m/z	eV	
(4,4,2,2)-d4-Ursodeoxycholic acid	d4-UDCA	8.68	395.2	395.2/377.2/349.2	0/26/33	192
Cholic acid	CA	9.38	407.2	407.2/343.2	0/35	135
Alanocholic acid	Ala-CA	8.34	478.2	416.3/88.0	15/18	135
Arginocholic acid	Arg-CA	5.13	563.3	173.0/131.0	28/46	210
Asparaginocholic acid	Asn-CA	7.27	521.3	406.2/96.0	24/26	184
Aspartocholic acid	Asp-CA	7.70	522.2	407.2/88.0	27/42	125
Glutaminocholic acid	Gln-CA	7.32	535.3	127.0/109.0	26/42	127
Glutamocholic acid	Glu-CA	7.69	536.2	407.2/127.9	28/25	90
Glycocholic acid	Gly-CA	8.08	464.2	402.2/74.0	27/36	140
Histidocholic acid	His-CA	5.18	544.3	154.0/110.0	34/42	129
Iso-/Leucholic acid	Ile/Leu-CA	9.78	520.3	458.3/456.3/130.0	29/34/32	124
Lysocholic acid	Lys1-CA	6.22	535.2	467.1/145.0	22/41	127
	Lys2-CA	5.05	535.2	467.1/145.0	22/41	127
Methionocholic acid	Met-CA	9.12	538.3	446.3/148.0	26/28	197
Ornithocholic acid	Orn1-CA	6.20	521.3	459.2/353.4/131.0	27/26/40	125
	Orn2-CA	5.11	521.3	459.2/353.4/131.0	27/26/40	125
Phenylalanocholic acid	Phe-CA	9.87	554.3	164.0/147.0	31/43	194
Serocholic acid	Ser-CA	7.63	494.3	464.3/74.0	23/36	151
Taurocholic acid	Tau-CA	13.87	514.2	123.9/106.9	44/45	229
Threonocholic acid	Thr-CA	7.97	508.3	464.3/74.0	22/38	122
Tryptophanocholic acid	Trp-CA	9.33	593.2	464.3/203.0	29/31	179
Tyrosocholic acid	Tyr-CA	8.24	570.2	179.9/162.8	31/30	154
Valocholic acid	Val-CA	9.31	506.3	444.3/116.0	32/40	134
Chenodeoxycholic acid	CDCA	10.67	391.2	391.2/373.2/345.2	0/26/33	192
Alanochenodeoxycholic acid	Ala-CDCA	9.55	462.2	400.0/88.0	30/37	141
Arginochenodeoxycholic acid	Arg-CDCA	5.89	547.3	173.0/131.0	29/43	151
Asparaginochenodeoxycholic acid	Asn-CDCA	8.47	505.3	487.3/96.0	22/28	133
Aspartochenodeoxycholic acid	Asp-CDCA	8.89	506.3	391.1/88.0	26/38	127
Glutaminochenodeoxycholic acid	Gln-CDCA	8.52	519.3	127.0/109.1	32/44	124
Glutamochenodeoxycholic acid	Glu-CDCA	8.86	520.3	392.2/128.0	28/27	120
Glycochenodeoxycholic acid	Gly-CDCA	9.34	448.2	386.3/74.0	28/31	147
Histidochenodeoxycholic acid	His-CDCA	6.00	528.3	153.9/109.9	29/43	126
Iso-/Leuchenodeoxycholic acid	Ile/Leu-CDCA	10.77	504.3	442.3/430.4/130.0	31/24/34	128
Lysochenodeoxycholic acid	Lys1-CDCA	7.24	519.3	451.3/145.0	18/38	124
	Lys2-CDCA	5.86	519.3	451.3/145.0	18/38	124
Methionochenodeoxycholic acid	Met-CDCA	10.16	522.2	474.3/148.0	26/29	125
Ornithinochenodeoxycholic acid	Orn1-CDCA	7.18	505.3	461.3/443.3/131.0	27/29/32	128
	Orn2-CDCA	5.85	505.3	461.3/443.3/131.0	27/29/32	128
Phenylalanochenodeoxycholic acid	Phe-CDCA	10.79	538.3	164.0/147.0	31/42	139
Serochenodeoxycholic acid	Ser-CDCA	8.84	478.2	448.2/74.0	25/31	126
Taurochenodeoxycholic acid	Tau-CDCA	18.02	498.2	123.9/106.9	44/49	269
Threonochenodeoxycholic acid	Thr-CDCA	9.18	492.2	448.3/74.1	22/36	131
Tryptophanochenodeoxycholic acid	Trp-CDCA	10.34	577.2	448.1/202.9	26/32	136
Tyrosochenodeoxycholic acid	Tyr-CDCA	9.37	554.1	179.9/162.8	29/41	131

Compound	Abbr.	RT	Precursor	Product	CE	S-Lens
		min	m/z	m/z	eV	
Valochenodeoxycholic acid	Val-CDCA	10.35	490.2	428.3/116.0	32/32	131
Deoxycholic acid	DCA	10.84	391.2	391.2/373.2/345.2	0/26/33	192
Alanodeoxycholic acid	Ala-DCA	9.88	462.2	400.0/88.0	30/37	141
Arginodeoxycholic acid	Arg-DCA	6.13	547.3	173.0/131.0	29/43	151
Asparaginodeoxycholic acid	Asn-DCA	8.77	505.3	487.3/96.0	22/28	133
Aspartodeoxycholic acid	Asp-DCA	9.23	506.3	391.1/88.0	26/38	127
Glutaminodeoxycholic acid	Gln-DCA	8.86	519.3	127.0/109.1	32/44	124
Glutamodeoxycholic acid	Glu-DCA	9.20	520.3	392.2/128.0	28/27	120
Glycodeoxycholic acid	Gly-DCA	9.63	448.2	386.3/74.0	28/31	147
Histidodeoxycholic acid	His-DCA	6.26	528.3	153.9/109.9	29/43	126
Iso-/Leudeoxycholic acid	Ile/Leu-DCA	11.13	504.3	442.3/430.4/130.0	31/24/34	128
Lysodeoxycholic acid	Lys1-DCA	7.53	519.3	451.3/145.0	18/38	124
	Lys2-DCA	6.07	519.3	451.3/145.0	18/38	124
Methionodeoxycholic acid	Met-DCA	10.53	522.2	474.3/148.0	26/29	125
Ornithinodeoxycholic acid	Orn1-DCA	7.50	505.3	461.3/443.3/131.0	27/29/32	128
	Orn2-DCA	6.10	505.3	461.3/443.3/131.0	27/29/32	128
Phenylalanodeoxycholic acid	Phe-DCA	11.14	538.3	164.0/147.0	31/42	139
Serodeoxycholic acid	Ser-DCA	9.27	478.2	448.2/74.0	25/31	126
Taurodeoxycholic acid	Tau-DCA	19.02	498.2	123.9/106.9	44/49	269
Threonodeoxycholic acid	Thr-DCA	9.56	492.2	448.3/74.1	22/36	131
Tryptophanodeoxycholic acid	Trp-DCA	10.63	577.2	448.1/202.9	26/32	136
Tyrosodeoxycholic acid	Tyr-DCA	9.66	554.1	179.9/162.8	29/41	131
Valodeoxycholic acid	Val-DCA	10.73	490.2	428.3/116.0	32/32	131
Hyodeoxycholic acid	HDCA	9.08	391.2	391.2/373.2/345.2	0/26/33	192
Alanohyodeoxycholic acid	Ala-HDCA	7.83	462.2	400.0/88.0	30/37	141
Arginohyodeoxycholic acid	Arg-HDCA	4.75	547.3	173.0/131.0	29/43	151
Asparaginohyodeoxycholic acid	Asn-HDCA	6.63	505.3	487.3/114.0/96.0	22/35/28	133
Aspartohyodeoxycholic acid	Asp-HDCA	7.10	506.3	391.1/88.0	26/38	127
Glutaminohyodeoxycholic acid	Gln-HDCA	6.72	519.3	127.0/109.1	32/44	124
Glutamohyodeoxycholic acid	Glu-HDCA	7.20	520.3	392.2/128.0	28/27	120
Glycohyodeoxycholic acid	Gly-HDCA	7.50	448.2	386.3/74.0	28/31	147
Histidohyodeoxycholic acid	His-HDCA	4.76	528.3	153.9/109.9	29/43	126
Iso-/Leuhyodeoxycholic acid	Ile/Leu-HDCA	9.31	504.3	442.3/430.4/130.0	31/24/34	128
Lysohyodeoxycholic acid	Lys1-HDCA	5.73	519.3	451.3/145.0	18/38	124
	Lys2-HDCA	4.71	519.3	451.3/145.0	18/38	124
Methionohyodeoxycholic acid	Met-HDCA	8.61	522.2	474.3/148.0	26/29	125
Ornithohyodeoxycholic acid	Orn1-HDCA	5.60	505.3	461.3/443.3/131.0	27/29/32	128
	Orn2-HDCA	4.66	505.3	461.3/443.3/131.0	27/29/32	128
Phenylalanohyodeoxycholic acid	Phe-HDCA	9.33	538.3	164.0/147.0	31/42	139
Serohyodeoxycholic acid	Ser-HDCA	6.96	478.2	448.2/74.0	25/31	126
Taurohyodeoxycholic acid	Tau-HDCA	10.01	498.2	123.9/106.9	44/49	269
Threonohyodeoxycholic acid	Thr-HDCA	7.38	492.2	448.3/74.1	22/36	131
Tryptophanohyodeoxycholic acid	Trp-HDCA	8.87	577.2	448.1/202.9	26/32	136
Tyrosohyodeoxycholic acid	Tyr-HDCA	7.82	554.1	179.0/162.8	29/41	131
Valohyodeoxycholic acid	Val-HDCA	8.80	490.2	428.3/116.0	32/32	131
Lithocholic acid	LCA	11.97	375.2	375.2/357.2	0/33	169
Alanolithocholic acid	Ala-LCA	10.88	446.3	402.2/88.0	25/34	148
Arginolithocholic acid	Arg-LCA	6.90	531.3	173.0/131.0	30/43	183

Compound	Abbr.	RT	Precursor	Product	CE	S-Lens
		min	m/z	m/z	eV	
Asparaginolithocholic acid	Asn-LCA	9.85	489.3	471.3/114.0/96.0	25/28/40	132
Aspartolithocholic acid	Asp-LCA	10.30	490.2	374.3/88.0	31/32	131
Glutaminolithocholic acid	Gln-LCA	9.92	503.3	127.0/109.1	27/43	124
Glutamolithocholic acid	Glu-LCA	10.23	504.3	375.2/127.9	28/28	128
Glycolithocholic acid	Gly-LCA	10.68	432.2	388.4/74.0	24/25	154
Histidolithocholic acid	His-LCA	7.05	512.3	154.0/109.9	28/48	123
Iso-/Leulithocholic acid	Ile/Leu-LCA	11.94	488.3	444.3/414.2/130.0	28/37/37	132
Lysolithocholic acid	Lys1-LCA	8.46	503.3	357.1/145.0	35/34	128
	Lys2-LCA	6.86	503.3	357.1/145.0	35/34	128
Methionolithocholic acid	Met-LCA	11.41	506.2	458.3/148.0	23/26	127
Ornitholithocholic acid	Orn1-LCA	8.43	489.3	445.3/131.0	27/33	132
	Orn2-LCA	6.88	489.3	445.3/131.0	27/33	132
Phenylalanolithocholic acid	Phe-LCA	11.91	522.3	164.0/147.2	34/37	125
Serolithocholic acid	Ser-LCA	10.22	462.3	432.3/74.1	21/38	141
Threonolithocholic acid	Thr-LCA	10.55	476.3	432.3/74.1	20/32	135
Tryptophanolithocholic acid	Trp-LCA	11.42	561.3	432.4/203.0	24/28	133
Tyrosolithocholic acid	Tyr-LCA	10.62	538.3	179.9/162.8	29/48	128
Valolithocholic acid	Val-LCA	11.60	474.3	430.3/116.0	30/32	136
Ursodeoxycholic acid	UDCA	8.67	391.2	391.2/373.2/345.2	0/26/33	192
Alanoursodeoxycholic acid	Ala-UDCA	7.54	462.2	400.0/88.0	30/37	141
Arginoursodeoxycholic acid	Arg-UDCA	4.63	547.3	173.0/131.0	29/43	151
Asparaginoursodeoxycholic acid	Asn-UDCA	6.47	505.3	487.3/114.0/96.0	22/35/28	133
Aspartoursodeoxycholic acid	Asp-UDCA	6.89	506.3	391.1/88.0	26/38	127
Glutaminoursodeoxycholic acid	Gln-UDCA	6.51	519.3	127.0/109.1	32/44	124
Glutamoursodeoxycholic acid	Glu-UDCA	6.93	520.3	392.2/128.0	28/27	120
Glycoursodeoxycholic acid	Gly-UDCA	7.20	448.2	386.3/74.0	28/31	147
Histidoursodeoxycholic acid	His-UDCA	4.68	528.3	153.9/109.9	29/43	126
Iso-/Leuursodeoxycholic acid	Ile/Leu-UDCA	9.02	504.3	442.3/430.4/130.0	31/24/34	128
Lysoursodeoxycholic acid	Lys1-UDCA	5.53	519.3	451.3/145.0	18/38	124
	Lys2-UDCA	4.59	519.3	451.3/145.0	18/38	124
Methionoursodeoxycholic acid	Met-UDCA	8.36	522.2	474.3/148.0	26/29	125
Ornithoursodeoxycholic acid	Orn1-UDCA	5.43	505.3	461.3/443.3/131.0	27/29/32	128
	Orn2-UDCA	4.57	505.3	461.3/443.3/131.0	27/29/32	128
Phenylalanoursodeoxycholic acid	Phe-UDCA	9.03	538.3	164.0/147.0	31/42	139
Seroursodeoxycholic acid	Ser-UDCA	6.75	478.2	448.2/74.0	25/31	126
Tauroursodeoxycholic acid	Tau-UDCA	9.80	498.2	123.9/106.9	44/49	269
Threonoursodeoxycholic acid	Thr-UDCA	7.13	492.2	448.3/74.1	22/36	131
Tryptophanoursodeoxycholic acid	Trp-UDCA	8.66	577.2	448.1/202.9	26/32	136
Tyrosoursodeoxycholic acid	Tyr-UDCA	7.57	554.1	179.9/162.8	29/41	131
Valoursodeoxycholic acid	Val-UDCA	8.51	490.2	428.3/116.0	32/32	131

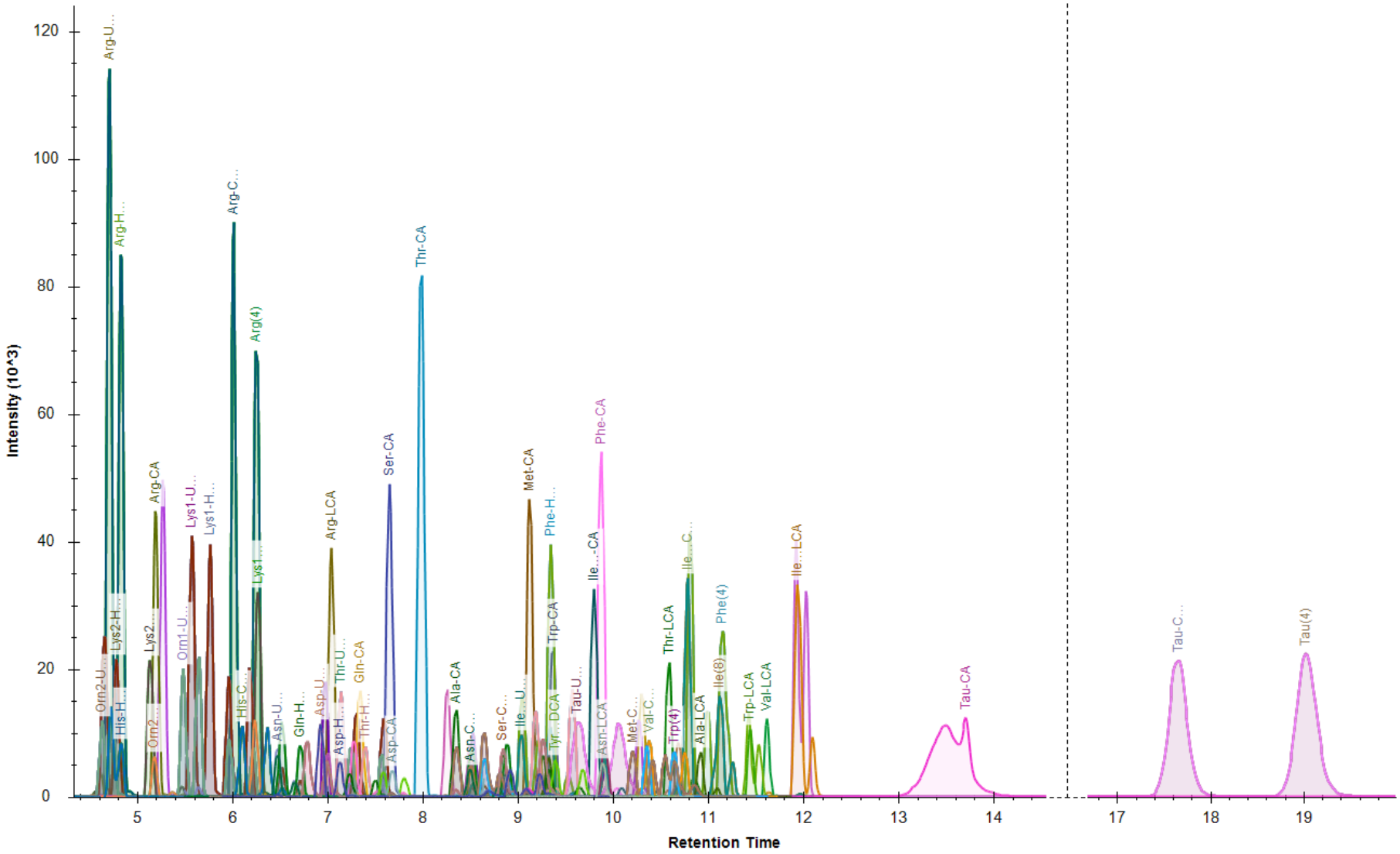

Figure 8. An extracted ion chromatogram of all 125 conjugates covered by the developed method from a multi-analyte reference standard.

4.2.2 Choice of column and eluents

A full list of tested columns and eluents can be found in Tab. 5. Columns and eluents were tested mostly on their potential to separate the isomeric conjugates formed by reaction of AAs with UDCA, HDCA, CDCA and DCA, as a separation simply by mass alone would be inadequate. A secondary factor was keeping the method runtime as short as possible. The Kinetex® column featured the best runtime but showed inadequate separation of isomers and was therefore quickly excluded. While the Acquity HSS T3 showed decent separation of isomers, the retention was also drastically higher than seen on the Kinetex®. A middle ground in runtime could be found in the Atlantis® T3, which in turn exhibited very good separation of isomers. Despite the only slightly shorter runtime necessary, likely caused by the greater column length, the Atlantis® T3 was eventually chosen over the Acquity HSS T3 for further testing.

The default solvent chosen for eluent A was water with 0.1% FA, which was also added in the same concentration to all organic eluents B that were tested. The 1:1 (v/v) mixture of methanol and acetonitrile displayed the best resolution for peaks of isomeric conjugates. This combination of solvents shifted the retention only slightly ahead over a pure acetonitrile phase and also featured the best separation (Fig. 9). As this phase still featured acetonitrile as a major component, water up to 2% of overall volume was added as a preventive measure to avoid acetonitrile polymer buildup on components of the HPLC pump, which can interfere with the HPLC system.[63,64]

Table 5. Tested columns and eluent systems for the separation of conjugates via LC before subsequent detection on the MS.

Tested columns	Tested eluents (B)
Phenomenex Kinetex® 2.6µm Biphenyl-phase, 100 Å (150 x 3 mm)	Methanol
Waters Acquity UPLC® HSS T3 1.8µm C18-phase, 100 Å (100 x 2.1 mm)	Acetonitrile
Waters Atlantis® T3 3µm C18-phase (150 x 3 mm)	2-Propanol/Acetonitrile (3:1 v/v)
	Methanol/Acetonitrile (1:1 v/v)

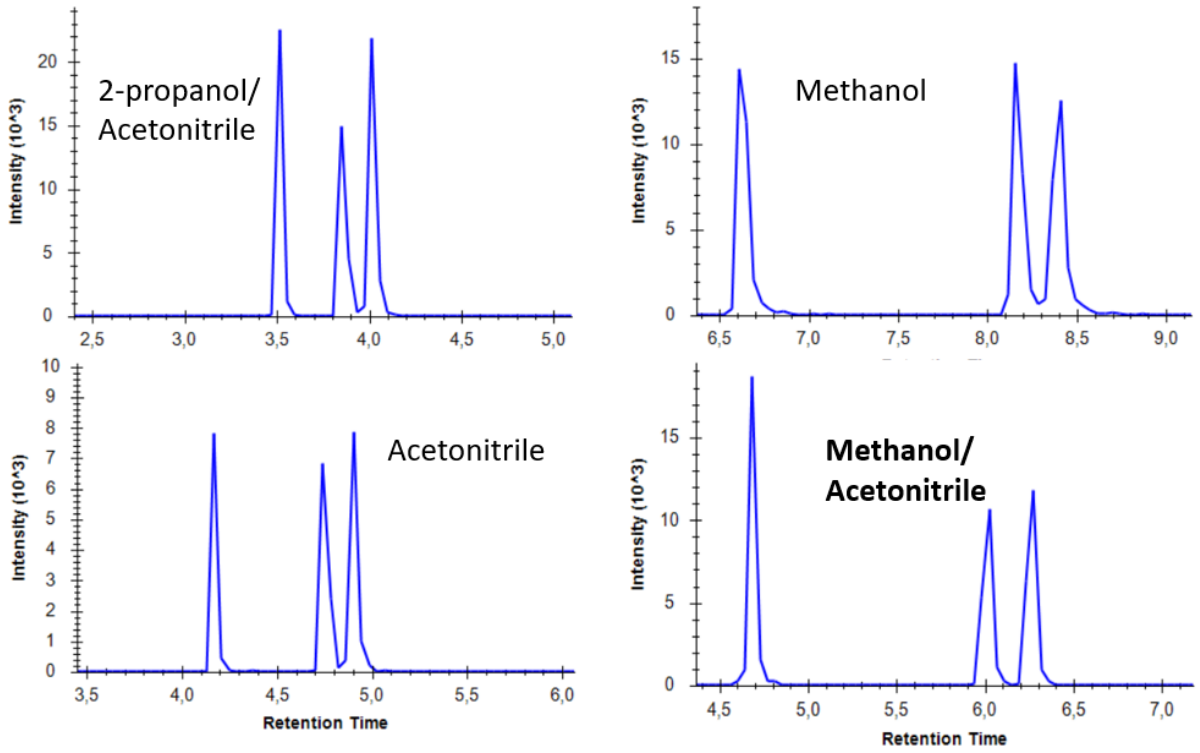

Figure 9. Comparison of chromatograms from dihydroxy bile acid-Arg conjugates. The methanol/acetonitrile mixture was the only eluent system to provide base line separation in initial experiments.

4.2.3 Optimization of flow rate and gradient

The chosen column and eluents (Atlantis® T3 with MeOH/ACN 1:1) were tested on flow rates ranging between 0.4 and 0.6 mL/min. The increase of the flow rate resulted in an expected shortening of retention time and sharpening of peak shapes across all analytes, while simultaneously retaining separation efficiency (Fig. 10). Even at the highest flow rate tested the back pressure throughout chromatographic runs was well within the allowed maximum limit of 400 bar, according to the manufacturer.[65] Therefore it was decided to adopt a flow rate of 0.6 mL/min for the method.

The optimization of the gradient was started from a linear increase from 5% to 95% B over 9 min. Even with this rudimentary test gradient, separation of dihydroxy BA conjugates could be achieved. This was very promising as it was the most important criterion for identification among these isomers. However, most conjugates eluted relatively late and none before 6.9 min. This was a likely and anticipated downside of choosing the longer Atlantis® T3 column over the Acquity HSS T3. Another factor contributing to the strong retention was likely the fact that amino acids and taurine are in most cases much smaller than the bile acids they are coupled to. This would indicate that the chemical properties of the sterol structure, which is fairly lipophilic, would be expected to predominate the conjugates behavior and its distribution among a given stationary and mobile phase.

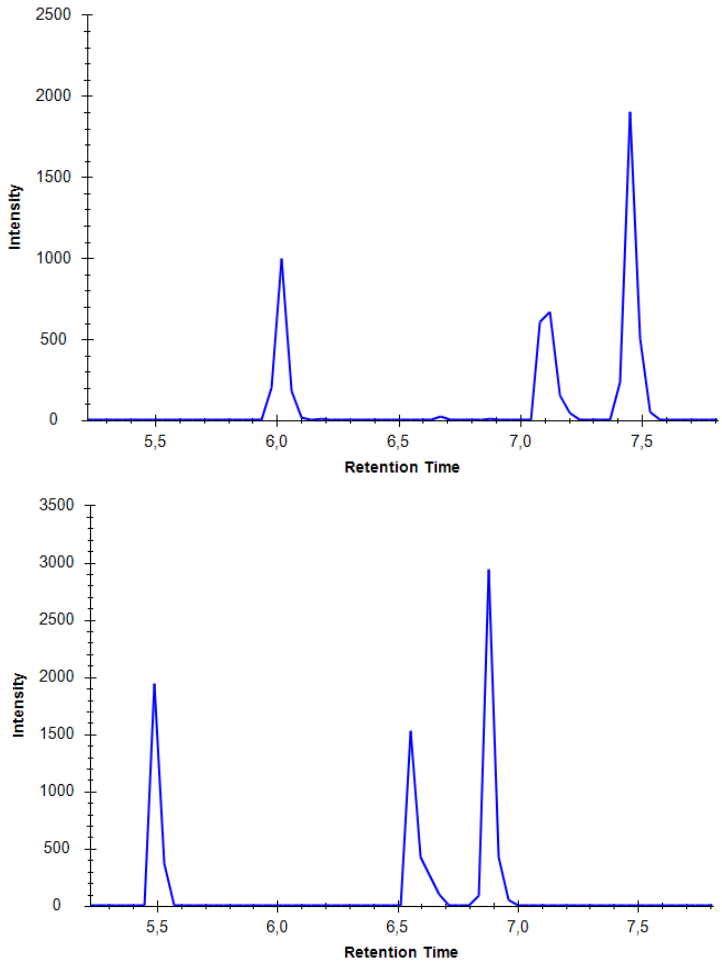

Figure 10. Comparison between a 0.5 (top) and 0.6 (bottom) mL/min flow rate chromatogram of dihydroxy BA-Ser conjugates on the Atlantis® T3. Peaks continue to be base line separated at higher flow rates while sharpening peak shape.

Given this, in an attempt to reduce run time for heightened throughput, a steep increase from 5% B at 1 min to 20-50% B within half a minute and then followed by a linear increase to 95% B until 10 min as before was tested. Even with 50% B starting at 1.5 min the separation of isobaric conjugates continued to be very good while shifting retention times forward by as much as 1.6 min with the last analyte at 11.9 min. As this represented a considerable improvement, the method was modified to include the steep rise to 50% B after the starting conditions.

4.2.4 Separation of isobaric analytes

Overall, all isobaric molecules that relied on chromatographic means to be split apart, could be separated successfully except for Ile and Leu conjugates. Therefore, the signals of Ile and Leu conjugates were evaluated as a combined product. In rare cases, the conjugates of the same amino acids coupled to HDCA and UDCA could not be completely baseline separated. This is true for Gln and His. The bile acids HDCA and UDCA are particularly similar, since their hydroxy groups are at the same

position and the only difference between them is in their α- or β-configuration. This fact is probably responsible for the observed relative closeness in elution between the conjugates of HDCA and UDCA. While this results in very close, not baseline separated peaks between Gln-HDCA and Gln-UDCA, or His-HDCA and His-UDCA, the overlap is inconsequential for the purpose of identification (Fig. 11). Also, in practice it does not really interfere with peak integration, therefore no significant effort was put into achieving perfect baseline separation in fear of compromising other aspects of the method.

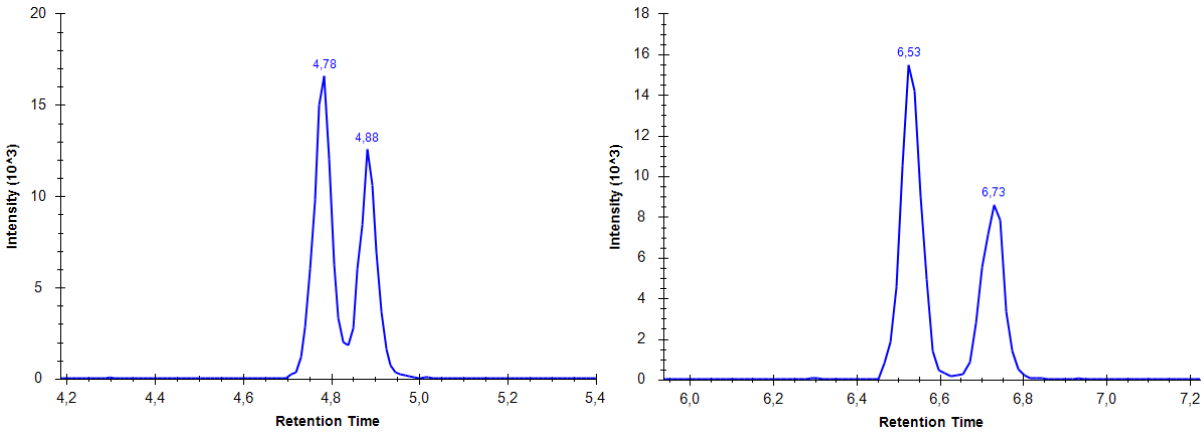

Figure 11. Chromatograms of His-UDCA and His-HDCA (left), as well as Gln-UDCA and Gln-HDCA (right). The separation is almost complete in the case of the Gln conjugates.

4.2.5 Elution pattern of bile acids and their respective conjugates

In essence, the coupling of a given amino acid to the different bile acids merely constitutes structural extension of the latter by the same element. As such, the pattern of elution among conjugates sharing the same amino acids was expected to mirror that of the base components. Indeed, this pattern was constant across all isobaric compounds, with conjugates of UDCA eluting first, followed by HDCA, then CDCA and finally DCA. Interestingly, UDCA and HDCA conjugates also consistently eluted before CA conjugates, despite the lack of a third hydroxy group, which was expected to be the largest contributor to the retention behavior. Contrary to that, conjugates of LCA, which only features one hydroxy group on its sterol backbone, consistently eluted last.

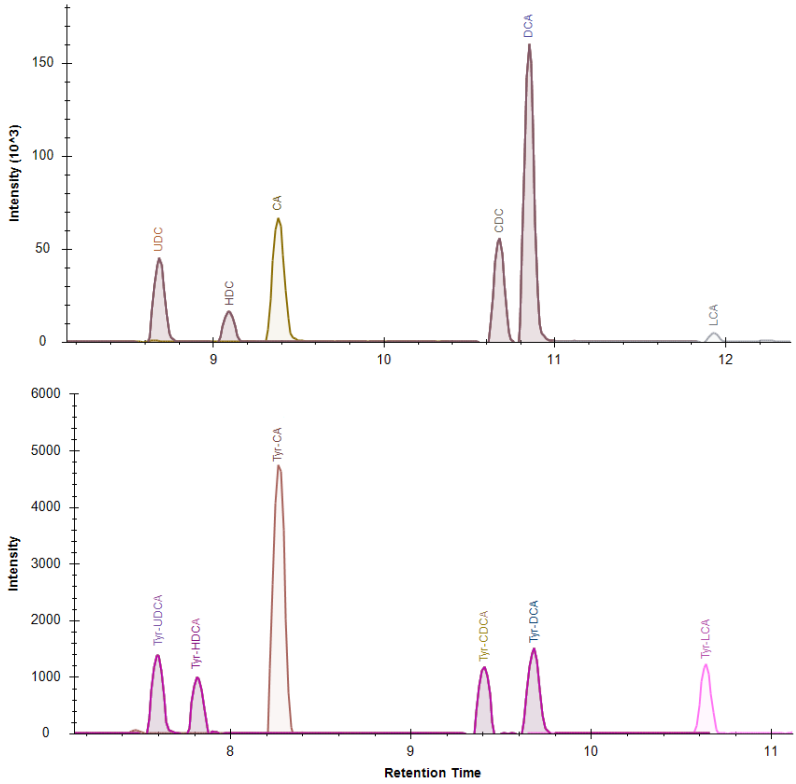

Figure 12. A comparison of native bile acid elution order compared to synthesized BA-AAs (Tyr). While there are slight offsets among the individual pairs, the order stays the same through all conjugates.

4.2.6 Taurine conjugates

Considerable work was spent on incorporating the Tau conjugates of the respective bile acids into the method. Similar to the Gly conjugates, these do not constitute new conjugates and are in fact a known part of the endogenous human bile salts. As such, interest was taken into their distribution in comparison to the new conjugates. While standards of certain Tau conjugates are actually commercially available, it also features an amine group that can be coupled to bile acids in the same manner as amino acids and so it was decided to integrate it into the mixtures for batch synthesis instead.

The tuning of Tau conjugates was without difficulty, similar to the rest of the analytes. Though it was noted that Tau conjugates required much larger collision energies for fragmentation and had a vastly different optimal S-Lens values than most other compounds, it was still well within the capabilities of the instrument and of no concern. Issues arose during the LC-method development stage, as it was found that Tau conjugates were subject to significant carryover. Under the conditions that were optimal and chosen for all other BA-AAs, Tau conjugates appeared to exhibit extreme affinity and retention on the column material. In fact, with the conditions established during the testing of flow rates and gradients, only Tau-CA, Tau-UDCA and Tau-HDCA could be found within chromatograms of

standard mixtures, while peaks pertaining to the other conjugates could be found eluting in following blank runs (Fig. 13).

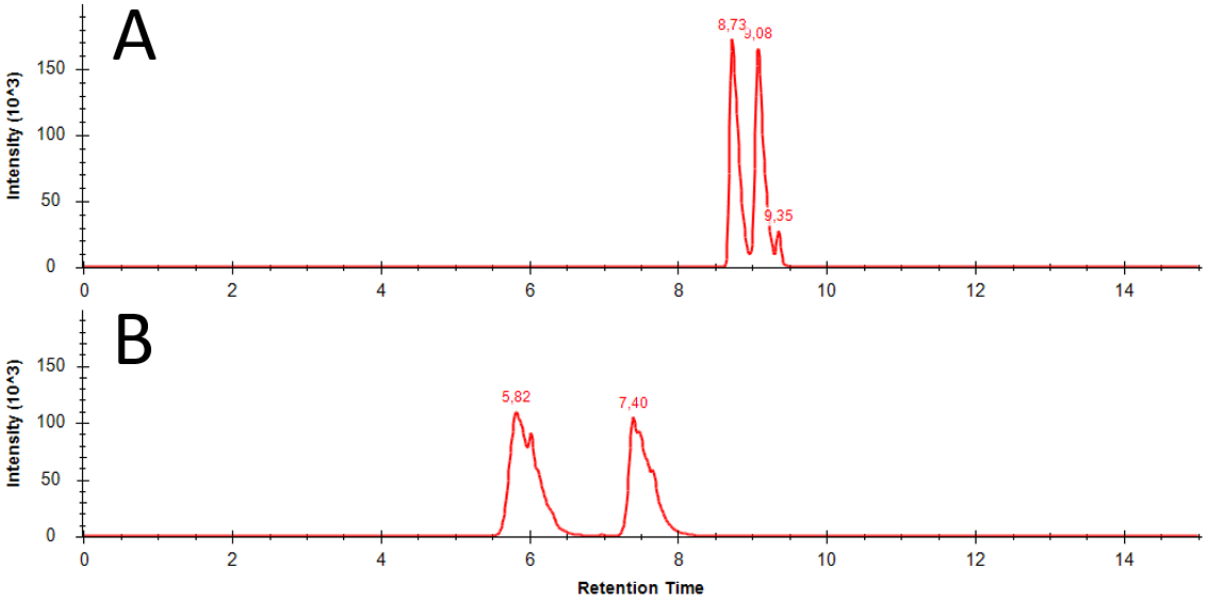

Figure 13. (A) An extracted chromatogram for dihydroxy-BA-Tau conjugates after a run with initially tested gradient conditions. There should be four signals yet only two are visible. **(B)** The blank injection following shows very broad peaks of the conjugates that were missing, indicating they were stuck in the column and only eluted after.

After synthesizing single standards of all Tau conjugates an investigation was conducted into their elution behavior under set conditions. At first it was assumed these substances would simply require longer flushing with high organic percentage mobile phase to elute and so the time at 95% B was extended. While this did bring forth the other analytes within a single run, it took a significant amount of time and the peaks were extremely wide. Lowering the amount of organic solvent in the isocratic part of the mobile phase incrementally revealed an elution optimum at around 75% B for Tau conjugates. This could possibly be attributed to a pH-sensitivity of the sulfate group present in taurine, which could impact the retention behavior significantly depending on the state of protonation. Both eluents used in the method had an addition of 0.1% formic acid, but since the strength of an acid is not only determined by its concentration but also the solvent composition it is surrounded by, a unique environment could have formed around 75% B allowing for quicker elution of Tau conjugates.[66] This is further supported when looking at other work that focuses on traditional bile acids and conjugates of Gly and Tau. A method developed by Reiter *et al.* actually shows Tau conjugates eluting as some of the earliest analytes.[67] A major difference to the method discussed in this work is the introduction of 5 mM ammonium acetate to both eluents in addition to 0.1% FA to create a buffered system. Considering this, pH as the major contributor to Tau conjugate elution behavior seems likely.

At this point, the method worked exceedingly well for the identification and determination of all other conjugates and so further insertion of additives was tried to be avoided. As a workaround in order to still capture the Tau conjugates a period of isocratic flow at 75% B for 6 minutes was added to the end of the established method (Fig. 14). This ensured that RTs of other conjugates would not be altered and still enabled the elution of Tau-CDCA and Tau-DCA towards the end of the run. Tau-LCA could unfortunately not be incorporated this way, as the method would have required to be considerably longer. The amount and diversity of secondary bile acids increases stepwise as the microbiota of the host develops over time along the own endogenous BA metabolism.[68] Indeed, traces of LCA have been shown to only appear in human infants after a minimum of 6 months.[69] Therefore, Tau-LCA is unlikely to be relevant in the context of the samples measured and was excluded.

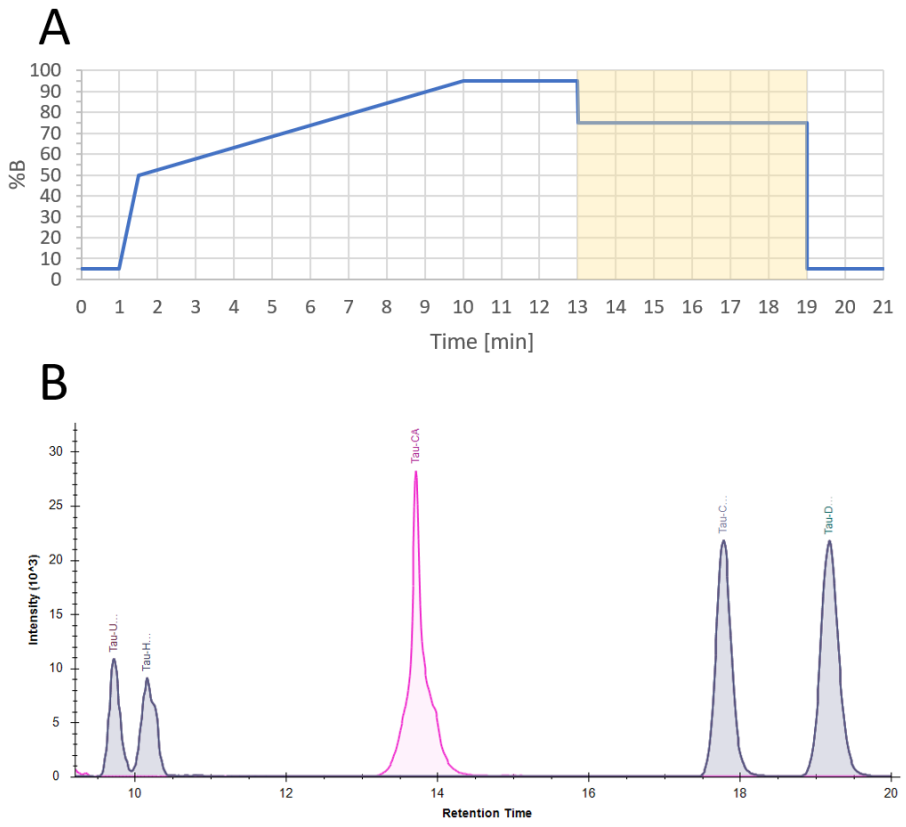

Figure 14. (A) Compromised change in gradient to incorporate all Tau-conjugates apart from Tau-LCA. The yellow area shows the added time to the end of the run in order to eluate the conjugates. **(B)** Resulting chromatogram, now featuring all tracked Tau-conjugates in one run.

4.3 Isomeric anomalies and interferences

Another challenge was encountered in the cases of lysine and ornithine during method development. Both of these amino acids feature an additional amino group on the side chain, which can also react with the activated carboxy group of the bile acids. Therefore, it is very likely for two distinct reaction products to occur per amino acid (Fig. 15). Proof of this could be found early during the optimization

process, as two distinct peaks featuring the same transitions at different retention times would appear for each conjugate (Fig. 16). As it was not possible to elucidate which peak belonged to which reaction product, much less which product would be of biological significance, they were split and retention times of both were included as separate entries Lys1, Lys2 and Orn1, Orn2 respectively.

A similar, but less understood issue, is the appearance of multiple peaks of analytes for which no additional product was expected. This effect would manifest itself as a smaller peak eluting shortly after a large one, and was most pronounced in conjugates of Ala, Asp, Ile/Leu, Met and Phe. In the case of Ile/Leu, the distinctively different peaks were at first interpreted as a successful separation of Ile and Leu conjugates in the mixed standards. It was later discovered that both features could be seen in single standards of Ile and Leu conjugates synthesized separately. Fractions of Ile-LCA were collected manually during a chromatographic run with the intention of isolating the peaks, as an attempt to determine, whether this was an elution phenomenon of the conjugates or different molecules altogether. Injecting the single fractions separately revealed the peaks to be indeed separate molecules, as fractions would only have one of the prominent signals appear at their given RT (Fig. 17A). This is further supported by findings of Phe conjugates within biological samples only featuring the major of the two peaks that can be found in synthesized standard material (Fig. 17B). It is therefore likely that this phenomenon arises due to some kind of rearrangement during the synthesis of BA-AAs, forming a side product. The nature and structure of the resulting molecules is unknown and would require other means to be determined, but given their absence in biological samples this was decided to be redundant.

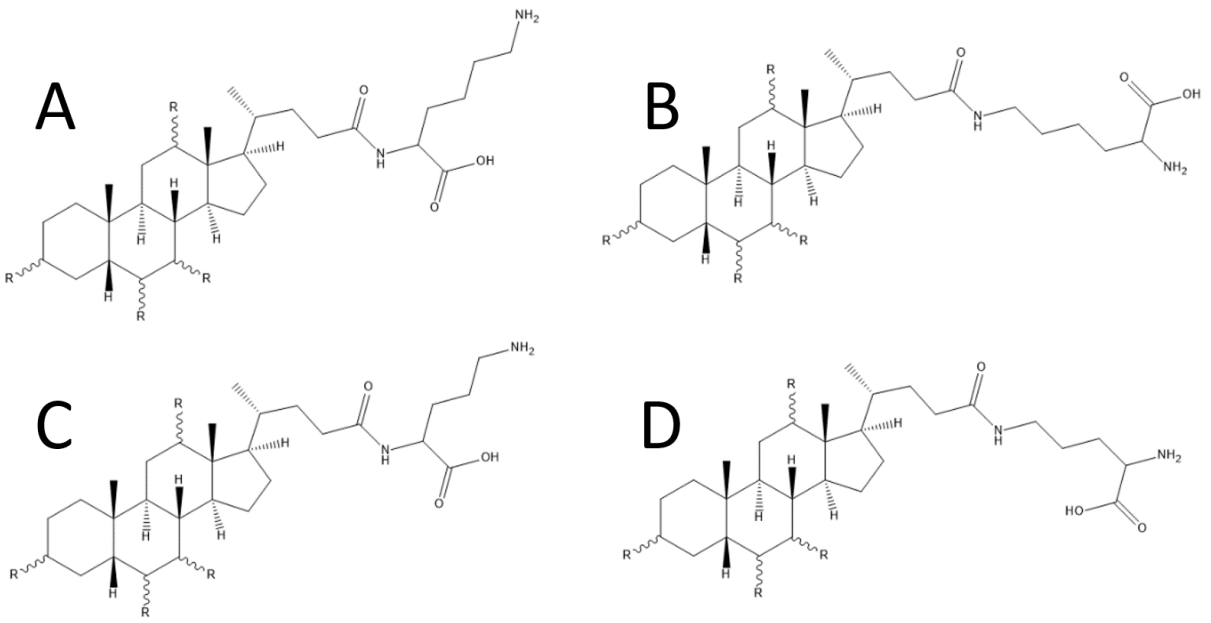

Figure 15. Possible reaction products for lysine (top) bound either at the α-amino **(A)** or ε-amino group **(B)** and ornithine (bottom) bound either at the α-amino **(C)** or δ-amino group **(D)**.

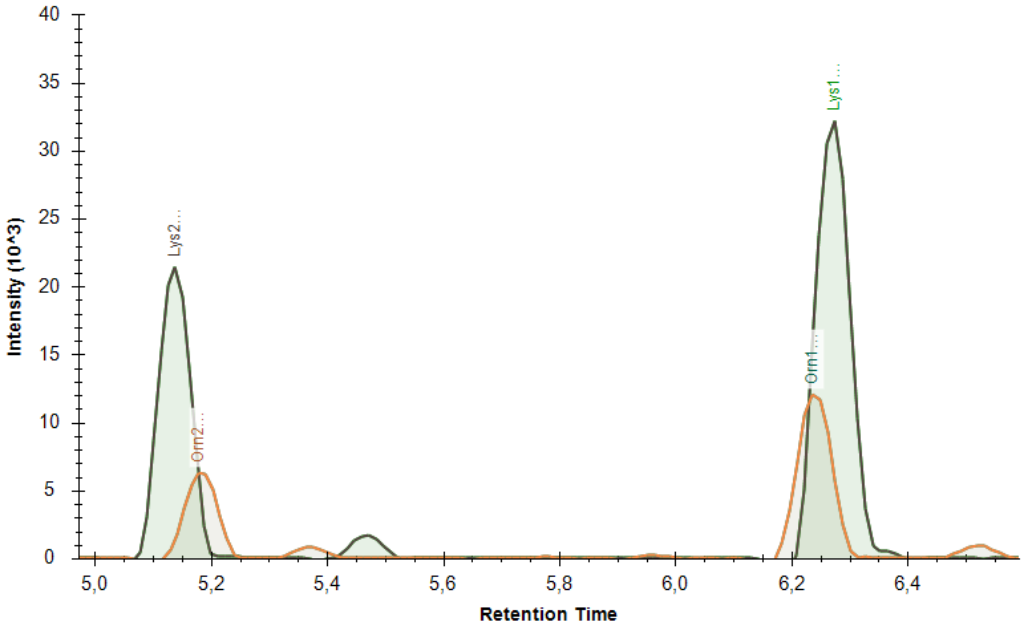

Figure 16. Shown here on the example of CA conjugates, both Lys and Orn featured two distinct peaks each in their chromatograms, likely relating to the two different reaction products as shown in Fig. 15.

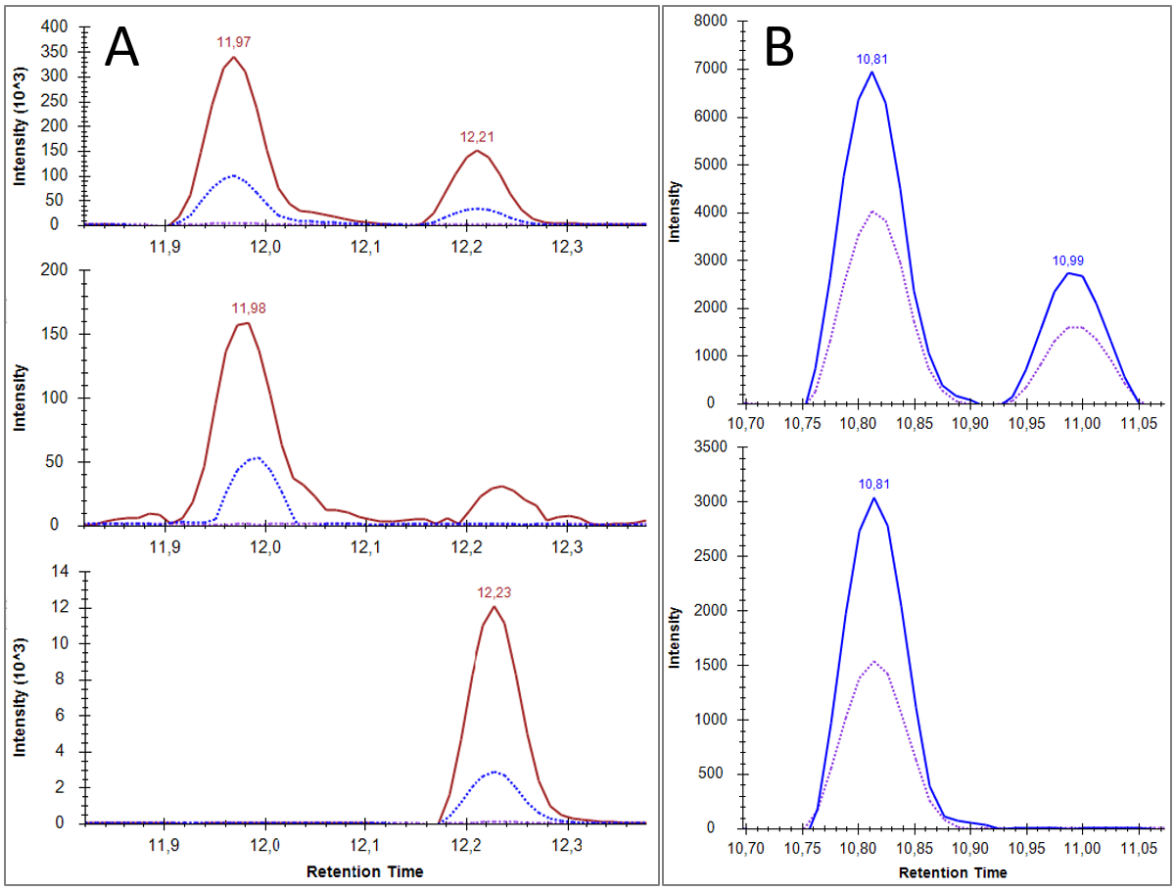

Figure 17. (A) Top: Synthesized Ile-LCA chromatogram, middle: First peak fraction caught separately and injected, bottom: Second peak fraction caught separately and injected. **(B)** Top: Phe-CDCA from synthesis, bottom: Phe-CDCA as detected in unspiked biological sample material**.**

Furthermore, while it is clear that the conjugates of dihydroxy bile acids CDCA, DCA, HDCA and UDCA would share the same masses and likely the same fragments, the same is interestingly also true for some conjugates made from completely different bile acids and amino acids. For example, while being constitutionally different, dihydroxy bile acids coupled to Ser exhibits the same mass as Ala-CA. This was not surprising, as the mass of the additional hydroxy group present in CA is the same as the mass of the hydroxy group in the Ser side chain. However, this introduced additional need of choosing the right product ions for the MRM measurements and making sure they are separated from similar molecules during the run, as some fragments could be shared among them. In cases where it was not possible to avoid shared fragments, due to lack of other product ions with sufficient intensity, it was made sure that no peak overlap occurred to allow the differentiation based on retention time (Fig. 18).

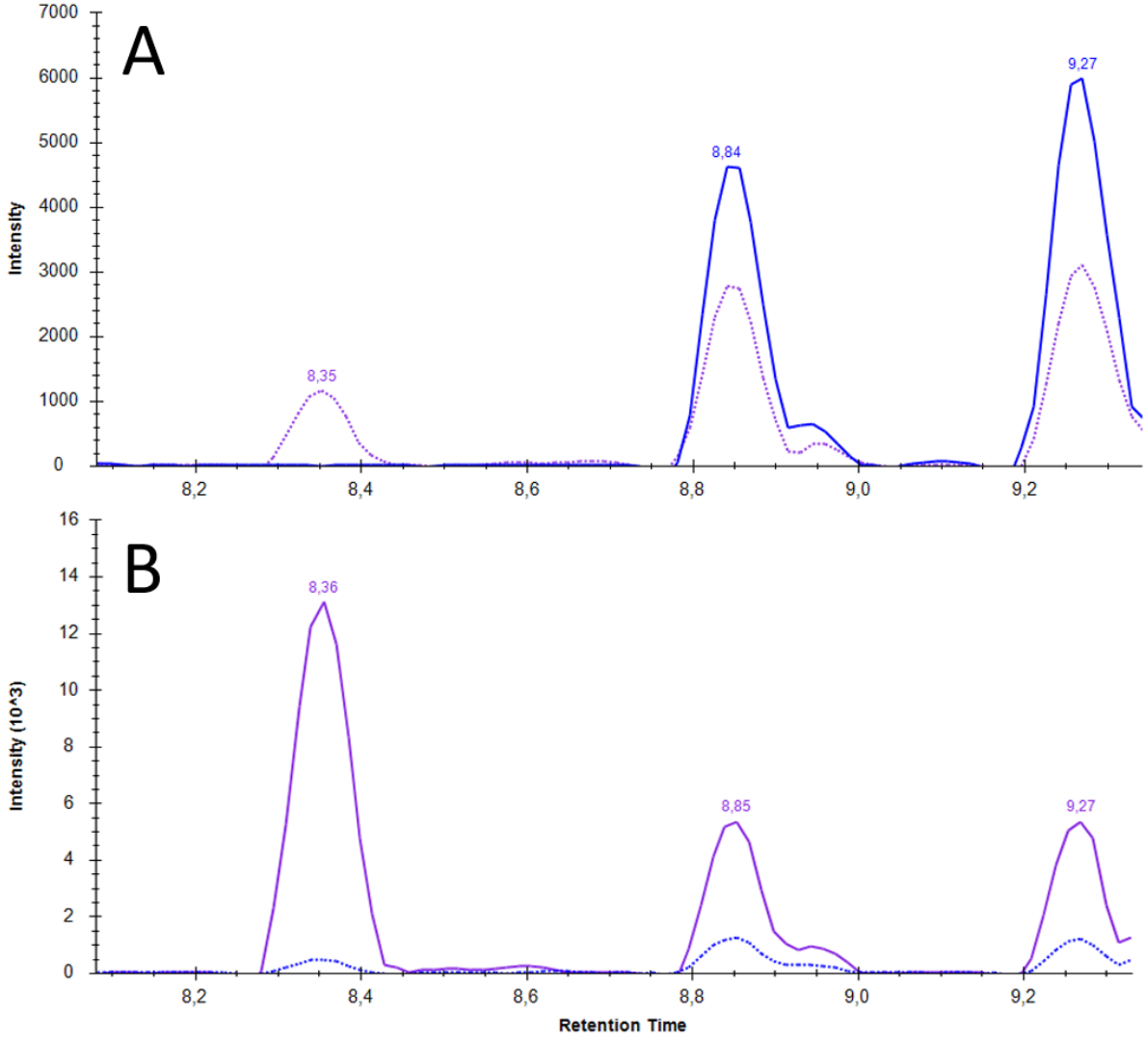

Figure 18. **(A)** Chromatogram for Ser-CDCA (RT = 8.84 min) and Ser-DCA (RT = 9.27 min) shows an interference of qualifier mass at 8.35 min. **(B)** Likewise, Ala-CA (RT = 8.36 min) has the masses corresponding to Ser-CDCA and Ser-DCA infringing on the chromatogram. Differentiation between Ala-CA and Ser-CDCA could be achieved based on retention time.

4.4 Biological samples

4.4.1 Human infant plasma

A full overview of the amount and frequency of detection in regard to bile acids and their conjugates can be found in Fig. 19. Examples of comparisons between plasma samples and standard chromatograms for all positively identified analytes can be found in Fig. 23. Most conjugates that were found in plasma samples were primary BAs bound to either Gly or Tau. Their presence is not at all surprising, as it is a well-known fact that small amounts of BAs are released from the enterohepatic circulation and enter systemic circulation.[70] In fact, circulating bile acids are reported to be higher in newborns and decrease with age and is thought to be the result of immature enterohepatic circulation.[71] Signals were largest and most abundant for Tau-CDCA and Tau-CA as opposed to Gly conjugates, which is consistent with data found on term and preterm neonates.[72] This is likely due to dietary availability of free Tau in breast milk and formula. Interestingly, free CDCA was sparsely found in comparison to CA. This is contrary to reported data in newborns, where CDCA should not just be present but the predominant form of unconjugated BAs.[73] Whether this is due to extremely low levels that challenge the sensitivity of the instrument or distinctive for extremely premature infants is unknown. As for secondary BAs and conjugates, Tau-DCA and Tau-HDCA could be determined in a relatively large number of samples while Gly-HDCA, Tau-UDCA and Gly-UDCA were less frequent. This, again, runs contrary to reference values mentioning DCA and Gly-DCA as the major constituents.[73] Though this may simply be a case of secondary bile acid concentrations being low in infants in general, caused by an undeveloped microbiota.

New bile acid amino acid conjugates could barely be detected in plasma with sporadic signals of Thr-CA, Met-CDCA, Orn2-CDCA, Orn1-LCA and Trp-UDCA. Again, considering the undeveloped microbiota this is not entirely unexpected and the total number for secondary bile acids were low overall. Furthermore, not only would these substances have to be absorbed coming from the large intestine but also pass the liver and be subject to deconjugations and phase I/II metabolism, making it unlikely for them to pass over into systemic circulation, and thus making their appearance unlikely despite many being present in feces.

The analyte “Tau-Undefined” represents a special case. Throughout many measurements another peak could be found alongside Tau-CA, eluting slightly later and featuring the same transitions. From this information, it was assumed to be another trihydroxy bile acid, such as muricholic acid, conjugated with Tau that was not included in the method. Due to the sheer abundance of samples it could be found in, an entry was made in the evaluation software and the peaks integrated accordingly. Of course, the possibility that this molecule is unrelated to bile acid conjugates and only coincidentally

shares mass and fragments indicative of this cannot be excluded. Another unknown signal could be found in some chromatograms relating to unconjugated CA, which further validates the theory, however.

4.4.2 Human infant feces

A full overview of the amount and frequency of detection in regard to bile acids and their conjugates can be found in Fig. 20. Examples of comparisons between fecal samples and standard chromatograms for all positively identified analytes can be found in Fig. 24. Immediately apparent compared to the results of the plasma samples is the much greater amount and frequency of new bile acid amino acid conjugates. Also, while Tau and Gly conjugates of primary bile acids could be seen dominating the profile in plasma, the unconjugated forms appear ubiquitous in feces. This is consistent with our knowledge of the microbiome deconjugating bile acids as part of their biotransformation pathways and defense mechanism, since bile salts are also recognized to be potent antimicrobial agents.[74] Unconjugated secondary bile acids are equally more represented in feces than they were in plasma, with DCA appearing in a decent number of samples.

The majority of new bile acid amino acid conjugates were those of the primary bile acids CA and CDCA. This suggests that reconjugation of primary BAs is either preferred, a competing reaction to transformation into secondary BAs or simply up to relative concentrations. However, this stands in contrast to the frequency in which Phe-DCA and Tau-HDCA could also be discovered and whether conjugates themselves could undergo modification of the sterol backbone without preceding deconjugation.

The CA conjugates of Ile/Leu, Phe and Tyr, originally reported in the work of Quinn *et al.* could be confirmed.[31] The most abundant new conjugates were those of primary BAs bound to Arg, Gln, Glu, His, Phe and Thr. Conjugates of Asn, Ile/Leu, Lys2, Orn2, Trp and Tyr could also be seen with reasonable frequency. All other conjugates could be seen sporadically or not at all. This is partly consistent with reports of Dorrestein *et al.* mentioning His, Phe, Trp, Tyr, Ile/Leu and Lys as the most frequently observed amino acid conjugations in database searches.[33] Furthermore, Tau-Undefined being represented in almost every feces sample further shows the need for follow up studies on its identity.

It is worth mentioning, that absence of some conjugates could simply be an issue of sensitivity. While conjugates of, for example, UDCA were exceptionally rare in these measurements, the signals that could be found were a very clear representation of the respective substances in comparison to QCs. Together with the arbitrary requirements set for peak evaluation, some signals showed similarity but were eventually judged to be too ambiguous for integration. The TSQ Vantage system that was utilized in the acquisition of the data does not represent the most sensitive tool available today. It is therefore

very much possible, that more modern systems could resolve or reveal signals in the samples tested that were otherwise inexplicit and thus increase the number of conjugates.

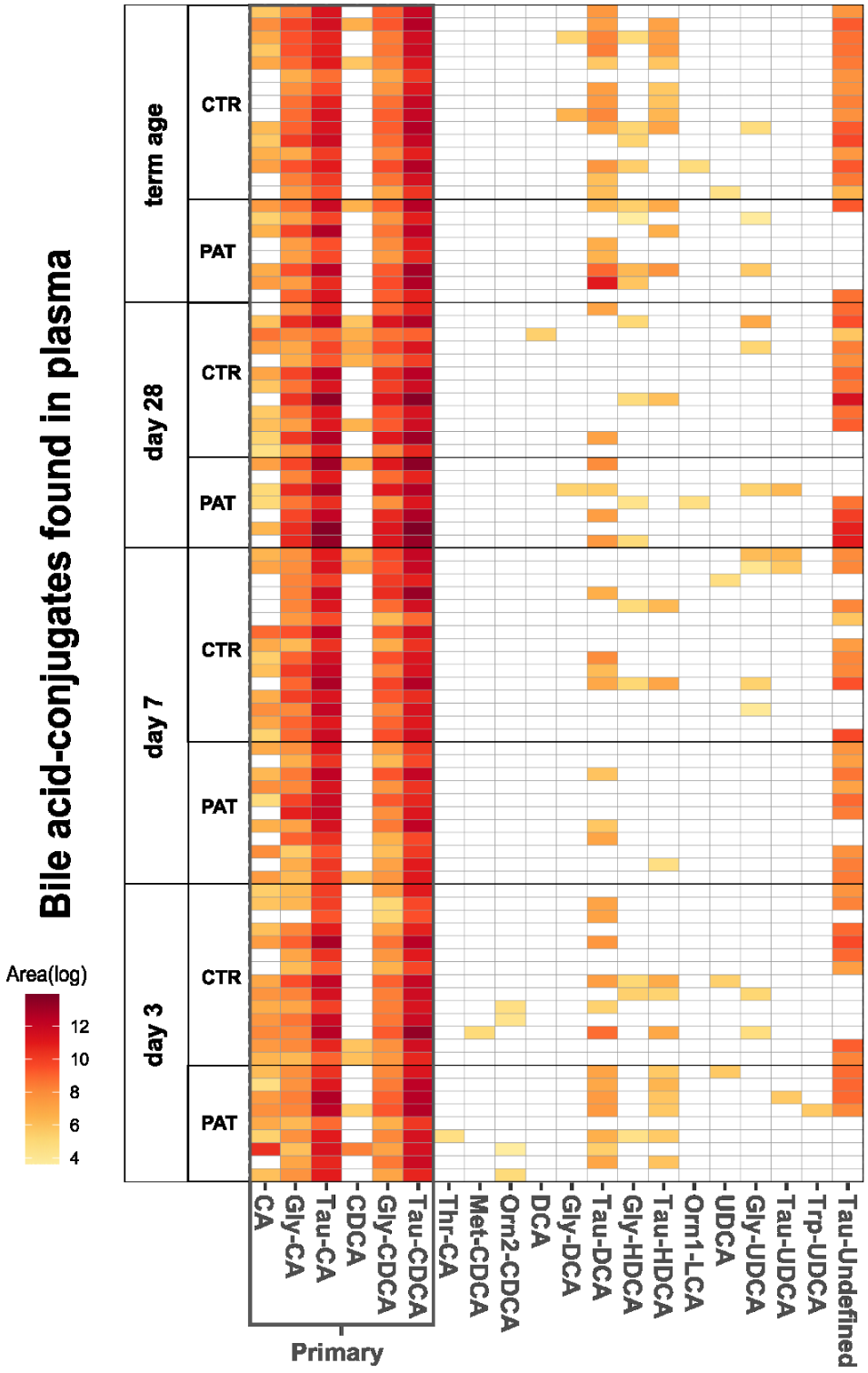

Figure 19. BA-AAs found in plasma of extremely premature infants. The section labeled "Primary" relates to endogenous bile acids and conjugates, everything else is therefore a product of the microbiome that was taken up. Image created and provided by Manuel Pristner.

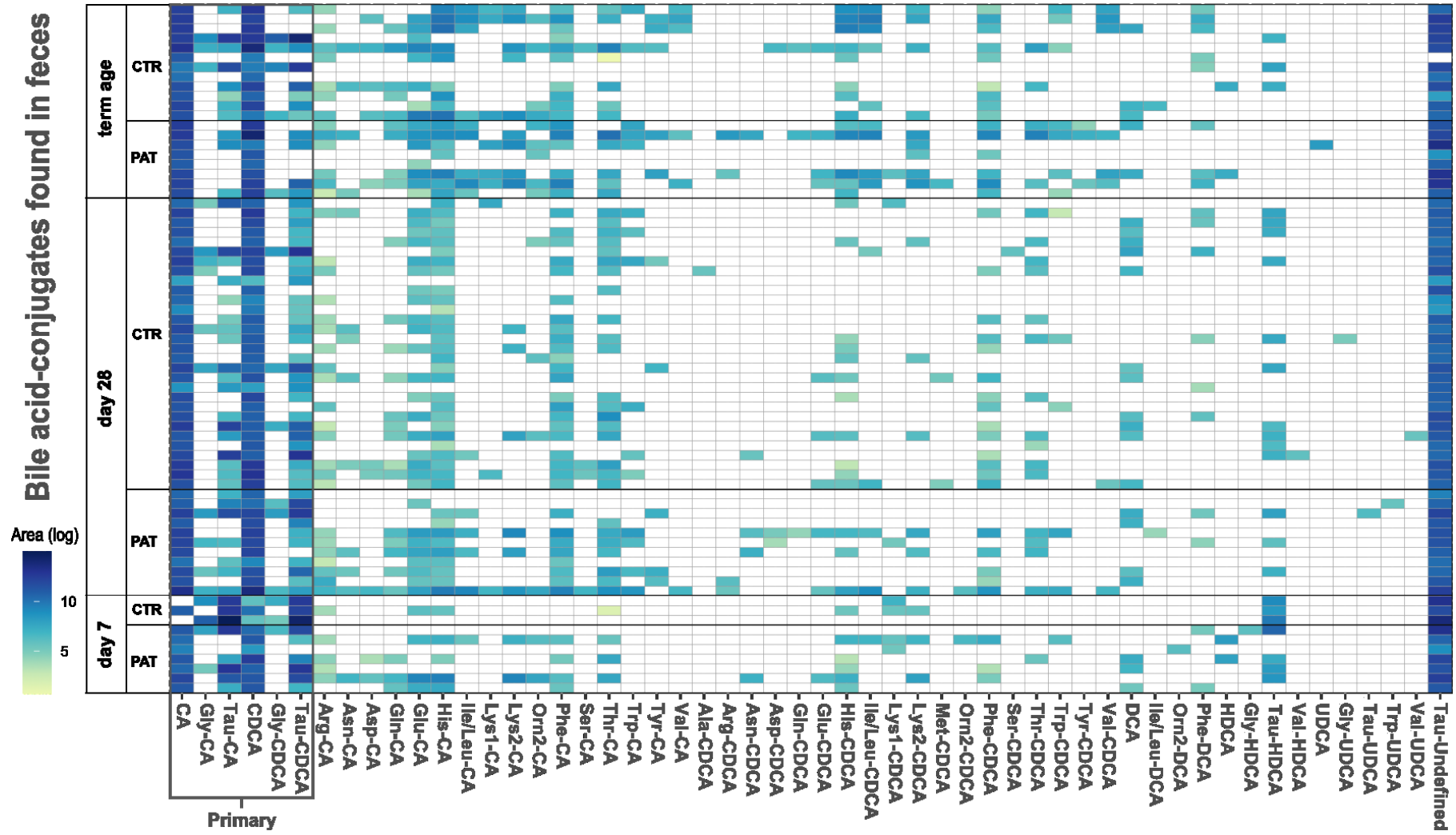

Figure 20. BA-AAs found in feces of extremely premature infants. The section labeled “Primary” relates to endogenous bile acids and conjugates, everything else is therefore a product of the microbiome. Image created and provided by Manuel Pristner.

4.4.3. QC during measurement of real-life samples

Over the run time of a sequence of LC-MS measurements a drift in MS sensitivity can occur leading to variations in signal intensity between samples with a technical origin rather than a biological origin. Therefore, it is necessary to employ quality control measures to avoid any bias in the results introduced by a drift in sensitivity. A common approach is the repeated injection of the same QC sample at the beginning, between samples and at the end of a sequence, to monitor a change in sensitivity. A sample of the same matrix spiked with a standard mix of the analytes, was used as QC sample for the measurements. The sequences both started with five extracted matrix injections and five QC injections to condition the column. After that, QC measurements were repeated around every 20 injections to check for consistency during the measurements. Fig. 21 shows the signal of selected QCs throughout the measurements. In plasma, a trend can be seen, that the QC measurements start out inconsistent but after the conditioning continue to be more stable over the rest of the sequence. This highlights the importance of the conditioning step to ensure comparable results between samples.

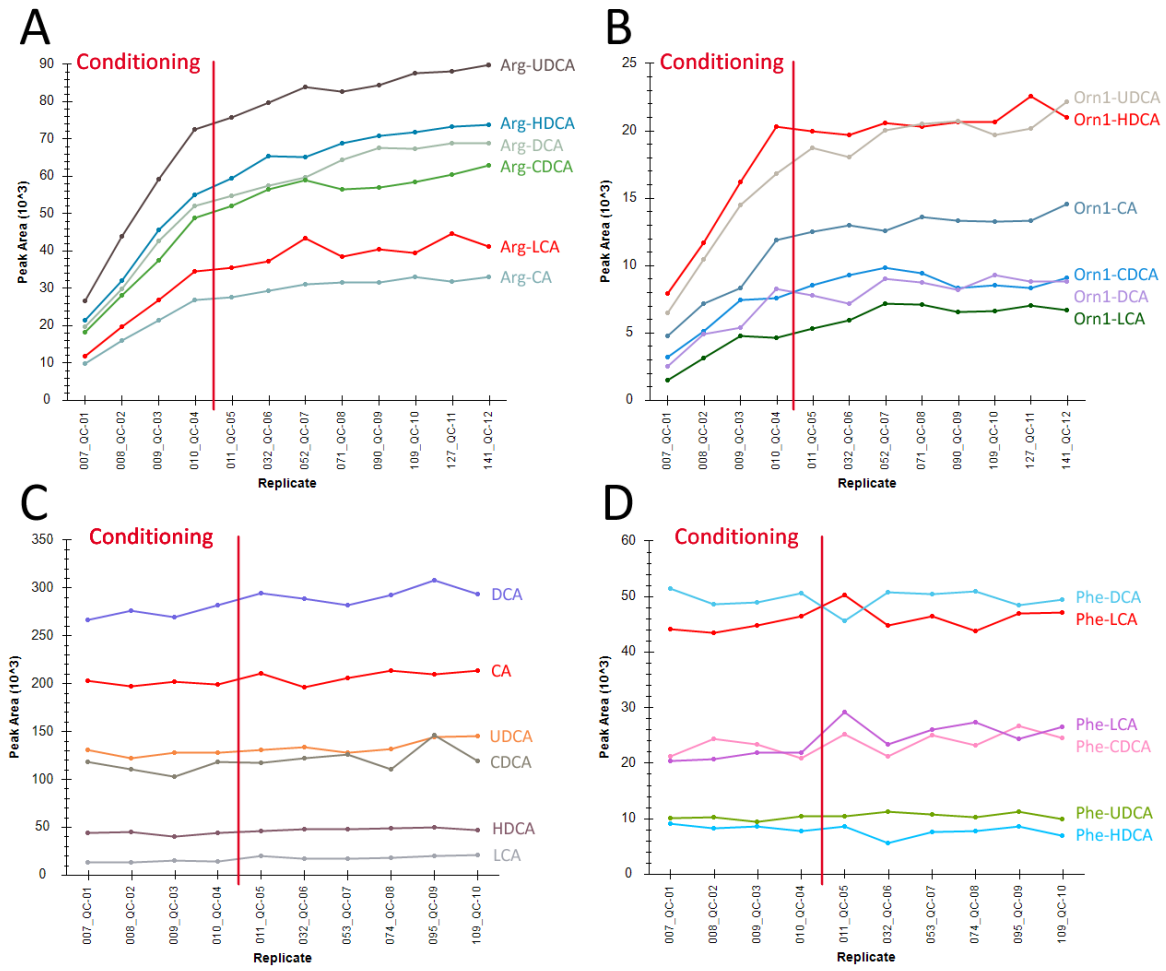

Figure 21. QCs in plasma samples **(A, B)** exhibit a steep increase in signal in the first few measurements, then stay relatively stable. QCs from fecal samples **(C, D)** on the other hand show consistency from the start.

The extracted ion chromatograms of the samples were compared between samples containing the reference standards and the biological samples obtained from the extremely premature infants. This included the comparison of retention time, peak shape and ion ratio between transitions, to ensure a correct identification of analytes. In Fig. 22 examples of sample and reference peaks are shown, exhibiting high congruency, proving the correct identification of the respective compounds found in the biological samples.

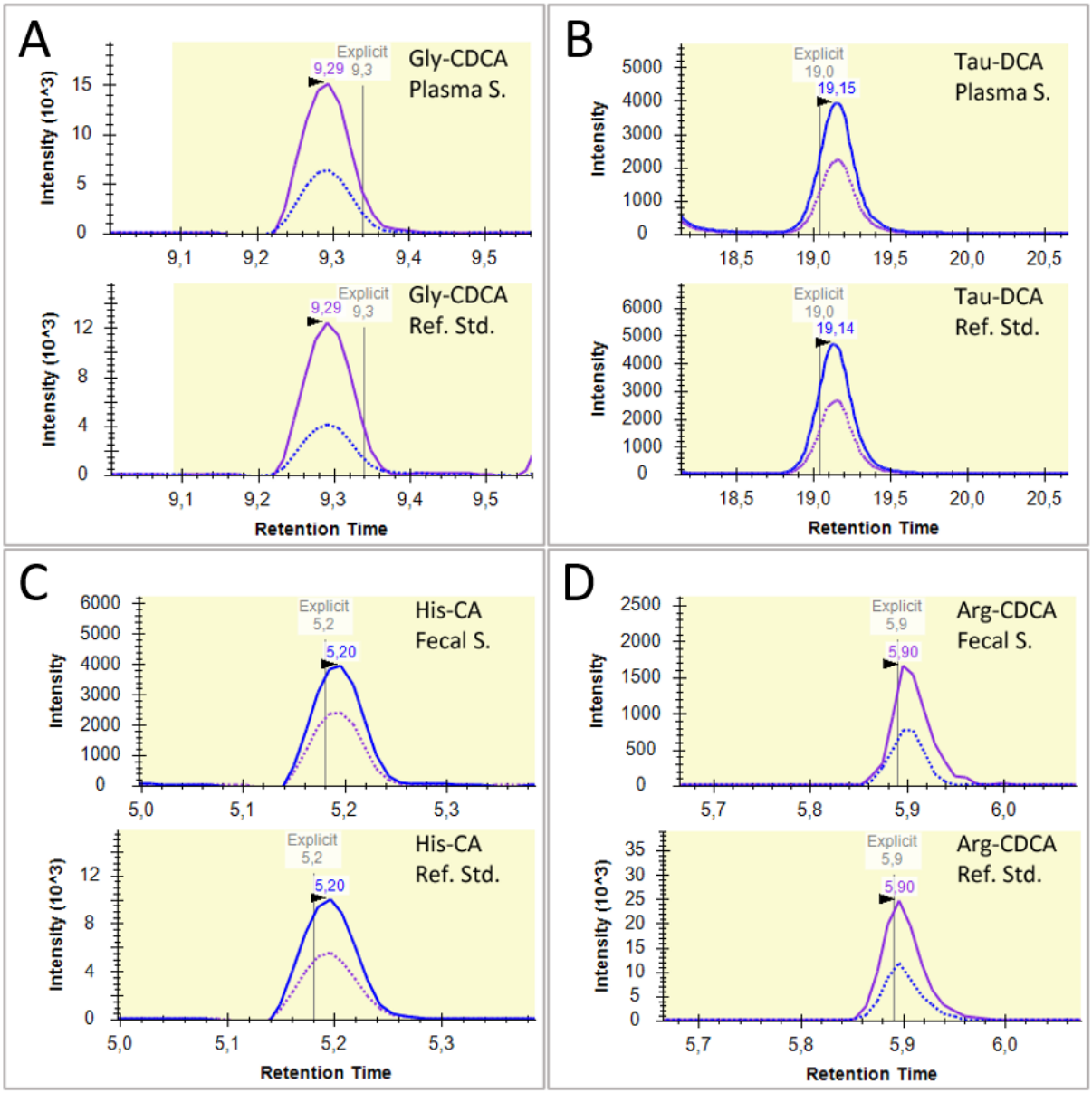

Figure 22. Comparisons of extracted ion chromatograms of analytes from plasma samples **(A, B)** and fecal samples **(C, D)** compared to their counterpart in the sample containing the reference standards. A full set of example figures for every detected analyte can be found in the appendix (Fig. 23 & 24).

5 Conclusion and outlook

The metabolomic diversity of humans and the microbiome alike are far from fully explored and new molecules are constantly discovered. LC-MS method development for newly discovered compounds is often hindered by the commercial inaccessibility of reference standard material due to their novelty. Inspired by their recent discovery, 120 new bile acid amino acid conjugates were successfully synthesized employing straight-forward coupling chemistry with the goal of using them for the development of a LC-MS/MS method. Most compounds could be produced by the batch synthesis in sufficient yields to be tuned on the TSQ Vantage triple quadrupole mass spectrometer, obtaining the necessary parameters for method development. In rare cases, single synthesis had to be performed to ensure a high enough concentration for the tuning procedure. As such, the viability of the batch procedure should be rated as very high but not flawless. The synthesized bile acid amino acid conjugates were used to establish the HPLC method, where all isomeric structures with the exception of leucine- and isoleucine-conjugates could be separated successfully. Overall, this resulted in a LC-MS/MS method for over 120 analytes, mainly consisting of the recently described compounds. In proof-of-principle experiments, plasma and feces samples of extremely premature infants were processed and measured, revealing many of the new conjugates at appreciable signal intensities. However, a transfer of the method to instruments featuring higher sensitivity could be considered as interesting follow up. A statement about statistically significant differences between pathological and control groups will be part of a future project.

Chromatographic resolution of taurine-conjugates was problematic, requiring significant elongation of the method, reducing its throughput and still leading to the exclusion of Tau-LCA from the method. In the future, this should be revisited to find a way to include the compound, perhaps through adjusting additives in the eluent systems. While easily explained for lysine- and ornithine-conjugates, which feature two amine moieties and thus two possible reaction products per molecule, the nature of the additional peaks found with some other synthesized compounds is not clear. As they can be separated through fractionation, they clearly represent different molecules, yet feature the exact same fragmentation patterns. They might be stereoisomers caused by rearrangement during the synthesis. More work in the future could be directed towards their structure elucidation, although the lack of their presence in the infant samples might indicate that they do not occur in biological settings. While this method is only applicable for qualitative and semi-quantitative questions, it represents, to the best of our knowledge, the first method produced for the targeted analysis of a wide range of the novel bile acid amino acid conjugates that can be directly applied for the measurement of human plasma and fecal samples.

6 References

1. Franzosa, E. A. *et al.* Identifying personal microbiomes using metagenomic codes. *Proc. Natl. Acad. Sci.* 112 (**2015**).

2. Umesaki, Y. & Setoyama, H. Structure of the intestinal flora responsible for development of the gut immune systemin a rodent model. *Microbes Infect.* 2, 1343–1351 (**2000**).

3. Savage, D. C. Gastrointestinal Microflora in Mammalian Nutrition. *Annu. Rev. Nutr.* 6, 155–178 (**1986**).

4. Hooper, L. V., Midtvedt, T. & Gordon, J. I. How host-microbial interactions shape the nutrient environment of the mammalian intestine. *Annu. Rev. Nutr.* 22, 283–307 (**2002**).

5. Visconti, A. *et al.* Interplay between the human gut microbiome and host metabolism. *Nat. Commun.* 10, 4505 (**2019**).

6. Claus, S. P. *et al.* Systemic multicompartmental effects of the gut microbiome on mouse metabolic phenotypes. *Mol. Syst. Biol.* 4, 219 (**2008**).

7. Wikoff, W. R. *et al.* Metabolomics analysis reveals large effects of gut microflora on mammalian blood metabolites. *Proc. Natl. Acad. Sci.* 106, 3698–3703 (**2009**).

8. DeMoss, R. D. & Moser, K. Tryptophanase in Diverse Bacterial Species. *J. Bacteriol.* 98, 167–171 (**1969**).

9. Karbownik, M. *et al.* Indole-3-propionic acid, a melatonin-related molecule, protects hepatic microsomal membranes from iron-induced oxidative damage: Relevance to cancer reduction. *J. Cell. Biochem.* 81, 507–513 (**2001**).

10. Sanna, S. *et al.* Causal relationships among the gut microbiome, short-chain fatty acids and metabolic diseases. *Nat. Genet.* 51, 600–605 (**2019**).

11. Flint, H. J., Duncan, S. H., Scott, K. P. & Louis, P. Links between diet, gut microbiota composition and gut metabolism. *Proc. Nutr. Soc.* 74, 13–22 (**2015**).

12. Miller, T. L. & Wolin, M. J. Pathways of acetate, propionate, and butyrate formation by the human fecal microbial flora. *Appl. Environ. Microbiol.* 62, 1589–1592 (**1996**).

13. Morrison, D. J. & Preston, T. Formation of short chain fatty acids by the gut microbiota and their impact on human metabolism. *Gut Microbes* 7, 189–200 (**2016**).

14. Cani, P. D. *et al.* Changes in Gut Microbiota Control Metabolic Endotoxemia-Induced Inflammation in High-Fat Diet–Induced Obesity and Diabetes in Mice. *Diabetes* 57, 1470–1481 (**2008**).

15. Lee, B., Moon, K. M. & Kim, C. Y. Tight Junction in the Intestinal Epithelium: Its Association with Diseases and Regulation by Phytochemicals. *J. Immunol. Res.* 2018, 1–11 (**2018**).

16. He, J. *et al.* Short-Chain Fatty Acids and Their Association with Signalling Pathways in Inflammation, Glucose and Lipid Metabolism. *Int. J. Mol. Sci.* 21, 6356 (**2020**).

17. Chen, M. X., Wang, S.-Y., Kuo, C.-H. & Tsai, I.-L. Metabolome analysis for investigating host-gut microbiota interactions. *J. Formos. Med. Assoc.* 118, 10–22 (**2019**).

18. Vemuri, R., Shankar, E. M., Chieppa, M., Eri, R. & Kavanagh, K. Beyond Just Bacteria: Functional Biomes in the Gut Ecosystem Including Virome, Mycobiome, Archaeome and Helminths. *Microorganisms* 8, 483 (**2020**).

19. Monte, M. J., Marin, J. J., Antelo, A. & Vazquez-Tato, J. Bile acids: Chemistry, physiology, and pathophysiology. *World J. Gastroenterol.* 15, 804 (**2009**).

20. Axelson, M. *et al.* Bile acid synthesis in cultured human hepatocytes: support for an alternative biosynthetic pathway to cholic acid. *Hepatology* 31, 1305–1312 (**2000**).

21. Mukhopadhyay, S. & Maitra, U. Chemistry and Biology of Bile Acids. *Curr. Sci.* 87, 1666–1683 (**2004**).

22. Guzior, D. V. & Quinn, R. A. Review: microbial transformations of human bile acids. *Microbiome* 9, 140 (**2021**).

23. Kotti, T. J., Ramirez, D. M. O., Pfeiffer, B. E., Huber, K. M. & Russell, D. W. Brain cholesterol turnover required for geranylgeraniol production and learning in mice. *Proc. Natl. Acad. Sci.* 103, 3869–3874 (**2006**).

24. Hylemon, P. B. *et al.* Bile acids as regulatory molecules. *J. Lipid Res.* 50, 1509–1520 (**2009**).

25. Han, S. I. *et al.* Bile acids enhance the activity of the insulin receptor and glycogen synthase in primary rodent hepatocytes. *Hepatology* 39, 456–463 (**2004**).

26. Qi, Y. *et al.* Bile acid signaling in lipid metabolism: Metabolomic and lipidomic analysis of lipid and bile acid markers linked to anti-obesity and anti-diabetes in mice. *Biochim. Biophys. Acta - Mol. Cell Biol. Lipids* 1851, 19–29 (**2015**).

27. Schoenfeld, L. J. Chenodiol (Chenodeoxycholic Acid) for Dissolution of Gallstones: The National Cooperative Gallstone Study. *Ann. Intern. Med.* 95, 257 (**1981**).

28. Ridlon, J. M., Kang, D. J., Hylemon, P. B. & Bajaj, J. S. Bile acids and the gut microbiome. *Curr. Opin. Gastroenterol.* 30, 332–338 (**2014**).

29. Begley, M., Gahan, C. G. M. & Hill, C. The interaction between bacteria and bile. *FEMS Microbiol. Rev.* 29, 625–651 (**2005**).

30. Monteiro-Cardoso, V. F., Corlianò, M. & Singaraja, R. R. Bile Acids: A Communication Channel in the Gut-Brain Axis. *NeuroMolecular Med.* 23, 99–117 (**2021**).

31. Quinn, R. A. *et al.* Global chemical effects of the microbiome include new bile-acid conjugations. *Nature* 579, 123–129 (**2020**).

32. Cheng, J. *et al.* Therapeutic Role of Rifaximin in Inflammatory Bowel Disease: Clinical Implication of Human Pregnane X Receptor Activation. *J. Pharmacol. Exp. Ther.* 335, 32–41 (**2010**).

33. Dorrestein, P. *et al.* A Synthesis-Based Reverse Metabolomics Approach for the Discovery of Chemical Structures from Humans and Animals. *Res. Sq.* (**2021**).

34. Finegold, S. M. *et al.* Pyrosequencing study of fecal microflora of autistic and control children. *Anaerobe* 16, 444–453 (**2010**).

35. Wang, Y.-Z. *et al.* Discovery and Identification of New Amino Acid-Conjugated Bile Acids by Polarity-Switching Multiple Reaction Monitoring Mass Spectrometry. *ChemRxiv* (**2022**).

36. Fanali, S., Haddad, P. R., Poole, C. F. & Riekkola, M.-L. *Liquid Chromatography*. (Elsevier, **2017**).

37. Flasch, M. *et al.* Integrated exposomics/metabolomics for rapid exposure and effect analyses. *ChemRxiv* (**2022**).

38. Ekman, R., Silberring, J., Westman-Brinkmalm, A. & Kraj, A. *Mass Spectrometry*. (John Wiley &

Sons, Inc.), (**2008**).

39. Famiglini, G., Palma, P., Termopoli, V. & Cappiello, A. The history of electron ionization in LC-MS, from the early days to modern technologies: A review. *Anal. Chim. Acta* 1167, 338350 (**2021**).

40. El-Faham, A. & Albericio, F. Peptide Coupling Reagents, More than a Letter Soup. *Chem. Rev.* 111, 6557–6602 (**2011**).

41. Patchett, A. A. Excursions in drug discovery. *J. Med. Chem.* 36, 2051–2058 (**1993**).

42. de Gasparo, M. & Whitebread, S. Binding of valsartan to mammalian angiotensin AT1 receptors. *Regul. Pept.* 59, 303–311 (**1995**).

43. Ananthanarayanan, V. S., Tetreault, S. & Saint-Jean, A. Interaction of calcium channel antagonists with calcium: spectroscopic and modeling studies on diltiazem and its Ca2+ complex. *J. Med. Chem.* 36, 1324–1332 (**1993**).

44. Jursic, B. S. & Zdravkovski, Z. A Simple Preparation of Amides from Acids and Amines by Heating of Their Mixture. *Synth. Commun.* 23, 2761–2770 (**1993**).

45. Valeur, E. & Bradley, M. Amide bond formation: beyond the myth of coupling reagents. *Chem. Soc. Rev.* 38, 606–631 (**2009**).

46. Sheehan, J. C. & Hess, G. P. A New Method of Forming Peptide Bonds. *J. Am. Chem. Soc.* 77, 1067–1068 (**1955**).

47. Benoiton, N. L. & Chen, F. M. F. Not the alkoxycarbonylamino-acid O-acylisourea. *J. Chem. Soc. Chem. Commun.* 543 (**1981**).

48. Carpino, L. A. 1-Hydroxy-7-azabenzotriazole. An efficient peptide coupling additive. *J. Am. Chem. Soc.* 115, 4397–4398 (**1993**).

49. Matsueda, R., Maruyama, H., Ueki, M. & Mukaiyama, T. Peptide Synthesis by Oxidation-Reduction Condensation. II. The Use of Disulfide as an Oxidant. *Bull. Chem. Soc. Jpn.* 44, 1373–1378 (**1971**).

50. Higashi, T. *et al.* Simple and practical derivatization procedure for enhanced detection of carboxylic acids in liquid chromatography–electrospray ionization-tandem mass spectrometry. *J. Pharm. Biomed. Anal.* 52, 809–818 (**2010**).

51. Toyo'oka, T. *et al.* Precolumn fluorescence tagging reagent for carboxylic acids in high-performance liquid chromatography: 4-substituted-7-aminoalkylamino-2,1,3-benzoxadiazoles. *J. Chromatogr. A* 588, 61–71 (**1991**).

52. Santa, T., Matsumura, D., Huang, C., Kitada, C. & Imai, K. Design and synthesis of a hydrophilic fluorescent derivatization reagent for carboxylic acids, 4-N-(4-N-aminoethyl)piperazino-7-nitro-2,1,3-benzoxadiazole (NBD-PZ-NH2), and its application to capillary electrophoresis with laser-induced fluorescence detec. *Biomed. Chromatogr.* 16, 523–528 (**2002**).

53. Lu, Y., Yao, D. & Chen, C. 2-Hydrazinoquinoline as a Derivatization Agent for LC-MS-Based Metabolomic Investigation of Diabetic Ketoacidosis. *Metabolites* 3, 993–1010 (**2013**).

54. Aksenov, A. A., da Silva, R., Knight, R., Lopes, N. P. & Dorrestein, P. C. Global chemical analysis of biology by mass spectrometry. *Nat. Rev. Chem.* 1, 0054 (**2017**).

55. Hoffmann, M. A. *et al.* Assigning confidence to structural annotations from mass spectra with COSMIC. *bioRxiv* (**2021**).

56. Wang, M. *et al.* Mass spectrometry searches using MASST. *Nat. Biotechnol.* 38, 23–26 (**2020**).

57. Jarmusch, A. K. *et al.* ReDU: a framework to find and reanalyze public mass spectrometry data. *Nat. Methods* 17, 901–904 (**2020**).

58. Piraud, M. *et al.* ESI-MS/MS analysis of underivatised amino acids: a new tool for the diagnosis of inherited disorders of amino acid metabolism. Fragmentation study of 79 molecules of biological interest in positive and negative ionisation mode. *Rapid Commun. Mass Spectrom.* 17, 1297–1311 (**2003**).

59. Seki, D. *et al.* Aberrant gut-microbiota-immune-brain axis development in premature neonates with brain damage. *Cell Host Microbe* 29, 1558-1572 (**2021**).

60. Adams, K. J. *et al.* Skyline for Small Molecules: A Unifying Software Package for Quantitative Metabolomics. *J. Proteome Res.* 19, 1447–1458 (**2020**).

61. Thermo Scientific. Crosslinking Technical Handbook: easy molecular bonding crosslinking technology. https://tools.thermofisher.com/content/sfs/brochures/1602163-Crosslinking-Reagents-Handbook.pdf (accessed: 13.10.2022).

62. Danese, E. *et al.* Bile acids quantification by liquid chromatography-tandem mass spectrometry: Method validation, reference range, and interference study. *Diagnostics* 10, 1–13 (**2020**).

63. Heidorn, M. Why Solvent Grade and Purity Must Fit the U/HPLC System Needs. *ThermoFisher Scientific AnalyteGuru* https://www.analyteguru.com/t5/Blog/Why-Solvent-Grade-and-Purity-Must-Fit-the-U-HPLC-System-Needs/ba-p/3444 (accessed: 13.10.2022).

64. Haidar Ahmad, I. A. Necessary Analytical Skills and Knowledge for Identifying, Understanding, and Performing HPLC Troubleshooting. *Chromatographia* 80, 705–730 (**2017**).

65. Waters Corporation. Atlantis T3, DC18 and HILIC silica columns, care and use manual. https://www.waters.com/webassets/cms/support/docs/736000640.pdf (accessed: 13.10.2022).

66. Cox, B. G. *Acids and Bases: Solvent Effects on Acid-Base Strength*. (Oxford University Press), (**2013**).

67. Reiter, S. *et al.* Development of a Highly Sensitive Ultra-High-Performance Liquid Chromatography Coupled to Electrospray Ionization Tandem Mass Spectrometry Quantitation Method for Fecal Bile Acids and Application on Crohn's Disease Studies. *J. Agric. Food Chem.* 69, 5238–5251 (**2021**).

68. Tanaka, M. *et al.* The association between gut microbiota development and maturation of intestinal bile acid metabolism in the first 3 y of healthy Japanese infants. *Gut Microbes* 11, 205–216 (**2020**).

69. Hammons, J. L., Jordan, W. E., Stewart, R. L., Taulbee, J. D. & Berg, R. W. Age and Diet Effects on Fecal Bile Acids in Infants. *J. Pedriatic Gastroenterol. Nutr.* 7, 30–38 (**1988**).

70. Mertens, K. L., Kalsbeek, A., Soeters, M. R. & Eggink, H. M. Bile Acid Signaling Pathways from the Enterohepatic Circulation to the Central Nervous System. *Front. Neurosci.* 11 (**2017**).

71. Niijima, S. I. Studies on the conjugating activity of bile acids in children. *Pediatr. Res.* 19, 302–307 (**1985**).

72. Zöhrer, E. *et al.* Serum bile acids in term and preterm neonates A case-control study determining reference values and the influence of early-onset sepsis. *Med. (United States)* 95

(**2016**).

73. Jahnel, J. *et al.* Reference ranges of serum bile acids in children and adolescents. *Clin. Chem. Lab. Med.* 53, 1807–1813 (**2015**).

74. Sannasiddappa, T. H., Lund, P. A. & Clarke, S. R. In Vitro Antibacterial Activity of Unconjugated and Conjugated Bile Salts on Staphylococcus aureus. *Front. Microbiol.* 8 (**2017**).

Appendix

Reference and sample chromatograms

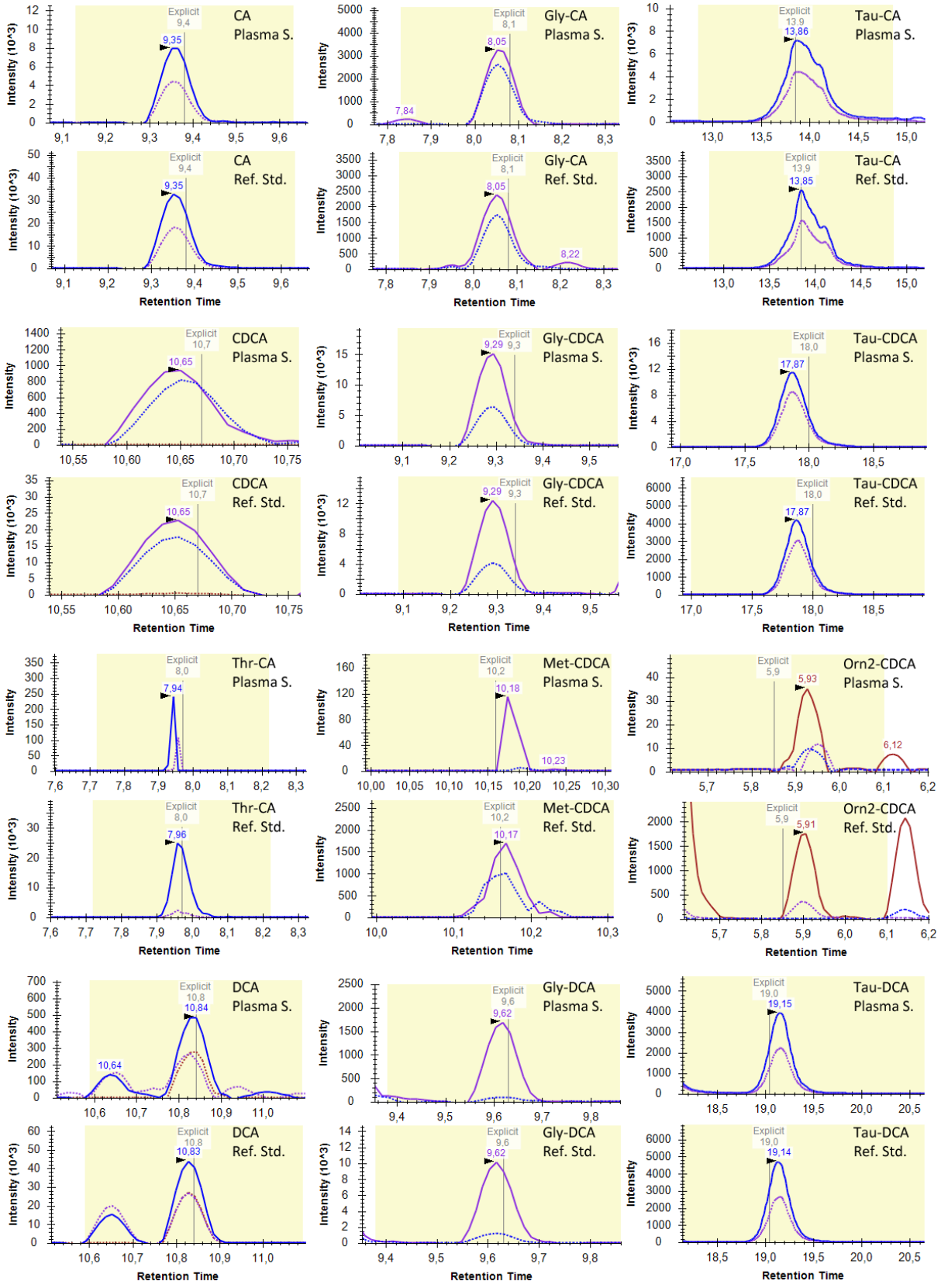

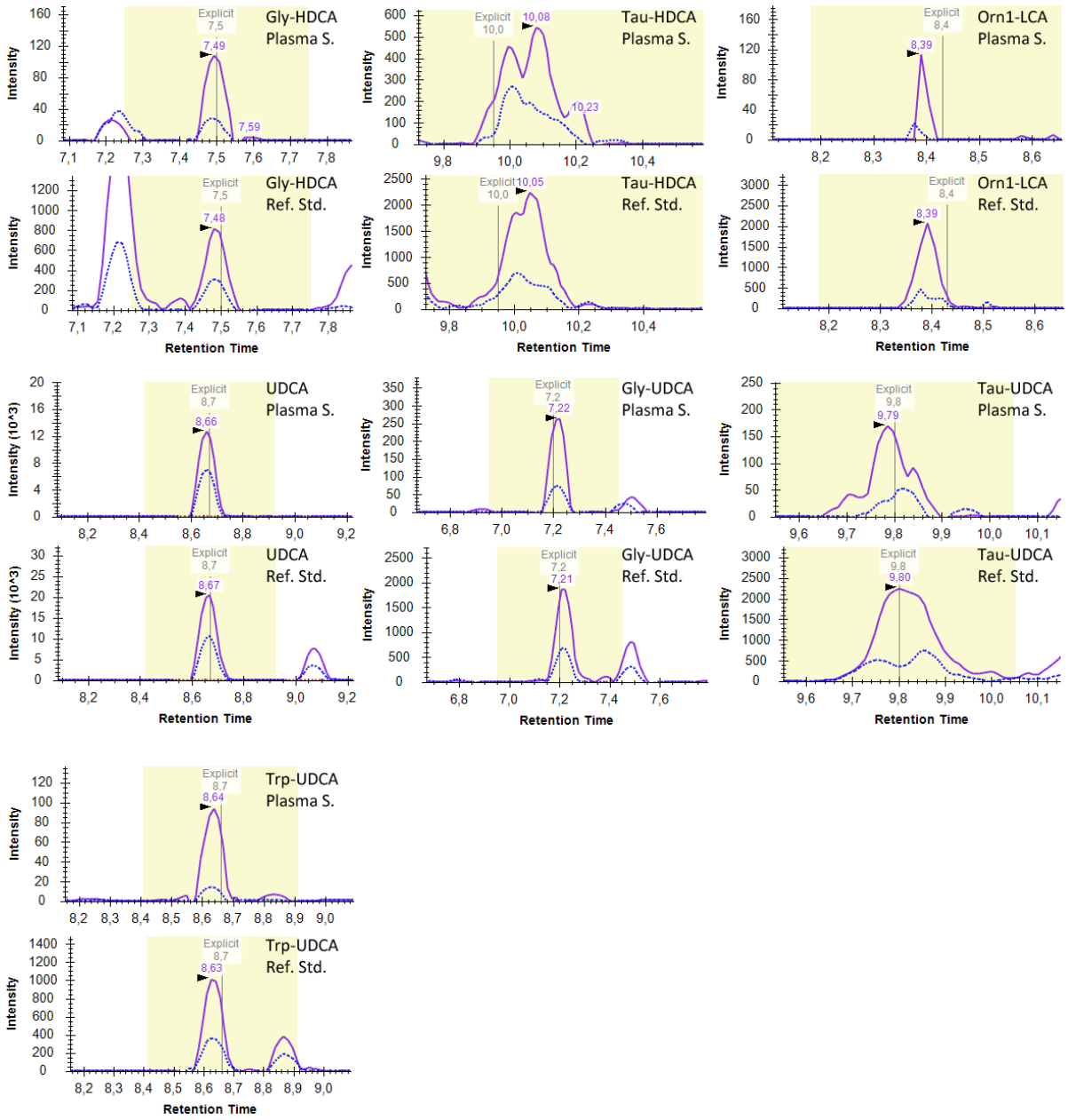

Figure 23. Comparisons between the chromatograms from reference standard mixtures (Ref. Std.) used for identification of compounds in plasma samples obtained from extremely premature infants (Plasma S.).

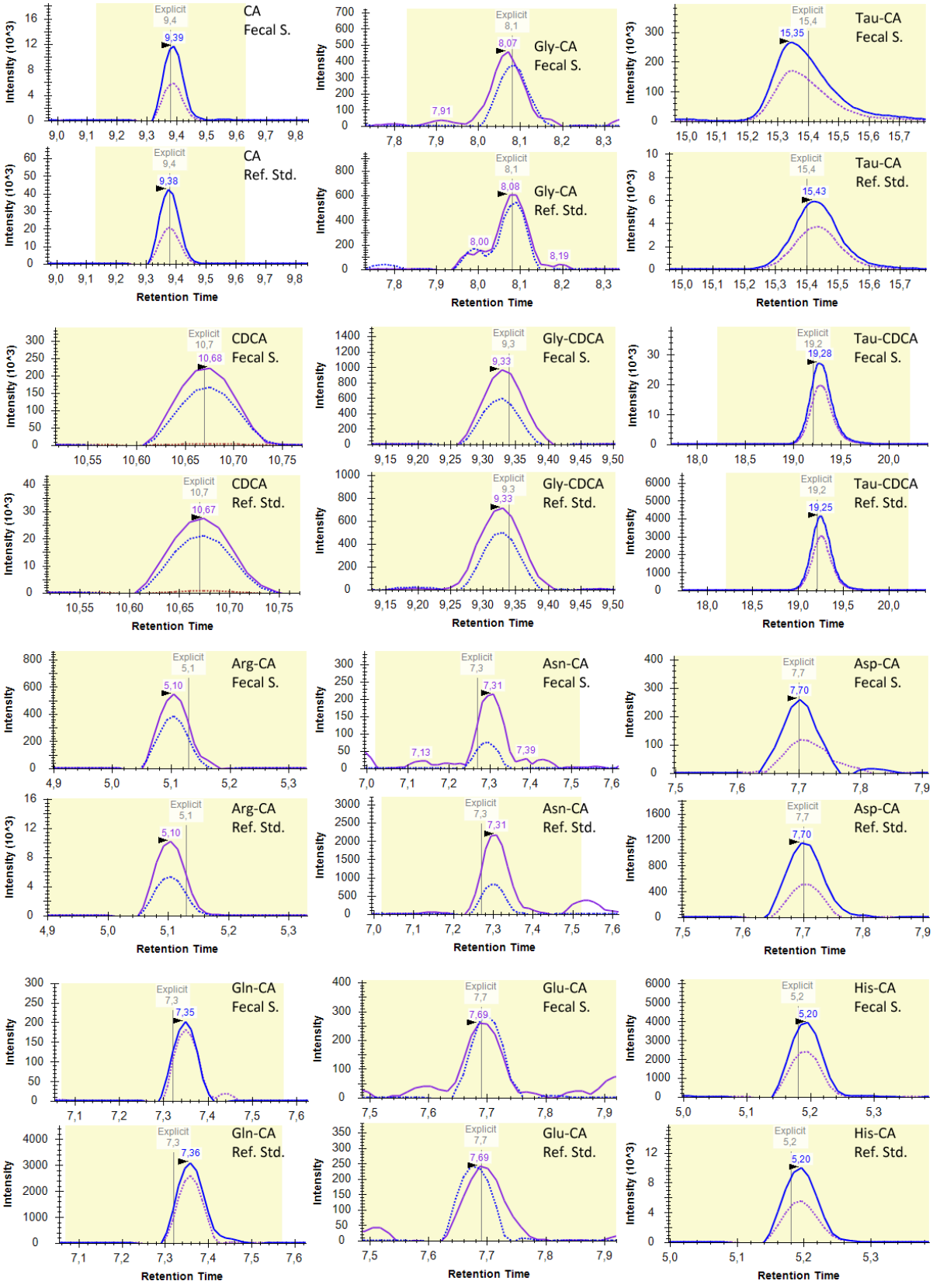
CA
Fecal S.
CA
Ref. Std.
Gly-CA
Fecal S.
Gly-CA
Ref. Std.
Tau-CA
Fecal S.
Tau-CA
Ref. Std.
CDCA
Fecal S.
CDCA
Ref. Std.
Gly-CDCA
Fecal S.
Gly-CDCA
Ref. Std.
Tau-CDCA
Fecal S.
Tau-CDCA
Ref. Std.
Arg-CA
Fecal S.
Arg-CA
Ref. Std.
Asn-CA
Fecal S.
Asn-CA
Ref. Std.
Asp-CA
Fecal S.
Asp-CA
Ref. Std.
Gln-CA
Fecal S.
Gln-CA
Ref. Std.
Glu-CA
Fecal S.
Glu-CA
Ref. Std.
His-CA
Fecal S.
His-CA
Ref. Std.
Intensity
Intensity (10^3)
Retention Time

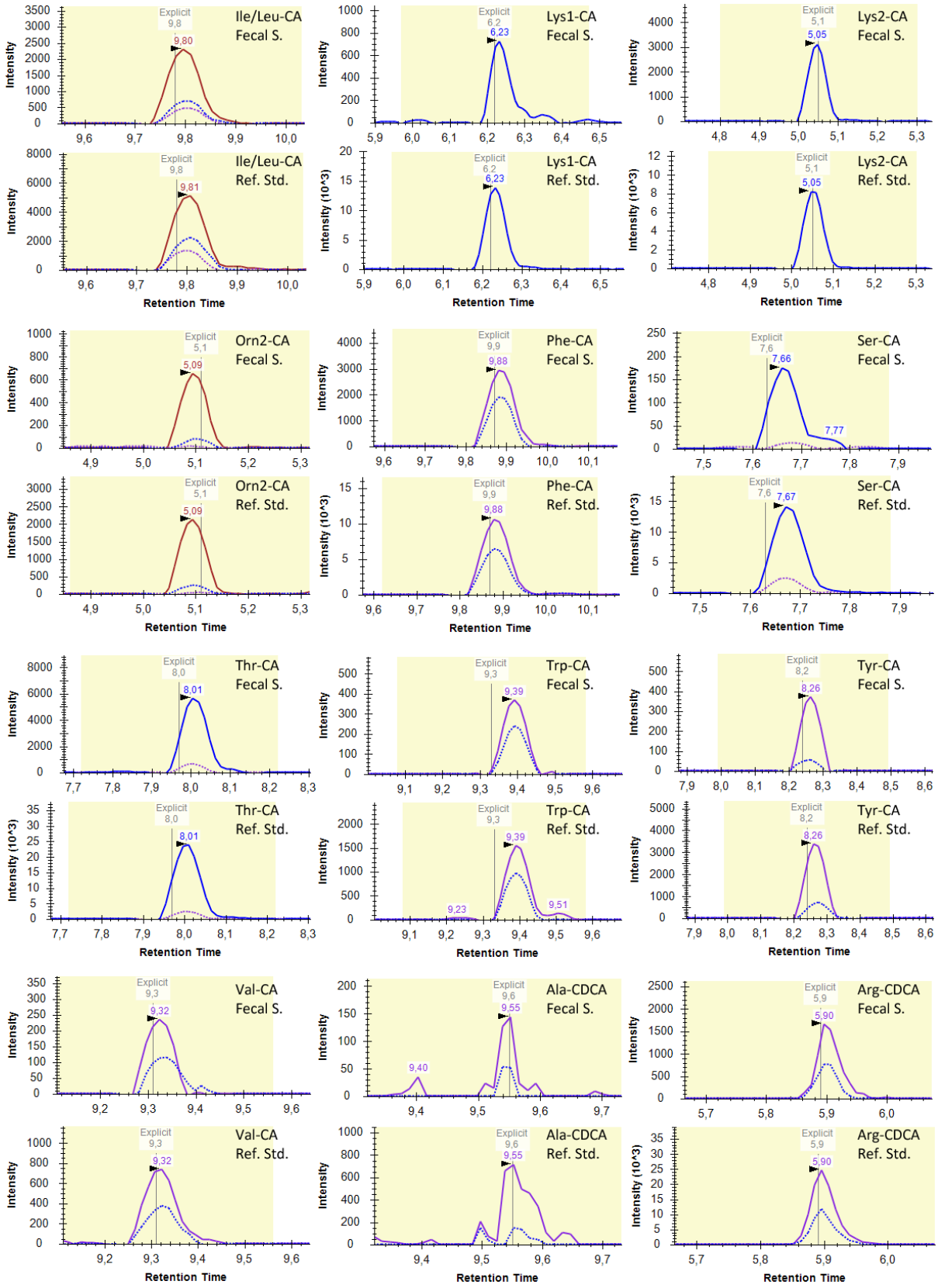
Ile/Leu-CA
Fecal S.
Ile/Leu-CA
Ref. Std.
Lys1-CA
Fecal S.
Lys1-CA
Ref. Std.
Lys2-CA
Fecal S.
Lys2-CA
Ref. Std.
Orn2-CA
Fecal S.
Orn2-CA
Ref. Std.
Phe-CA
Fecal S.
Phe-CA
Ref. Std.
Ser-CA
Fecal S.
Ser-CA
Ref. Std.
Thr-CA
Fecal S.
Thr-CA
Ref. Std.
Trp-CA
Fecal S.
Trp-CA
Ref. Std.
Tyr-CA
Fecal S.
Tyr-CA
Ref. Std.
Val-CA
Fecal S.
Val-CA
Ref. Std.
Ala-CDCA
Fecal S.
Ala-CDCA
Ref. Std.
Arg-CDCA
Fecal S.
Arg-CDCA
Ref. Std.
Intensity
Intensity (10^3)
Retention Time

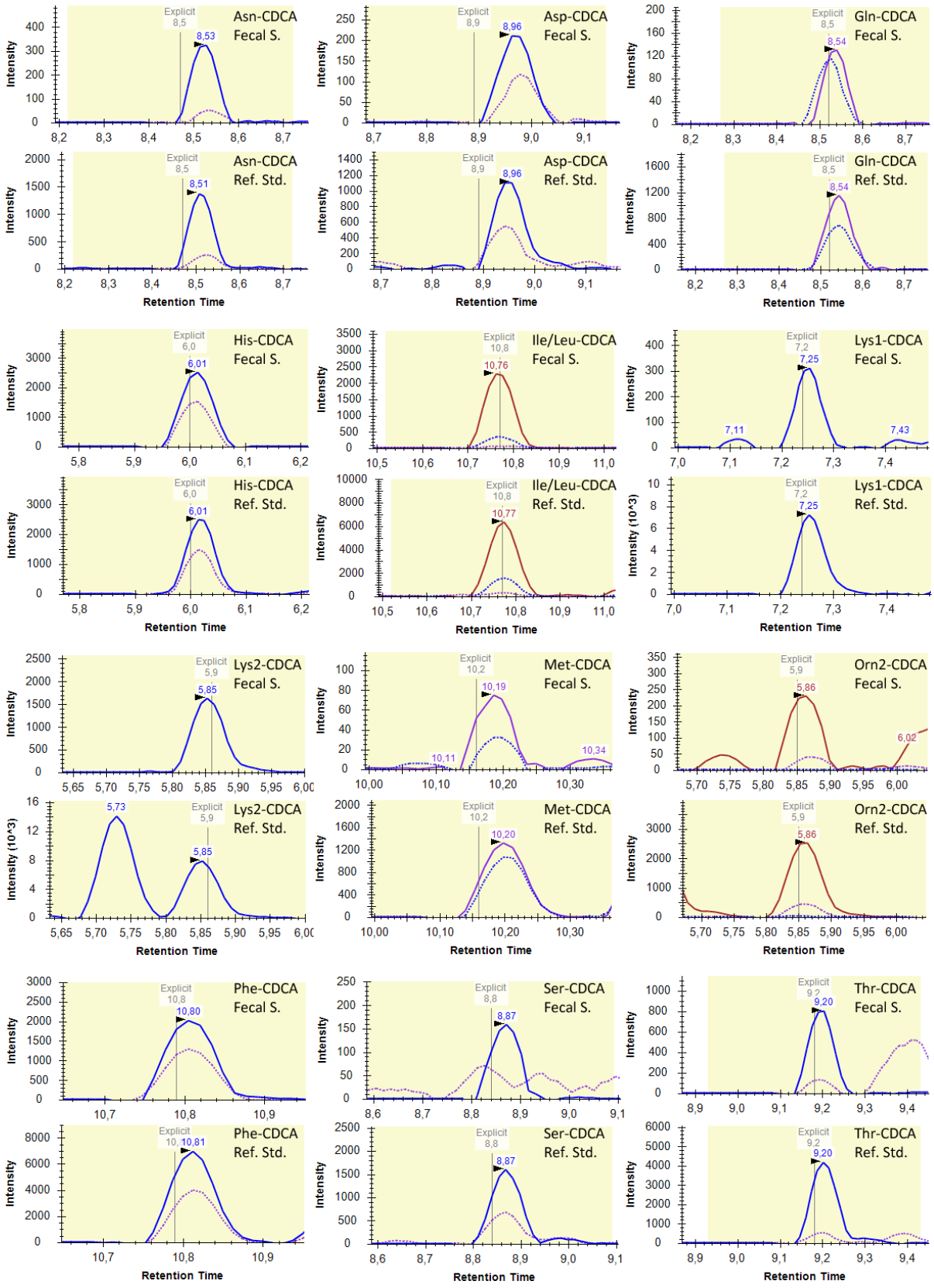
Asn-CDCA Fecal S.
Asp-CDCA Fecal S.
Gln-CDCA Fecal S.
Asn-CDCA Ref. Std.
Asp-CDCA Ref. Std.
Gln-CDCA Ref. Std.
His-CDCA Fecal S.
Ile/Leu-CDCA Fecal S.
Lys1-CDCA Fecal S.
His-CDCA Ref. Std.
Ile/Leu-CDCA Ref. Std.
Lys1-CDCA Ref. Std.
Lys2-CDCA Fecal S.
Met-CDCA Fecal S.
Orn2-CDCA Fecal S.
Lys2-CDCA Ref. Std.
Met-CDCA Ref. Std.
Orn2-CDCA Ref. Std.
Phe-CDCA Fecal S.
Ser-CDCA Fecal S.
Thr-CDCA Fecal S.
Phe-CDCA Ref. Std.
Ser-CDCA Ref. Std.
Thr-CDCA Ref. Std.
Intensity
Intensity (10^3)
Retention Time
Explicit

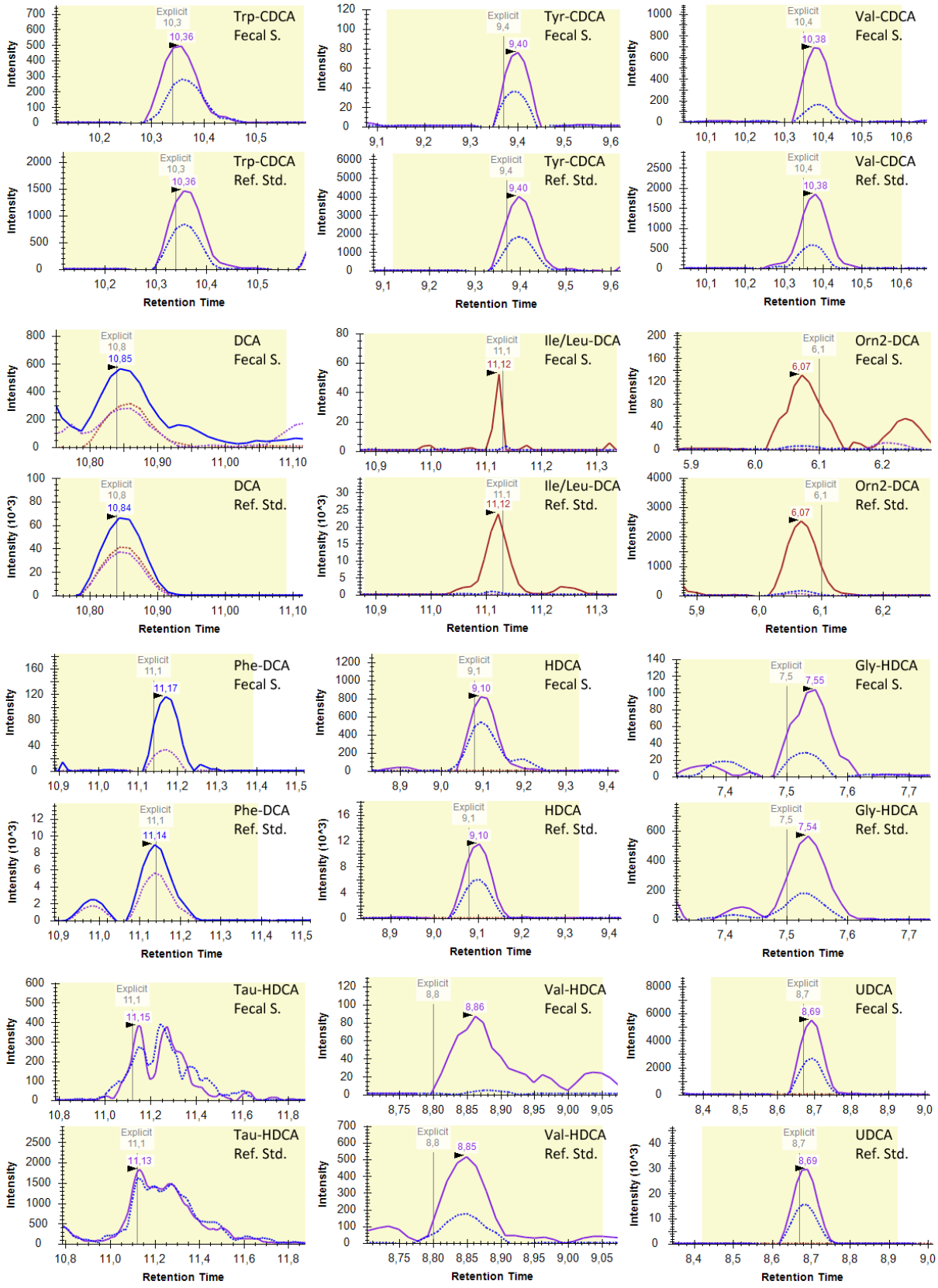
Trp-CDCA Fecal S.
Tyr-CDCA Fecal S.
Val-CDCA Fecal S.
Trp-CDCA Ref. Std.
Tyr-CDCA Ref. Std.
Val-CDCA Ref. Std.
DCA Fecal S.
Ile/Leu-DCA Fecal S.
Orn2-DCA Fecal S.
DCA Ref. Std.
Ile/Leu-DCA Ref. Std.
Orn2-DCA Ref. Std.
Phe-DCA Fecal S.
HDCA Fecal S.
Gly-HDCA Fecal S.
Phe-DCA Ref. Std.
HDCA Ref. Std.
Gly-HDCA Ref. Std.
Tau-HDCA Fecal S.
Val-HDCA Fecal S.
UDCA Fecal S.
Tau-HDCA Ref. Std.
Val-HDCA Ref. Std.
UDCA Ref. Std.
Intensity
Intensity (10^3)
Retention Time

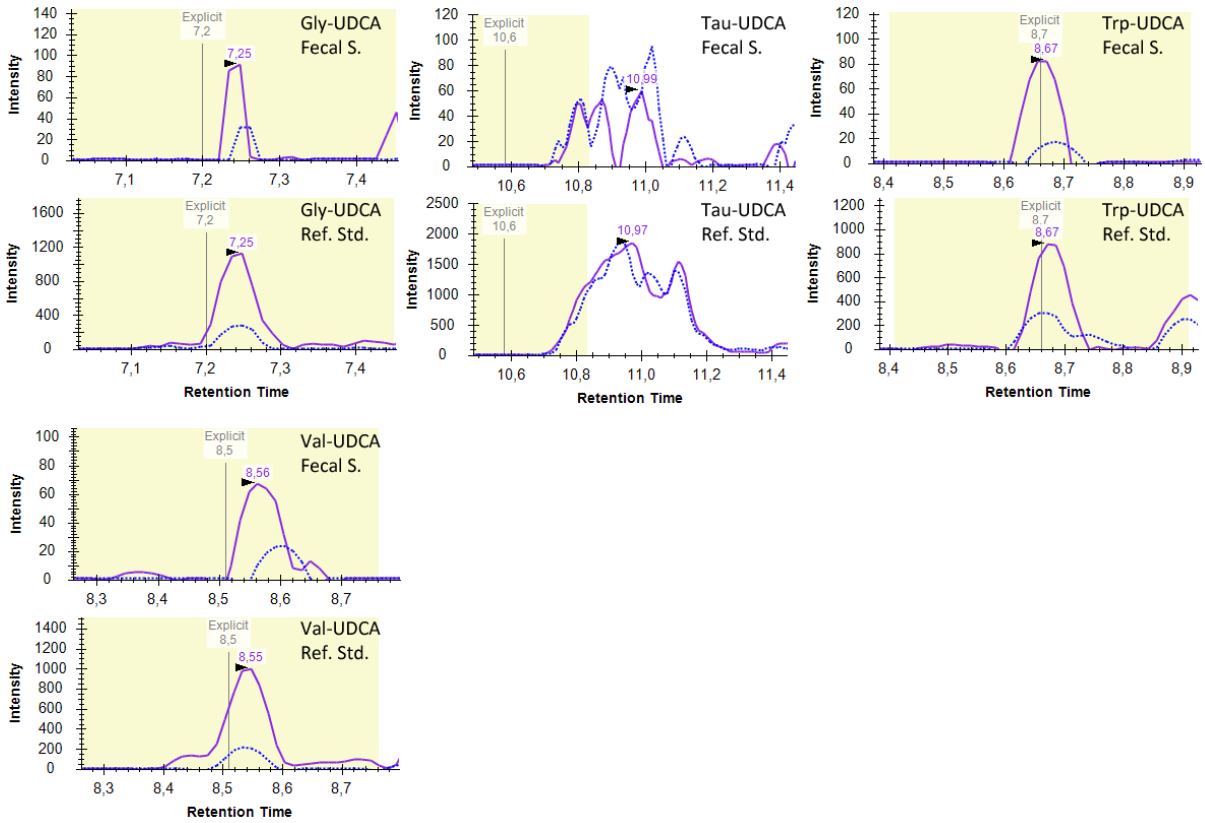

Figure 24. Comparisons between the chromatograms from reference standard mixtures (Ref. Std.) used for identification of compounds in fecal samples obtained from extremely premature infants (Fecal S.).

Abbreviations

AA	Amino acid
ACN	Acetonitrile
Ala	Alanine
APCI	Atmospheric pressure chemical ionization
APPI	Atmospheric pressure photoionization
Arg	Arginine
Asn	Asparagine
Asp	Aspartic acid
BA-AA	Bile acid amino acid conjugate
CA	Cholic acid
CDCA	Chenodeoxycholic acid
DC	Direct current
DCA	Deoxycholic acid
DCC	Dicyclohexylcarbodiimide
DPDS	2,2’-dipyridyldisulfide
EDC	N-(3-Dimethylaminopropyl)-N’-ethylcarbodiimide
EI	Electron ionization
ESI	Electrospray ionization
FA	Formic acid
FXR	Farnesoid X receptor
GC	Gas chromatography
GF	Germ-free
Gln	Glutamine
Glu	Glutamic acid
Gly	Glycine
HDCA	Hyodeoxycholic acid
HESI	Heated electrospray ionization
HIC	Hydrophobic interaction chromatography
HILIC	Hydrophilic interaction chromatography
His	Histidine
HPLC	High-performance liquid chromatography
IBD	Inflammatory bowel disease
Ile	Isoleucine

IPA	Indole-3-propionic acid
LCA	Lithocholic acid
Leu	Leucine
Lys	Lysine
m/z	Mass-to-charge ratio
MeOH	Methanol
Met	Methionine
MRM	Multiple reaction monitoring
MS	Mass spectrometry
NP(C)	Normal phase (chromatography)
Orn	Ornithine
Phe	Phenylalanine
Q1	First quadrupole in a triple quadrupole
Q2	Second quadrupole in a triple quadrupole
Q3	Third quadrupole in a triple quadrupole
QC	Quality control
QqQ	Triple quadrupole
RF	Radio frequency
RP(C)	Reversed phase (chromatography)
RT	Retention time
SCFA	Short-chain fatty acid
SEC	Size-exclusion chromatography
Ser	Serine
sMRM	Scheduled multiple reaction monitoring
SRM	Selected reaction monitoring
Tau	Taurine
Thr	Threonine
TOF	Time-of-flight
TPP	Triphenylphosphine
Trp	Tryptophan
Tyr	Tyrosine
UDCA	Ursodeoxycholic acid
UV	Ultra-violet
Val	Valine

List of Figures

List of Tables

List of sequences

Table 6. List of all sequences submitted over the course of the project in chronological order. All sequences and respective data can be found in the file path: E:\Manuel\Daniel\Raw_Data\

Sequence	Description/Purpose	Methods
First_Test_HSST3_4KP	Test for rudimentary CA-conjugate separation from a small batch, as well as checking fecal/plasma samples.	Test_CA-AA5Mix_Acquity_SRM
First_Test_HSST3_4KP_220303	Tested necessary injection volumes of first BA conjugate master mix on Acquity column.	BAConj_Test_v1
First_Test_HSST3_4KP_220304	Tested 0.4 flow rate and adjusted/replaced ESI needle due to sensitivity issues.	BAConj_Test_v1 220304_BAConj_Test_v2
TempSequence_220307	Further testing of new needle.	220304_BAConj_Test_v2
Column_Test_220308	Comparison of Acquity & Kinetex columns at different flow rates.	220304_BAConj_Test_v2 220304_BAConj_Test_v3
Column_Test_220314	Tested Atlantis column at same flow rates as Acquity & Kinetex.	220304_BAConj_Test_v2 220304_BAConj_Test_v3
Column_Test_220315	Tested Kinetex column at higher flow rates and different gradients.	220304_BAConj_Test_v2 220304_BAConj_Test_v4 220304_BAConj_Test_v5
Column_Test_220316	Tested eluent A (water) without FA additive and higher flow rates on Atlantis and Kinetex.	220304_BAConj_Test_v5 220316_BAConj_Test_v6 220316_BAConj_Test_v7
Eluent_Test_220317	Tested eluent systems MeOH and 2-propanol/acetonitrile.	220315_BAConj_Test_v5 220316_BAConj_Test_v7
Eluent_Test_220318	Tested MeOH/ACN eluent system and extracted fecal matrix with and without standard spike on Atlantis.	220315_BAConj_Test_v5 220316_BAConj_Test_v7
220331_RT-Determination_Atlantis_ACN-MeOH	Injection of separate BA-AA batches in succession to compare with standard mix and determine retention times of all conjugates.	220316_BAConj_Test_v7

Sequence	Description/Purpose	Methods
220404_NewMM+Plasma-Test_Atlantis_ACN-MeOH	Prepared new “master mix” containing all conjugates and tested it spiked onto processed plasma samples.	220316_BAConj_Test_v7
220407_sMRM-Segment-test	Started creating sMRM segments to optimize the method in regard to scan time.	220407_BAConj_Test_v8
220412_sMRM-Segment-test_03	Tightened windows for more optimization and tested with master mix.	220412_BAConj_v01
220413_NIST-Serum-Standard	Measured NIST serum standard but was unable to find any new conjugates.	220412_BAConj_v01
220413_04_NPHDeriv_U-ABC-Mix_Test	Tested further derivatization of BA-AAs with 3-nitrophenylhydrazine.	220413_NPHDeriv_Test_v01
220420_BA-NPH_CE-Tests	Further experiments on derivatization with 3-nitrophenylhydrazine.	220420_NPHDeriv_Test_v02
220425_BAConj_EZMethod-Test	Discovered an alternative sMRM input method (EZ mode) that is more flexible, using scan windows instead of segments. Transferred and tested the method.	220425_BAConj_Test_v10
220426_BAConj_CycleTime-Test	Tested cycle times on EZ mode method.	220426_BAConj_v02
220427_BAConj_ CycleTime-Test-v03	Further optimized cycle time on EZ mode method.	220427_BAConj_v03
220428_BAConj_FecesWaterProteinExtractionComparison	Compared relative signal strength between differently processed and extracted fecal samples.	220427_BAConj_v03 220428_BAConj_v04
220517_BAConj_SingleBA-AAMixes+Feces	Injected single standards of specific conjugates that were synthesized in isolation. Also remeasured differently processed fecal samples.	220428_BAConj_v05
220519_BAConj_IleLeu+OldMethodConfirmation	Remeasured fecal samples with old, segmented method to confirm findings. Injected single standards of Ile and Leu conjugates to check, if additional peaks are separate molecules or a different phenomenon.	220519_BAConj_v06 220316_BAConj_Test_v7

Sequence	Description/Purpose	Methods
220519_BAConj_Ile-fractioning	Manually fractioning dual peaks visible in Ile chromatogram over two runs by disconnecting tubing at expected RT and diverting flow into separate vials.	220519_BAConj_v06_fractioning
220519_BAConj_Ile-Fr1-2	Injected manually fractioned Ile peaks and determined that separation is possible, therefore likely to not be an elution phenomenon.	220524_BAConj_v07
220524_BAConj_Ba-Tau-single-standards+EDCMix-Ile	Injected Ile conjugates synthesized with EDC as a coupling reagent to check if additional peaks persist. Furthermore, checked single standards of Tau conjugates.	220524_BAConj_v07
220524_BAConj_BA-Tau_Elution-tests_01	Started testing a variety of different eluent compositions to efficiently eluate Tau conjugates.	220525_BAConj_TauElution_Test-01 220525_BAConj_TauElution_Test-02 220525_BAConj_TauElution_Test-03 220525_BAConj_TauElution_Test -04
220524_BAConj_BA-Tau_Elution-tests_02	Further Tau conjugate elution testing.	220601_BAConj_TauElution_Test-05 220601_BAConj_TauElution_Test-06 220601_BAConj_TauElution_Test-07 220601_BAConj_TauElution_Test-08
220602_BAConj_BA-Tau_Elution-tests_03	Further Tau conjugate elution testing overnight.	220602_BAConj_TauElution_Test-09 220602_BAConj_TauElution_Test-10 220602_BAConj_TauElution_Test-11 220602_BAConj_TauElution_Test-12 220602_BAConj_TauElution_Test-13 220602_BAConj_TauElution_Test-14 220602_BAConj_TauElution_Test-15 220602_BAConj_TauElution_Test-16 220602_BAConj_TauElution_Test-17 220602_BAConj_TauElution_Test-18 220602_BAConj_TauElution_Test-19

Sequence	Description/Purpose	Methods
220603_BAConj_BA-Tau_Elution-tests_04	Tried to confirm the most viable gradient elongations for Tau conjugates.	220602_BAConj_TauElution_Test-17 220602_BAConj_TauElution_Test-18 220602_BAConj_TauElution_Test-19
220608_BAConj_BA-Tau_Elution-tests_05	Final Tau conjugate elution testing and establishment of final gradient.	220608_BAConj_TauElution_Test-20
220609_BAConj_NeedleTests+ISTD+Feces	Tested the method for the newly obtained internal standard 4d-UDCA, including spiking of extracted fecal samples. Also tested different ESI needle positions for possible sensitivity gain.	220608_BAConj_v08
220712_BAConj_PrecolumnStabilityTest	Affixed a new pre-column to the Atlantis column and tested/conditioned it with successive injections of fecal samples.	220711_BAConj_v09 & 220712_BAConj_v10
220712_BAConj_ColumnHealthTest+Cycle Time	Tested state of column after a communication error caused the eluent reservoir to drain completely and pump air for a short time. No damage could be found. Experimented with lower cycle times for more data points.	220712_BAConj_v10
220714_BAConj_Stability+CT_Test	Checked stability of measurements by injecting the same matrix sample 20 times. Finalized optimal cycle time for the method.	220712_BAConj_v10 & 220712_BAConj_v11
220718_BAConj_PlasmaQCTest	Created a QC sample for plasma measurements and confirmed its viability.	220718_BAConj_v12
220718_BAConj_PremiBrain-Plasma	Measurement of all infant plasma samples.	220718_BAConj_v12b
220721_BAConj_PremiBrain-Feces_PooledMatrixTest	Broadly assessed severity of matrix effect in concentrated, pooled extracted fecal samples.	220718_BAConj_v12c
220722_BAConj_PremiBrain-Feces	Measurement of all infant fecal samples.	220718_BAConj_v12c

Table 7. Detailed list of infant plasma and fecal sample batches submitted for measurement, including file name, path and injection volumes in µL.

Batch					
220718_BAConj_PremiBrain-Plasma			220722_BAConj_PremiBrain-Feces		
File Name	**File Path**	**Inj. Vol. [µL]**	**File Name**	**File Path**	**Inj. Vol. [µL]**
220718_001_Blank	E:\Manuel\Daniel\Raw_Data\	5	220721_001_Blank	E:\Manuel\Daniel\Raw_Data\	5
220718_002_Matrix	E:\Manuel\Daniel\Raw_Data\	5	220721_002_Matrix	E:\Manuel\Daniel\Raw_Data\	5
220718_003_Matrix	E:\Manuel\Daniel\Raw_Data\	5	220721_003_Matrix	E:\Manuel\Daniel\Raw_Data\	5
220718_004_Matrix	E:\Manuel\Daniel\Raw_Data\	5	220721_004_Matrix	E:\Manuel\Daniel\Raw_Data\	5
220718_005_Matrix	E:\Manuel\Daniel\Raw_Data\	5	220721_005_Matrix	E:\Manuel\Daniel\Raw_Data\	5
220718_006_Matrix	E:\Manuel\Daniel\Raw_Data\	5	220721_006_Matrix	E:\Manuel\Daniel\Raw_Data\	5
220718_007_QC-01	E:\Manuel\Daniel\Raw_Data\	5	220721_007_QC-01	E:\Manuel\Daniel\Raw_Data\	5
220718_008_QC-02	E:\Manuel\Daniel\Raw_Data\	5	220721_008_QC-02	E:\Manuel\Daniel\Raw_Data\	5
220718_009_QC-03	E:\Manuel\Daniel\Raw_Data\	5	220721_009_QC-03	E:\Manuel\Daniel\Raw_Data\	5
220718_010_QC-04	E:\Manuel\Daniel\Raw_Data\	5	220721_010_QC-04	E:\Manuel\Daniel\Raw_Data\	5
220718_011_QC-05	E:\Manuel\Daniel\Raw_Data\	5	220721_011_QC-05	E:\Manuel\Daniel\Raw_Data\	5
220718_012_TP-040	E:\Manuel\Daniel\Raw_Data\	5	220721_012_TF-001	E:\Manuel\Daniel\Raw_Data\	5
220718_013_TP-124	E:\Manuel\Daniel\Raw_Data\	5	220721_013_TF-002	E:\Manuel\Daniel\Raw_Data\	5
220718_014_TP-030	E:\Manuel\Daniel\Raw_Data\	5	220721_014_TF-003	E:\Manuel\Daniel\Raw_Data\	5
220718_015_TP-012	E:\Manuel\Daniel\Raw_Data\	5	220721_015_TF-004	E:\Manuel\Daniel\Raw_Data\	5
220718_016_TP-123	E:\Manuel\Daniel\Raw_Data\	5	220721_016_TF-005	E:\Manuel\Daniel\Raw_Data\	5
220718_017_TP-122	E:\Manuel\Daniel\Raw_Data\	5	220721_017_TF-006	E:\Manuel\Daniel\Raw_Data\	5
220718_018_TP-117	E:\Manuel\Daniel\Raw_Data\	5	220721_018_TF-007	E:\Manuel\Daniel\Raw_Data\	5
220718_019_TP-094	E:\Manuel\Daniel\Raw_Data\	5	220721_019_TF-008	E:\Manuel\Daniel\Raw_Data\	5
220718_020_TP-047	E:\Manuel\Daniel\Raw_Data\	5	220721_020_TF-009	E:\Manuel\Daniel\Raw_Data\	5
220718_021_TP-039	E:\Manuel\Daniel\Raw_Data\	5	220721_021_TF-010	E:\Manuel\Daniel\Raw_Data\	5
220718_022_TP-021	E:\Manuel\Daniel\Raw_Data\	5	220721_022_TF-011	E:\Manuel\Daniel\Raw_Data\	5

File Name	File Path	Inj. Vol. [µL]	File Name	File Path	Inj. Vol. [µL]
220718_023_TP-001	E:\Manuel\Daniel\Raw_Data\	5	220721_023_TF-014	E:\Manuel\Daniel\Raw_Data\	5
220718_024_TP-002	E:\Manuel\Daniel\Raw_Data\	5	220721_024_TF-015	E:\Manuel\Daniel\Raw_Data\	5
220718_025_TP-003	E:\Manuel\Daniel\Raw_Data\	5	220721_025_TF-016	E:\Manuel\Daniel\Raw_Data\	5
220718_026_TP-004	E:\Manuel\Daniel\Raw_Data\	5	220721_026_TF-017	E:\Manuel\Daniel\Raw_Data\	5
220718_027_TP-005	E:\Manuel\Daniel\Raw_Data\	5	220721_027_TF-018	E:\Manuel\Daniel\Raw_Data\	5
220718_028_TP-006	E:\Manuel\Daniel\Raw_Data\	5	220721_028_TF-019	E:\Manuel\Daniel\Raw_Data\	5
220718_029_TP-008-1	E:\Manuel\Daniel\Raw_Data\	5	220721_029_TF-020	E:\Manuel\Daniel\Raw_Data\	5
220718_030_TP-008-2	E:\Manuel\Daniel\Raw_Data\	5	220721_030_TF-021	E:\Manuel\Daniel\Raw_Data\	5
220718_031_TP-009	E:\Manuel\Daniel\Raw_Data\	5	220721_031_TF-022	E:\Manuel\Daniel\Raw_Data\	5
220718_032_QC-06	E:\Manuel\Daniel\Raw_Data\	5	220721_032_QC-06	E:\Manuel\Daniel\Raw_Data\	5
220718_033_TP-010	E:\Manuel\Daniel\Raw_Data\	5	220721_033_TF-023	E:\Manuel\Daniel\Raw_Data\	5
220718_034_TP-011	E:\Manuel\Daniel\Raw_Data\	5	220721_034_TF-024	E:\Manuel\Daniel\Raw_Data\	5
220718_035_TP-013	E:\Manuel\Daniel\Raw_Data\	5	220721_035_TF-025	E:\Manuel\Daniel\Raw_Data\	5
220718_036_TP-014	E:\Manuel\Daniel\Raw_Data\	5	220721_036_TF-026	E:\Manuel\Daniel\Raw_Data\	5
220718_037_TP-015	E:\Manuel\Daniel\Raw_Data\	5	220721_037_TF-027	E:\Manuel\Daniel\Raw_Data\	5
220718_038_TP-017	E:\Manuel\Daniel\Raw_Data\	5	220721_038_TF-028	E:\Manuel\Daniel\Raw_Data\	5
220718_039_TP-018	E:\Manuel\Daniel\Raw_Data\	5	220721_039_TF-029	E:\Manuel\Daniel\Raw_Data\	5
220718_040_TP-019	E:\Manuel\Daniel\Raw_Data\	5	220721_040_TF-030	E:\Manuel\Daniel\Raw_Data\	5
220718_041_TP-020	E:\Manuel\Daniel\Raw_Data\	5	220721_041_TF-031	E:\Manuel\Daniel\Raw_Data\	5
220718_042_TP-022	E:\Manuel\Daniel\Raw_Data\	5	220721_042_TF-032	E:\Manuel\Daniel\Raw_Data\	5
220718_043_TP-023	E:\Manuel\Daniel\Raw_Data\	5	220721_043_TF-033	E:\Manuel\Daniel\Raw_Data\	5
220718_044_TP-024	E:\Manuel\Daniel\Raw_Data\	5	220721_044_TF-034	E:\Manuel\Daniel\Raw_Data\	5
220718_045_TP-025	E:\Manuel\Daniel\Raw_Data\	5	220721_045_TF-035	E:\Manuel\Daniel\Raw_Data\	5
220718_046_TP-026	E:\Manuel\Daniel\Raw_Data\	5	220721_046_TF-036	E:\Manuel\Daniel\Raw_Data\	5
220718_047_TP-027	E:\Manuel\Daniel\Raw_Data\	5	220721_047_TF-037	E:\Manuel\Daniel\Raw_Data\	5
220718_048_TP-028	E:\Manuel\Daniel\Raw_Data\	5	220721_048_TF-038	E:\Manuel\Daniel\Raw_Data\	5
220718_049_TP-029	E:\Manuel\Daniel\Raw_Data\	5	220721_049_TF-039	E:\Manuel\Daniel\Raw_Data\	5

File Name	File Path	Inj. Vol. [µL]	File Name	File Path	Inj. Vol. [µL]
220718_050_TP-031	E:\Manuel\Daniel\Raw_Data\	5	220721_050_TF-040	E:\Manuel\Daniel\Raw_Data\	5
220718_051_TP-033	E:\Manuel\Daniel\Raw_Data\	5	220721_051_TF-041	E:\Manuel\Daniel\Raw_Data\	5
220718_052_QC-07	E:\Manuel\Daniel\Raw_Data\	5	220721_052_TF-042	E:\Manuel\Daniel\Raw_Data\	5
220718_053_TP-034	E:\Manuel\Daniel\Raw_Data\	5	220721_053_QC-07	E:\Manuel\Daniel\Raw_Data\	5
220718_054_TP-035	E:\Manuel\Daniel\Raw_Data\	5	220721_054_TF-043	E:\Manuel\Daniel\Raw_Data\	5
220718_055_TP-036	E:\Manuel\Daniel\Raw_Data\	5	220721_055_TF-044	E:\Manuel\Daniel\Raw_Data\	5
220718_056_TP-038	E:\Manuel\Daniel\Raw_Data\	5	220721_056_TF-045	E:\Manuel\Daniel\Raw_Data\	5
220718_057_TP-041	E:\Manuel\Daniel\Raw_Data\	5	220721_057_TF-046	E:\Manuel\Daniel\Raw_Data\	5
220718_058_TP-042	E:\Manuel\Daniel\Raw_Data\	5	220721_058_TF-049	E:\Manuel\Daniel\Raw_Data\	5
220718_059_TP-043	E:\Manuel\Daniel\Raw_Data\	5	220721_059_TF-050	E:\Manuel\Daniel\Raw_Data\	5
220718_060_TP-044	E:\Manuel\Daniel\Raw_Data\	5	220721_060_TF-051	E:\Manuel\Daniel\Raw_Data\	5
220718_061_TP-045	E:\Manuel\Daniel\Raw_Data\	5	220721_061_TF-052	E:\Manuel\Daniel\Raw_Data\	5
220718_062_TP-046	E:\Manuel\Daniel\Raw_Data\	5	220721_062_TF-053	E:\Manuel\Daniel\Raw_Data\	5
220718_063_TP-048	E:\Manuel\Daniel\Raw_Data\	5	220721_063_TF-054	E:\Manuel\Daniel\Raw_Data\	5
220718_064_TP-049	E:\Manuel\Daniel\Raw_Data\	5	220721_064_TF-055	E:\Manuel\Daniel\Raw_Data\	5
220718_065_TP-050	E:\Manuel\Daniel\Raw_Data\	5	220721_065_TF-056	E:\Manuel\Daniel\Raw_Data\	5
220718_066_TP-051	E:\Manuel\Daniel\Raw_Data\	5	220721_066_TF-057	E:\Manuel\Daniel\Raw_Data\	5
220718_067_TP-052	E:\Manuel\Daniel\Raw_Data\	5	220721_067_TF-058	E:\Manuel\Daniel\Raw_Data\	5
220718_068_TP-053	E:\Manuel\Daniel\Raw_Data\	5	220721_068_TF-059	E:\Manuel\Daniel\Raw_Data\	5
220718_069_TP-054	E:\Manuel\Daniel\Raw_Data\	5	220721_069_TF-060	E:\Manuel\Daniel\Raw_Data\	5
220718_070_TP-056	E:\Manuel\Daniel\Raw_Data\	5	220721_070_TF-061	E:\Manuel\Daniel\Raw_Data\	5
220718_071_QC-08	E:\Manuel\Daniel\Raw_Data\	5	220721_071_TF-062	E:\Manuel\Daniel\Raw_Data\	5
220718_072_TP-058	E:\Manuel\Daniel\Raw_Data\	5	220721_072_TF-063	E:\Manuel\Daniel\Raw_Data\	5
220718_073_TP-059	E:\Manuel\Daniel\Raw_Data\	5	220721_073_TF-064	E:\Manuel\Daniel\Raw_Data\	5
220718_074_TP-060	E:\Manuel\Daniel\Raw_Data\	5	220721_074_QC-08	E:\Manuel\Daniel\Raw_Data\	5
220718_075_TP-061	E:\Manuel\Daniel\Raw_Data\	5	220721_075_TF-065	E:\Manuel\Daniel\Raw_Data\	5
220718_076_TP-062	E:\Manuel\Daniel\Raw_Data\	5	220721_076_TF-066	E:\Manuel\Daniel\Raw_Data\	5

File Name	File Path	Inj. Vol. [µL]	File Name	File Path	Inj. Vol. [µL]
220718_077_TP-063	E:\Manuel\Daniel\Raw_Data\	5	220721_077_TF-067	E:\Manuel\Daniel\Raw_Data\	5
220718_078_TP-064	E:\Manuel\Daniel\Raw_Data\	5	220721_078_TF-068	E:\Manuel\Daniel\Raw_Data\	5
220718_079_TP-065	E:\Manuel\Daniel\Raw_Data\	5	220721_079_TF-069	E:\Manuel\Daniel\Raw_Data\	5
220718_080_TP-066	E:\Manuel\Daniel\Raw_Data\	5	220721_080_TF-070	E:\Manuel\Daniel\Raw_Data\	5
220718_081_TP-067	E:\Manuel\Daniel\Raw_Data\	5	220721_081_TF-071	E:\Manuel\Daniel\Raw_Data\	5
220718_082_TP-068	E:\Manuel\Daniel\Raw_Data\	5	220721_082_TF-072	E:\Manuel\Daniel\Raw_Data\	5
220718_083_TP-069	E:\Manuel\Daniel\Raw_Data\	5	220721_083_TF-073	E:\Manuel\Daniel\Raw_Data\	5
220718_084_TP-070	E:\Manuel\Daniel\Raw_Data\	5	220721_084_TF-074	E:\Manuel\Daniel\Raw_Data\	5
220718_085_TP-071	E:\Manuel\Daniel\Raw_Data\	5	220721_085_TF-075	E:\Manuel\Daniel\Raw_Data\	5
220718_086_TP-072	E:\Manuel\Daniel\Raw_Data\	5	220721_086_TF-076	E:\Manuel\Daniel\Raw_Data\	5
220718_087_TP-073	E:\Manuel\Daniel\Raw_Data\	5	220721_087_TF-077	E:\Manuel\Daniel\Raw_Data\	5
220718_088_TP-074	E:\Manuel\Daniel\Raw_Data\	5	220721_088_TF-078	E:\Manuel\Daniel\Raw_Data\	5
220718_089_TP-075	E:\Manuel\Daniel\Raw_Data\	5	220721_089_TF-079	E:\Manuel\Daniel\Raw_Data\	5
220718_090_QC-09	E:\Manuel\Daniel\Raw_Data\	5	220721_090_TF-080	E:\Manuel\Daniel\Raw_Data\	5
220718_091_TP-077	E:\Manuel\Daniel\Raw_Data\	5	220721_091_TF-082	E:\Manuel\Daniel\Raw_Data\	5
220718_092_TP-078	E:\Manuel\Daniel\Raw_Data\	5	220721_092_TF-083	E:\Manuel\Daniel\Raw_Data\	5
220718_093_TP-079	E:\Manuel\Daniel\Raw_Data\	5	220721_093_TF-084	E:\Manuel\Daniel\Raw_Data\	5
220718_094_TP-080	E:\Manuel\Daniel\Raw_Data\	5	220721_094_TF-085	E:\Manuel\Daniel\Raw_Data\	5
220718_095_TP-081	E:\Manuel\Daniel\Raw_Data\	5	220721_095_QC-09	E:\Manuel\Daniel\Raw_Data\	5
220718_096_TP-082	E:\Manuel\Daniel\Raw_Data\	5	220721_096_TF-086	E:\Manuel\Daniel\Raw_Data\	5
220718_097_TP-083	E:\Manuel\Daniel\Raw_Data\	5	220721_097_TF-087	E:\Manuel\Daniel\Raw_Data\	5
220718_098_TP-084	E:\Manuel\Daniel\Raw_Data\	5	220721_098_TF-088	E:\Manuel\Daniel\Raw_Data\	5
220718_099_TP-085	E:\Manuel\Daniel\Raw_Data\	5	220721_099_TF-089	E:\Manuel\Daniel\Raw_Data\	5
220718_100_TP-086	E:\Manuel\Daniel\Raw_Data\	5	220721_100_TF-090	E:\Manuel\Daniel\Raw_Data\	5
220718_101_TP-087	E:\Manuel\Daniel\Raw_Data\	5	220721_101_TF-091	E:\Manuel\Daniel\Raw_Data\	5
220718_102_TP-088	E:\Manuel\Daniel\Raw_Data\	5	220721_102_TF-092	E:\Manuel\Daniel\Raw_Data\	5
220718_103_TP-089	E:\Manuel\Daniel\Raw_Data\	5	220721_103_TF-093	E:\Manuel\Daniel\Raw_Data\	5

File Name	File Path	Inj. Vol. [µL]	File Name	File Path	Inj. Vol. [µL]
220718_104_TP-091	E:\Manuel\Daniel\Raw_Data\	5	220721_104_TF-094	E:\Manuel\Daniel\Raw_Data\	5
220718_105_TP-092	E:\Manuel\Daniel\Raw_Data\	5	220721_105_TF-095	E:\Manuel\Daniel\Raw_Data\	5
220718_106_TP-093	E:\Manuel\Daniel\Raw_Data\	5	220721_106_TF-096	E:\Manuel\Daniel\Raw_Data\	5
220718_107_TP-096	E:\Manuel\Daniel\Raw_Data\	5	220721_107_TF-097	E:\Manuel\Daniel\Raw_Data\	5
220718_108_TP-097	E:\Manuel\Daniel\Raw_Data\	5	220721_108_TF-098	E:\Manuel\Daniel\Raw_Data\	5
220718_109_QC-10	E:\Manuel\Daniel\Raw_Data\	5	220721_109_QC-10	E:\Manuel\Daniel\Raw_Data\	5
220718_110_TP-098	E:\Manuel\Daniel\Raw_Data\	5	220721_110_Blank	E:\Manuel\Daniel\Raw_Data\	5
220718_111_TP-099	E:\Manuel\Daniel\Raw_Data\	5	220721_111_Blank	E:\Manuel\Daniel\Raw_Data\	5
220718_112_TP-100	E:\Manuel\Daniel\Raw_Data\	5	220721_112_Shutdown	E:\Manuel\Daniel\Raw_Data\	5
220718_113_TP-101	E:\Manuel\Daniel\Raw_Data\	5			
220718_114_TP-102	E:\Manuel\Daniel\Raw_Data\	5			
220718_115_TP-103	E:\Manuel\Daniel\Raw_Data\	5			
220718_116_TP-104	E:\Manuel\Daniel\Raw_Data\	5			
220718_117_TP-105	E:\Manuel\Daniel\Raw_Data\	5			
220718_118_TP-106	E:\Manuel\Daniel\Raw_Data\	5			
220718_119_TP-107	E:\Manuel\Daniel\Raw_Data\	5			
220718_120_TP-109	E:\Manuel\Daniel\Raw_Data\	5			
220718_121_TP-110	E:\Manuel\Daniel\Raw_Data\	5			
220718_122_TP-111-1	E:\Manuel\Daniel\Raw_Data\	5			
220718_123_TP-111-2	E:\Manuel\Daniel\Raw_Data\	5			
220718_124_TP-113	E:\Manuel\Daniel\Raw_Data\	5			
220718_125_TP-114	E:\Manuel\Daniel\Raw_Data\	5			
220718_126_TP-115	E:\Manuel\Daniel\Raw_Data\	5			
220718_127_QC-11	E:\Manuel\Daniel\Raw_Data\	5			
220718_128_TP-119	E:\Manuel\Daniel\Raw_Data\	5			
220718_129_TP-120	E:\Manuel\Daniel\Raw_Data\	5			
220718_130_TP-121	E:\Manuel\Daniel\Raw_Data\	5			

File Name	File Path	Inj. Vol. [µL]	File Name	File Path	Inj. Vol. [µL]
220718_131_TP-126	E:\Manuel\Daniel\Raw_Data\	5			
220718_132_TP-128	E:\Manuel\Daniel\Raw_Data\	5			
220718_133_TP-130	E:\Manuel\Daniel\Raw_Data\	5			
220718_134_TP-131	E:\Manuel\Daniel\Raw_Data\	5			
220718_135_TP-132	E:\Manuel\Daniel\Raw_Data\	5			
220718_136_TP-133	E:\Manuel\Daniel\Raw_Data\	5			
220718_137_TP-134	E:\Manuel\Daniel\Raw_Data\	5			
220718_138_TP-135	E:\Manuel\Daniel\Raw_Data\	5			
220718_139_TP-136	E:\Manuel\Daniel\Raw_Data\	5			
220718_140_TP-137	E:\Manuel\Daniel\Raw_Data\	5			
220718_141_QC-12	E:\Manuel\Daniel\Raw_Data\	5			
220718_142_Blank	E:\Manuel\Daniel\Raw_Data\	5			
220718_143_Blank	E:\Manuel\Daniel\Raw_Data\	5			
220718_144_Shutdown	E:\Manuel\Daniel\Raw_Data\	5			